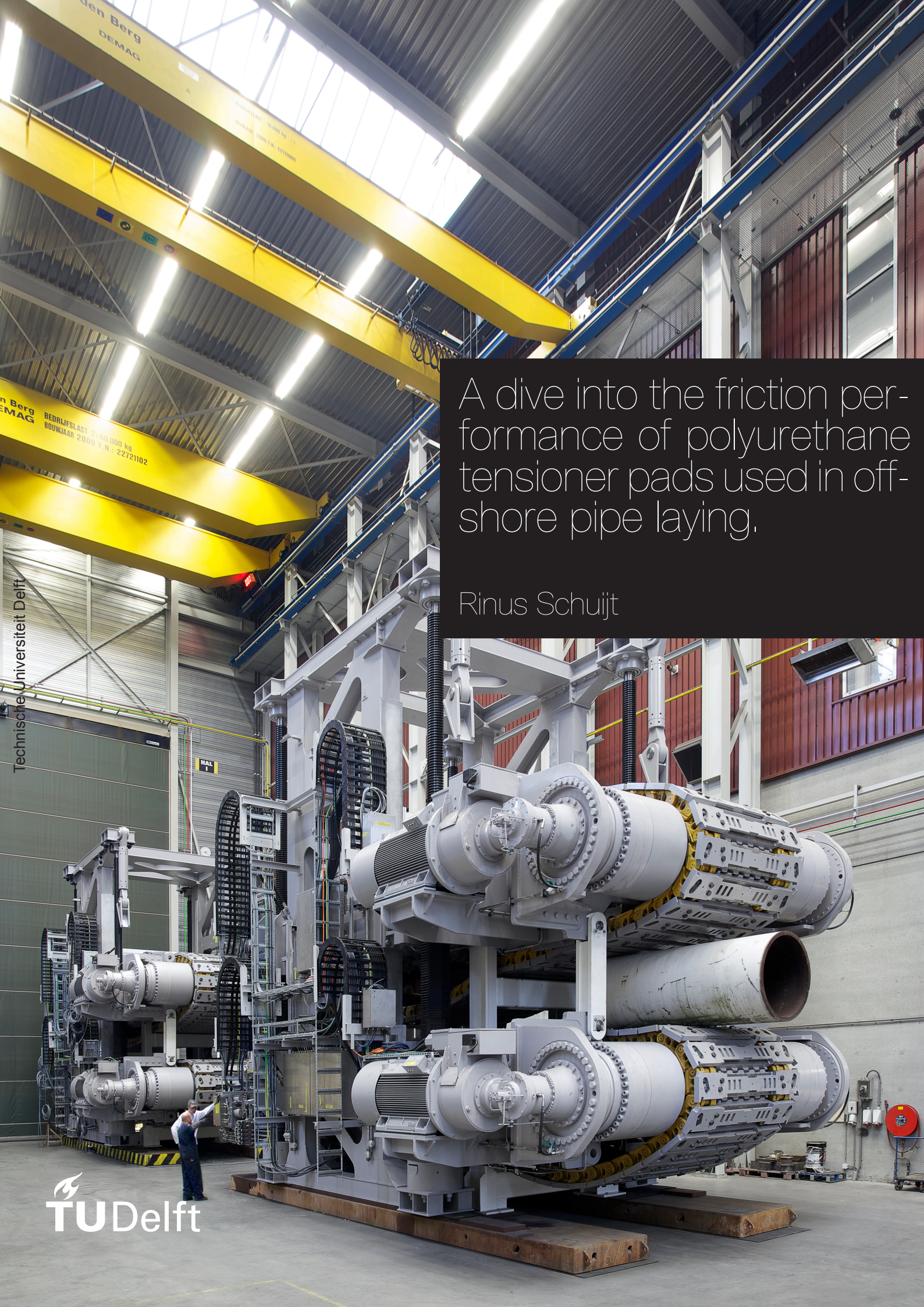

A dive into the friction performance of polyurethane tensioner pads used in offshore pipe laying.

Rinus Schuijt

TU Delft

A dive into the friction performance of polyurethane tensioner pads used in offshore pipe laying.

by

Rinus Schuijt

to obtain the degree of Master of Science
at the Delft University of Technology,
to be defended publicly on Thursday June 8, 2023 at 10:00 AM.

Student number:	4205286	
Project duration:	July 4, 2022 – June 8, 2023	
Thesis committee:	Prof. dr. ir. A. Cabboi,	TU Delft, supervisor
	Ir. E. Sulollari,	TU Delft
	Dr. ir. A. Grammatikopoulos,	TU Delft
	Dr. ir. J. Breukels,	Allseas Group S.A.

This thesis is confidential and cannot be made public until June 8, 2025.

TU Delft

Abstract

In this thesis, the friction performance of polyurethane tensioner pads used in offshore pipe-laying was investigated. Tensioner pads are used in pipe-lay to create tension in a pipe. The need to understand the pads better is because of the increased use of pipe coatings and pipe lay in deeper waters. Deep water leads to more pipe tension, and polymeric coating reduces friction.

A literature review was conducted on the friction of polyurethane. From the literature review, a few variables that influence polyurethane friction behaviour were summarised into the following research question: What is the influence of normal force on the pads, pad hardness, pad geometry, and pad temperature on the friction performance of polyurethane tensioner pads?

Experiments were performed at a full-scale setup. Polyurethane has a nonlinear coefficient of friction, making it difficult to upscale results from laboratory testing. In the full-scale setup, existing pads can be tested to find the influence of the different variables from the research question. The test setup was found to be flawed. Not only did it deform due to the massive forces, but the data gathered from the hydraulic pressures was not robust and accurate enough to estimate the static coefficient of friction, which is important in tensioners. Therefore, only trends in the pad behaviour were observed.

Increased normal force on the pads was found to increase the coefficient of friction. This contradicted the literature but was likely due to the geometry of flat pads versus round pipes, where the contact surface increased when the pads were loaded. Softer pads were found to yield higher friction than pads made from harder grades of polyurethane. This effect was also found in the literature. The influence of temperature was difficult to test. Since the pads could only be heated externally before testing, temperatures were inconsistent, and test results were inaccurate. The temperature did affect the friction significantly, though, so some newly produced pads were fitted with internal heating.

Next to the experiments, different pad geometries were tested in finite element analysis. A new pad shape was found that decreased stresses, leading to higher friction.

Next to the variables of the polyurethane itself, the relative humidity was recorded. The relative humidity changed significantly during the different tests, and it was found to affect friction more than anticipated.

Three sets of new pads were produced for future testing to validate the influence of geometry and further investigate the influence of the pad temperature. Moreover, a new test setup was designed to test the coefficient of friction more accurately.

Contents

1 Introduction

1.1. Background information

Friction has been used to people's benefit for thousands of years. Fires were likely started using friction from the middle stone age at least 30,000 years ago, and reportedly the early Egyptians even used lubrication to reduce friction to pull sledges with statues around 1880 BC [10]. Since then, many applications of using friction to mankind's advantage can be named. Evidence of systematic research into friction though is more recent.

Great thinkers like Hero, da Vinci, Hooke, Newton, Euler, and Coulomb all considered friction. Still, a complete description of its fundamental causes and a single quantitative model—generally applicable to any frictional situation— remains elusive [6].

The first two laws of friction, usually attributed to the Frenchman Guillaume Amontons (1699), are as follows:
1. The force of friction is directly proportional to the applied load.
2. The force of friction is independent of the apparent area of contact

Despite Amontons' association with these two fundamental "laws," the concepts attributed to him are paralleled in the detailed explanations in Leonardo da Vinci's earlier studies (1452–1519) [6].

There is a misconception in engineering that the coefficient of friction, the dimensionless scalar used to express friction, is a material property. Friction is a system property, meaning it is dependent on all components involved. Since there is an almost infinite number of systems containing friction, it is a very broad topic. For example, the amount of known materials that can interact with each other in friction is significant. Moreover, the COF is not only dependent on two materials making contact. If contaminants, like water or grease, are introduced between the contact surfaces, the COF could change significantly. The COF depends on many more parameters besides contaminants, some of which will be included in this report.

In some cases, the COF can be predicted accurately, primarily in cases of moderate loads on stiff solid materials like metals. Difficulties in predicting COF stem from contact with very small or very large normal loads. Another example where predicting the COF can be problematic is with very small or very large sliding velocities. The movement of tectonic plates is an example of low sliding velocity combined with extremely high loads. The movement of these plates cannot be represented by a COF.

1.2. Problem statement

The subject matter of this study is the friction between offshore pipe-lay vessels and the pipes they install on the seabed. Findings are mainly based on and related to the ship Pioneering Spirit, or PS in short. If essential factors are found regarding increasing friction, which lead to changes in offshore pipe-laying on the PS, these changes are likely to be transferable to other pipe-laying vessels. First, an introduction to offshore pipe-lay is given to understand the subject matter better.

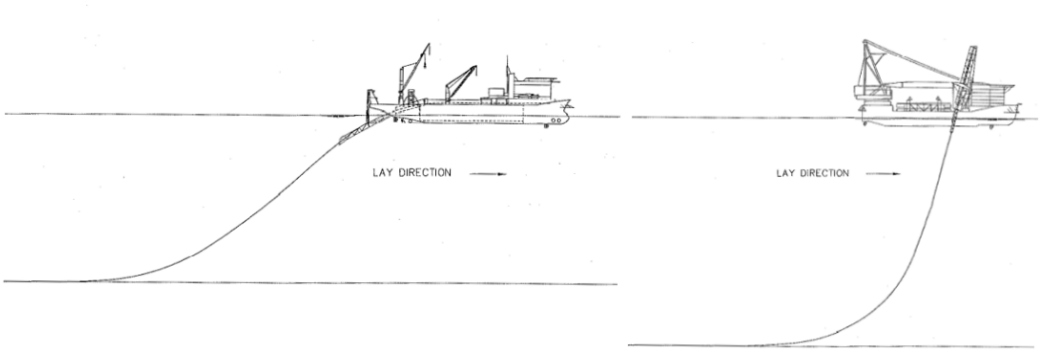

Figure 1.1: On the left, the S-lay pipe-laying method is shown. On the right, the J-lay method is shown.

There are two types of pipe-laying techniques. There is the S-lay method and the J-lay method, both seen in figure 1.1. The naming of the methods comes from the shape that the pipe makes during the pipe-laying process. Both methods have their advantages and disadvantages, which will be discussed in the following paragraphs. There are also some similarities between both methods of pipe-lay. For both methods, pipes arrive at the pipe-laying vessel in relatively small pieces. To make a continuous pipe, the small pieces must be welded together on the ship. Since the steel thickness of the pipe is typically more than 15mm, there are multiple passes of welds required. For example, the Nord Stream 2 pipes needed more than ten weld passes because of their steel wall thickness. After welding, the weld must pass inspection by either echo or x-ray. To prevent corrosion of the steel and the fresh welds, the pipe joints are then coated before the pipe can be lowered to the sea floor. In figure 1.2 an example of a welding station is given.

Figure 1.2: Example of a welding station on an S-lay type pipe-laying vessel from Allseas.

For the S-lay method, the main advantage is that the pipe is produced horizontally in the ship. This means that depending on the ship's length, it is possible to have many stations, like the aforementioned welding stations, to produce the pipe as quickly as possible. This is illustrated in figure 1.3, where it can be seen that thanks to the horizontal S-lay configuration, there is enough space for eight stations. The more stations the ship has, the less work has to be done on the pipe per station and the production rate goes up. One of the main disadvantages of the S-lay method is that the pipe has two bends from the ship to the seabed. To prevent the pipe from buckling, the bend from the ship towards the seabed has to be supported by a large steel structure at the bow or stern of the ship called the stinger. The stinger that guides the pipe to the seabed can be seen at the stern of the ship shown in figure 1.3. The radius of the stinger is typically too small for the pipe to bend elastically over, so it deforms plastically. Because of this plastic deformation, it is possible that in bad weather, the pipe has to be sealed and lowered onto the seabed to avoid fatigue damage.

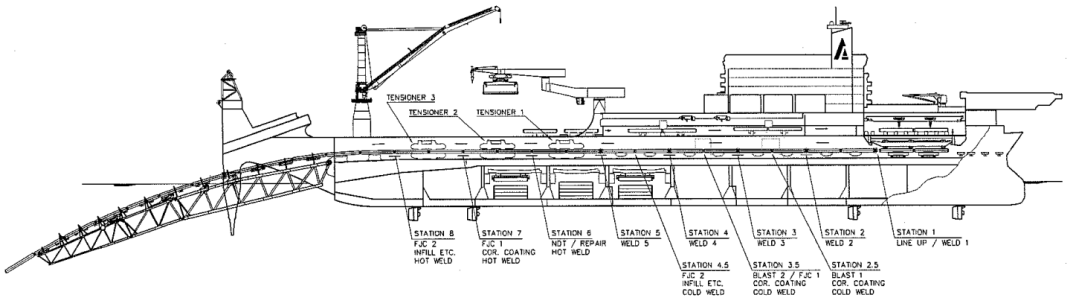

Figure 1.3: Schematic representation of different stations onboard Allseas' vessel Solitaire.

For J-lay, the main advantage is that it is very suitable to lay pipes in large water depths. Fatigue of the pipe in production is less of a problem since the pipe is only plastically deformed at the seabed. The main disadvantage is that because of the near-vertical production method, it is not possible to have as many stations to perform the necessary activities. This could require multiple activities to be performed at the same station, which slows down the production rate.

Regardless of the production method, either S-lay or J-lay, the pipe must be gripped on the ship to prevent slipping and loss of the pipe. Since the ship in question uses the S-lay method, from this point on, this report will fully focus on the S-lay production method. Much of the theory and results could be used for other purposes though.

The pipes produced in offshore pipe-lay are always heavier than the water surrounding them. This prevents the pipe from floating to the surface and interfering with shipping. Pipes are made from steel which has a high density. Still, larger diameter pipes may still need a concrete weight coating to prevent them from floating to the surface. Because the pipe is always heavier than the water surrounding it, there is always tension in the pipe during pipe-laying. To counter this tension in the pipe, the pipe is gripped on the ship. The tension in the pipe is even intentionally increased to prevent the pipe from buckling on the seabed, as was shown in figure 1.1.

To counter the tension in the pipe and to keep hold of it on the ship, large track-like machines called tensioners, as seen in figure 1.4, are used. It is recommended to maximize the friction between the tensioner tracks and the pipe, so the amount of tension needed to prevent pipe loss or buckling can always be provided. To provide the large amount of friction that is required, polyurethane tensioner pads are mounted on the tracks of the tensioners. These polyurethane pads then provide the grip on the pipe.

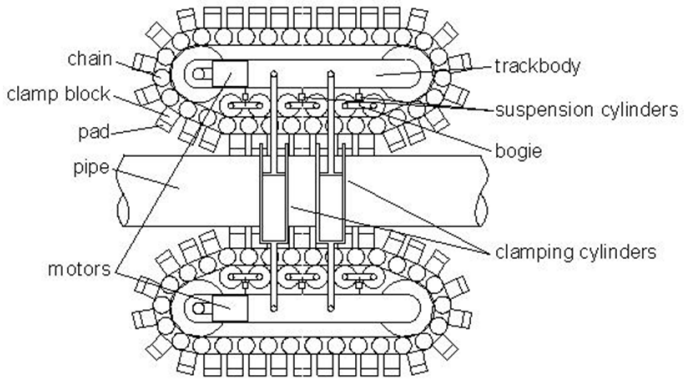

Figure 1.4: Schematic of a tensioner used in S-lay configuration.

Pipe-laying ships that use the S-lay method generally have 2-4 tensioners. These tensioners are in line with the pipe, so their number depends on the size of the vessel. The amount of tension a ship

can produce depends on the number of tensioners and their capacities. The tension capacity in turn, directly affects the water depth the ship can operate and lay pipes in. As mentioned before, the main focus of this research is the Pioneering Spirit. This vessel has four tensioners with a capacity of 500 metric tonnes each. Theoretically, it can provide 2000 metric tonnes of tension force, enough to lay large pipes in thousands of meters of water depth. In practice, the maximum tension the tensioners can provide is not reached. It should be noted that when the coefficient of friction between the pipe and the tensioner pads is too low, this capacity cannot even be reached.

There are different ways to increase the tension capacity of a vessel. One way would be to increase the number of tensioners or the tensioner track length and, therefore, the number of pads in contact with the pipe. This is not convenient in existing ships or could be a costly affair. Moreover, often there is not enough space to place more or larger tensioners. Another option is to increase the clamping force of the tensioner since the friction force is dependent on normal force. In this case, it is necessary to study the relationship between normal force and friction force, or in other words, the coefficient of friction, of the tensioner pads. The last way discussed here is to change the interface between the tensioners and the pipe. In other words, to change either the tensioner pads or the pipe coating. Since the pipe coating differs from project to project and is chosen by the client, it is easier to change the tensioner pads. The aim of this research is to improve the understanding of polyurethane tensioner pads and the influence that they have on the coefficient of friction of the system. Then, with this improved understanding, to try to increase the friction of the system.

In normal conditions, there is a surplus of tension capacity. There are some scenarios where more tension is required or where the capacity of the vessel is reduced. A few examples will be given. When sea states are rougher and the pipe-laying ship moves more, the inertia difference between the pipe and the ship will need to be compensated, especially in deep water. Another example is a wet buckle. A wet buckle is when a pipe buckles beneath the water line and is flooded with water. This changes the weight of the pipe, which is normally filled with air, drastically, thus increasing the tension in the pipe.

Figure 1.5: Example of inline structures during pipe-laying operations from Smit [20]

The tension capacity of the ship can be reduced in several ways. Pipelines are not necessarily simple round tubes that one can lay endlessly. Different pieces of equipment can be installed between the pipe sections called inline structures. These inline structures can have numerous functions, from valves to structures where other pipelines can be tied in. Figure 1.5 shows some inline structures for reference. These inline structures cannot pass through the tensioners in normal operation. The tensioners are therefore opened up by moving the tracks of the tensioner up and down, away from the pipe. Since this tensioner is now not gripping the pipe, all tension must be counteracted by the remaining tensioners in contact with the pipe.

The tension capacity of a ship is also reduced when the pipe must be pulled back in. This happens, for instance, in abandonment and recovery operations. When the sea is so rough that it cannot be

operated in anymore, the pipe can be plugged and lowered to the seafloor to avoid fatigue damage of the pipe from the movements of the ship. When the pipe is pulled back in to work on it again, it is wet and possibly contaminated with sediment from the seafloor. In previous slip testing by Allseas, it is found that water and/ or contaminants reduce the coefficient of friction of the pads on the pipe and, therefore, the total tension capacity of the ship.

Another factor of possible influence on the tension capacity of the ship is human error. A tensioner may be accidentally opened up due to miscommunication. Human error can also be coupled with inline structures. When inline structures pass through the tensioners, it is important that once an inline structure passes a tensioner, it is closed before the next tensioner is opened.

As stated before, under normal conditions, there is a surplus of tension capacity to account for most of the scenarios previously described. It could however happen that some of the scenarios take place simultaneously. This could lead to the pipe slipping in the tensioners, which causes a dangerous situation. When the grip is lost on the pipe, it is likely to slip from the ship and be lost completely. This is dangerous since the stations where people work on the pipe are all connected to the pipe to compensate for any ship motions. When the pipe slips out, it takes the stations with it until they reach their bump stops. The worst situation would be where grip is lost while there is an inline structure on the pipe since it will slam the tensioners and/or all other stations in its way with great force.

In conclusion, there is a high likelihood of losing grip on a pipe if multiple of the following events happen simultaneously:
- Rough sea states causing the ship to move more against the inertia of the pipe
- A wet buckle, increasing the weight of the pipe
- A pipe pull-in, where the pipe is covered wet and possibly covered in slick sediment
- Inline structures present in the pipeline, leaving fewer tensioners in operation
- Human error, accidentally opening one or more tensioners

Current tensioner pads are made from polyurethane, a material discovered in the 1930s by Otto Bayer and his coworkers [19]. This material is used because of its excellent load-bearing characteristics. Since the clamp forces in tensioners are in the order of hundreds, if not thousands of metric tonnes or tens of meganewtons, it is important to have a material that can withstand these compressive forces. Polyurethane is one of the few materials that can handle these forces well, as well as having a relatively large coefficient of friction against other materials.

The need for a better understanding of the polyurethane pads and with that, increasing friction is relatively new. It is somewhat connected to the exhaustion of large fossil fuel reserves but also to pipe-laying in deeper waters. Though mankind its need for fossil fuels is in decline, and a shift towards more renewable sources of energy is in place, there is still a large amount of fossil fuel needed in the coming decades. New fields are continuously taken into production, as the lifetime of fossil fuel fields is not infinite. Large oil/gas fields are discovered less frequently nowadays, creating the need to exploit smaller fields at harder-to-reach places. This increases the level of engineering required in the construction of pipelines. Nowadays, more effort is put into finding optimal pipe diameters and insulation for different pipes to different fields. Because fields are smaller and production rates are reduced, the need for large-diameter pipelines is declining, and the need for smaller pipelines is rising. This has an impact because large pipelines often have a concrete weight coating to keep them from floating up from the seabed. Rough concrete weight coating offers plenty of grip in combination with polyurethane pads, which negates the need for a better understanding of the polyurethane tensioner pad behaviour.

Smaller pipelines generally do not need a concrete weight coating because their diameter-to-wall thickness ratio (d/t ratio) is smaller. The steel wall then offers enough gravitational force to counter the buoyancy of the gas or oil flowing through the pipe. Pipelines sometimes need insulation too, when the fluids or gasses flowing through them have a large percentage of paraffin wax. The paraffin wax could potentially solidify and clot the pipeline when cooled down. An insulation layer can be added to the pipe to avoid the gas or oil from cooling down. Since there is no need for concrete but still a need for a coating to prevent oxidation and sometimes insulation, other materials are used to coat offshore pipes.

Figure 1.6: Example of concrete weight coating with a field joint of smooth polymeric material

Coating materials used nowadays are, for instance: three-layer polypropylene coating (3LPP), three-layer polyethylene coating (3LPE), and fusion-bonded epoxy coating (FBE). These polymer coatings are much smoother than the concrete weight coatings and, therefore, harder to get enough traction on. Figure 1.6 shows the difference between a smooth coated layer and a concrete weight coating. Getting enough traction on these new coatings requires more clamping force, but due to some factors, more clamping force does not necessarily mean more traction on the pipe.

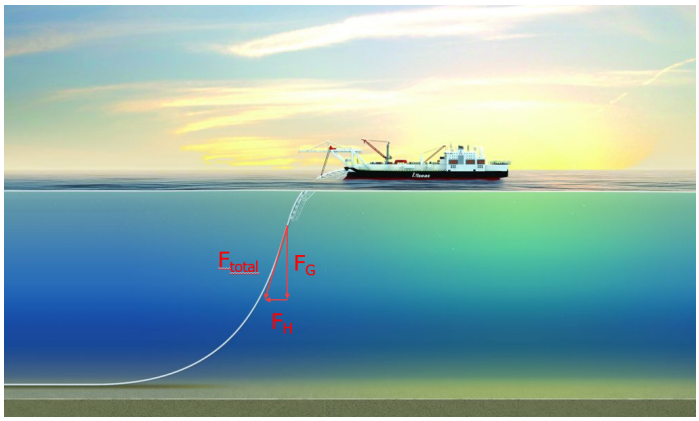

Figure 1.7: Example of forces while laying pipe in deep water.

The second reason for the need for increased friction between polyurethane pads and pipes is that pipelines are installed in increasingly deeper waters. When laying pipe in deeper waters, the span from ship to seabed is larger, and the tension in the pipe is larger. When the water is deeper, the pipe spans longer in the vertical direction. Since this pipe is designed to sink to the seabed, the longer the vertical span of the pipe, the larger the gravitational force on the pipe and the larger the tension. This is shown in figure 1.7 where the vertical force is depicted as F_G. A horizontal part in tension is also needed to avoid a buckle on the bottom part of the s-shape of the pipe. In the figure, this is depicted as F_H. The horizontal force is kept relatively constant independent of the water depth.

1.3. Research goal

The aim of this research is to find and understand what influence the hardness, geometry, and temperature of the pads have in the frictional behaviour between polyurethane tensioner pads and pipes used for offshore pipe-laying. Besides this, the influence of normal force on the pads and the influence of ambient temperature and relative humidity will be studied. By understanding the behaviour of the interface between pipe and pads, it is possible to tweak the parameters of the system in such a way

that the friction can be increased. This will improve the safety of all personnel working in the firing line by decreasing the risk of pipe slip.

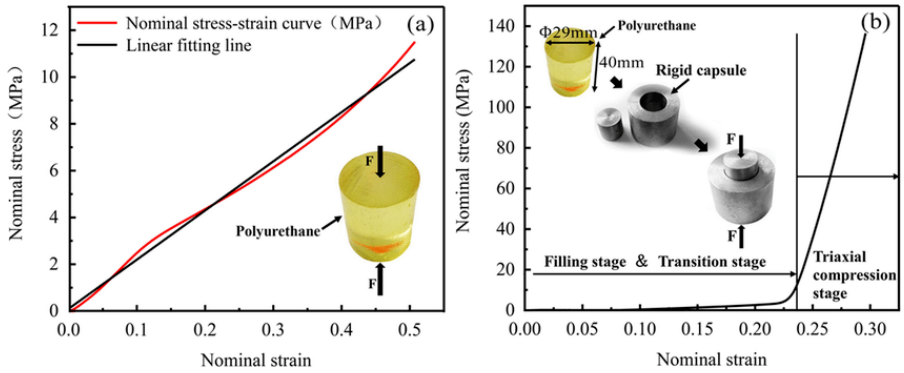

Figure 1.8: Nominal stress/strain behaviour of polyurethane that is, on the left: free to bulge out, and on the right: polyurethane that is enclosed. Image from Xie [23].

What is known is that polyurethane shows nonlinear behaviour in compression [23], as shown in figure 1.8. The reason for this nonlinear behaviour and how we can reduce its effects in tensioner pads is not clear. It must be researched to find if the nonlinear behaviour in compression leads to a nonlinear friction law for tensioner pads.

Friction research into polyurethane is mostly done with pin-on-disk tribometers or sled devices. These devices compress the material, which leads to pressure in the polyurethane. In most research, the pressures do not come close to the pressures in the polyurethane material in tensioners. For instance, the research from [8] is conducted on a sledge device to measure the static coefficient of friction. The pressures in the material range between 0.2-0.8 MPa, where pressures in the tensioner pads can exceed 10 MPa. It is possible to predict behaviour by extrapolating current results, but because of the nonlinear nature of compression of the material, predictions are tricky.

1.4. Research question

To answer the research goal, a main research question is formulated. This question is then divided into smaller parts, which will be answered separately.

Main research question:
What is the influence of normal force on the pads, pad hardness, pad geometry, and pad temperature on the friction performance of polyurethane tensioner pads?

Next to the research question influence of the ambient temperature and relative humidity on friction performance will be monitored. These ambient values are not thoroughly researched since they cannot be controlled in the current test setup.

1.5. Methodology

The methodology of this project is shown in figure 1.9. First, past research into the subject will be reviewed. This will create a rough understanding of the material behaviour and the influence of multiple parameters. At the same time as the literature review, a design is made to adapt the test rig. The test rig is a large machine at the Allseas yard in Heijningen, where full-scale tensioner pads can be tested. The adaptation design has to be made early because of the lead time of the one-off components.

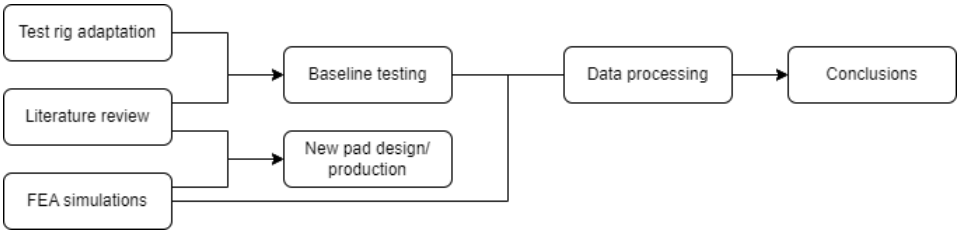

Figure 1.9: Overview of project scope

After part of the literature review is done and the components for the test rig are machined, the test rig is adapted, and experiments can be performed to answer the research question. During baseline testing, Finite Element Analysis (FEA) simulations are performed. In these simulations, some experiments in Heijningen are replicated. By replicating the experiments in FEA, pad behaviour can be compared to see if the deformation of the pads in FEA roughly matches the deformation of the pads observed in testing. Then, new pads can be designed and tested in FEA. After simulations indicate lower contact stresses for the new pads, the design is finalised, and pads are ordered.

After the baseline testing is finished, the data is processed and ordered. Finally, from the data of both the FEA simulations and baseline testing, conclusions can be drawn.

2

Literature about polyurethane and friction

This chapter will provide some background information about polyurethane and its influences on frictional behaviour. First, an explanation is given about what polyurethane is exactly. After that, a brief introduction is given about the coefficient of friction, or COF in short, and how it is found. After this introduction, the four parameters of the research question are discussed further.

2.1. Introduction to polyurethane and friction

2.1.1. Material composition

Polyurethane is not one particular material but rather a large family of materials with only one condition they must adhere to: polyurethanes must contain a urethane group in the molecular chain with some frequency. What the former exactly means will be explained in the next paragraph.

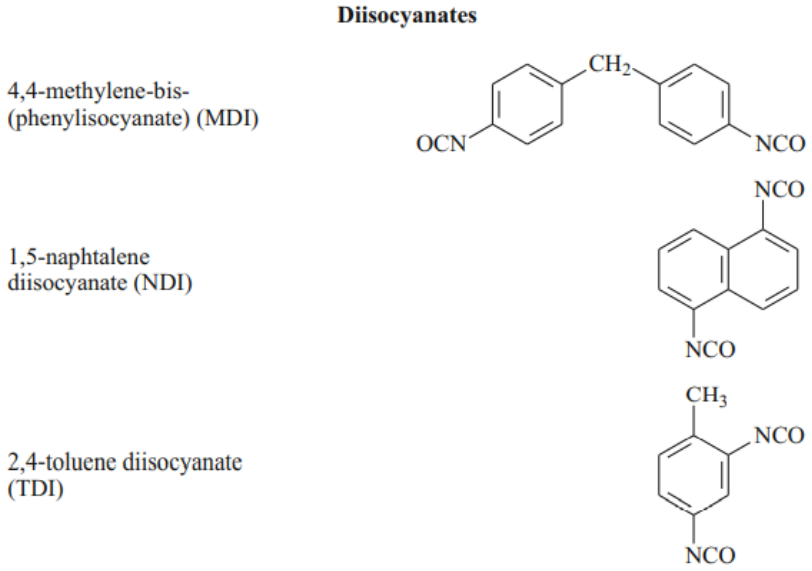

Figure 2.1: Examples of commonly used diisocyanates from Prisacariu [16]

Polyurethanes are produced by a polyaddition reaction between a diisocyanate with a polyol. Instead of a diisocyanate, a polymeric isocyanate can also be used. A few examples of the molecular forms of the diisocyanates can be found in figure 2.1. The polyol, also known as a long-chain diol or macro diol,

is generally a polyester or polyether. This will produce a long chain with urethane groups (-NHCO-O-) in some frequency. Because of the chemical incompatibility between the polyols and diisocyanates, the chain is divided into hard and soft segments like in figure 2.2. The ratio of hard segments to soft segments depends on multiple parameters such as the diisocyanates, polyols, chain extenders, and production process and reaction conditions [16]. As shown in figure 2.2, the chain length can be increased with so-called chain extenders.

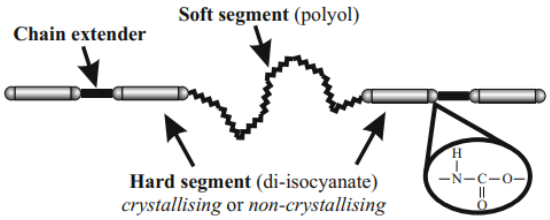

Figure 2.2: Polyurethane chain with hard and soft segments from Prisacariu [16]. Encircled is one of the urethane groups.

The reaction of the two chemicals can be enhanced with suitable additives and can be sped up with catalysts. The amount of different chemicals that can be used in different ratios promises an almost infinite number of different substances that are called polyurethanes. As mentioned before, the only condition to call a material polyurethane is the more or less frequent appearance of the urethane group depicted in figure 2.2.

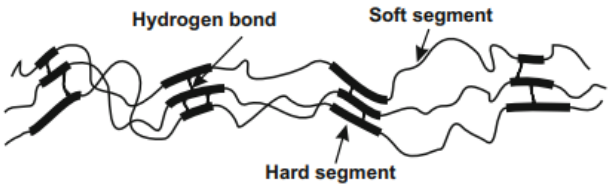

Figure 2.3: Multiple polyurethane chains with hydrogen bonding from Prisacariu [16]

There are two types of two categories of polyurethanes: namely thermoplastic polyurethane (TPU) and polyurethane elastomers (PU). The difference between the two is hydrogen bonding between the urethane groups. Whereas the TPU has no crosslinking between the urethane groups, the PU does have crosslinking like in figure 2.3. The hydrogen crosslinking influences the strength of the polyurethane elastomer.

It should be taken into account that chains are not necessarily as orderly as in figure 2.3. Often materials are not mixed fully, and chains vary in length. The production process, mixing, and other reaction conditions also influence the chains. After the polyurethane is produced, a choice can be made to anneal the material to gain greater uniformity in the polymer network, making the hydrogen crosslinking stronger.

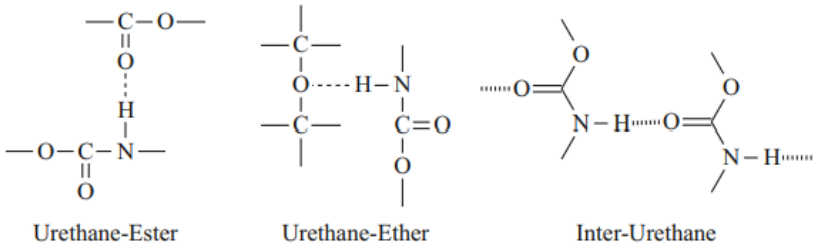

Figure 2.4: Hydrogen bonding interaction in polyurethanes from Prisacariu [16]

Hydrogen crosslinking is not the only factor in the strength of PU bonds [16]. There are also the ends of the PU chains. The ends of the PU chains can bond to hard segments in other chains. Examples of this are depicted in figure 2.4, where the rightmost figure shows the bonding between hard segments. The two left figures show the difference in the bonding of ester and ether polyols with hard segments. The difference between the two is the double bond of the oxygen atom. The hydrogen bonding of the ester polyol is much stronger than that of the ether. Therefore, polyester-based PUs have virtually no nonreactive ends as opposed to polyether-based PUs. This factor contributes substantially to the higher strength of polyester-based PUs.

There are advantages and drawbacks to both polyester and polyether PUs. Going into the exact differences between the two is beyond the scope of this report. The main thing to take away from the molecular structure of PUs is that the polyester ones are tougher, and the polyether ones perform better in humid conditions.

Since ageing is not part of the scope of this research, the breakdown of the chains due to humid conditions is not considered a problem. Therefore, the PUs of choice for tensioner pads are polyester PUs. From testing in the past by Allseas, the polyester PUs were also considered superior because of their load-bearing properties.

There is much more to say about the exact molecular formulas of the PUs. However, the exact formulas of the materials used for tensioner pads are unknown since the pads are bought and not developed and produced in-house. This means that it will not be possible in this report to try to break down friction phenomena to a molecular level.

2.1.2. Friction formulas

The well-known formula for (Coulomb) friction is:

$$\mu = F/N \tag{2.1}$$

Where F is the friction force, N is the normal force, and μ is the coefficient of friction as depicted in figure 2.5. There are two different kinds of friction coefficients μ. There is a static friction coefficient μ_s and a kinetic or sliding friction coefficient μ_k when an object is sliding. Generally, $\mu_s > \mu_k$, though in some cases, they are quite close.

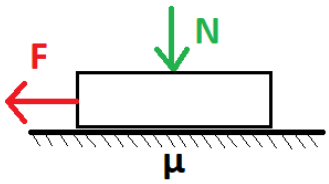

Figure 2.5: Graphic representation of friction formula.

Important to note is that the coefficient of friction is not a material property. While the materials do have a significant influence on the friction of a system, they do not encompass everything. The coefficient of friction is a system property dependent on the two materials in contact and possible lubrication in between. In fact, there are many factors that can influence the coefficient of friction.

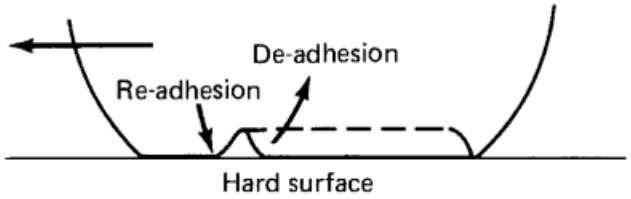

Figure 2.6: Schematic showing how a wave of detachment travels through the contact zone of a smooth rubber sliding over a smooth glass from Bhushan [5].

It is sometimes claimed that polyurethane does not even have a μ_s because the material is likely in movement when loaded. This is also observed in the testing of tensioner pads. The hyperelastic polyurethane is often partly losing grip and repositioning on the pipe without losing grip over the entire contact area. In this way, the polyurethane is slowly repositioning itself while the load in the slip direction increases. This effect has to do with the adhesion of the polyurethane on the surface and is also described as going in waves through the material. They were discovered by Schallamach in 1971 and are since known as waves of detachment, travelling from the front compression side to the rear at high speed [5]. A graphical representation of this is shown in figure 2.6.

For the sake of simplicity, the maximum coefficient of friction of systems will be called the static coefficient of friction μ_s. The kinetic or sliding COF will be named the kinetic COF μ_k. In the case of polyurethane tensioner pads, μ_k is not the most important value. Since the kinetic friction coefficient of polyurethane is smaller than that of the static coefficient, when the grip on the pipe is lost, it is not likely to return. In the best-case scenario, the pipe slides through the tensioners until a spot with more grip is found, while in the worst case, the pipe slips out of the tensioners into the sea, with all its consequences.

The static COF of polyurethane is around 0.2 for the harder grades to around 2-3 for the softest grades [11]. A large influence on friction is the contact surface area. The theory of Bowden & Tabor was the first to suggest that friction is not dependent on apparent contact area A_a, but rather on asperities and real contact area A_r. This will be further explained in section 2.2.

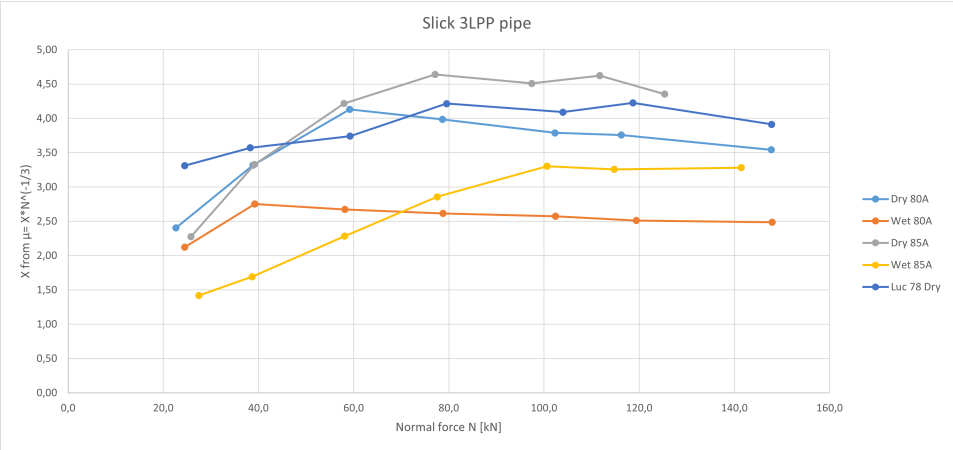

Figure 2.7: Results from friction testing at Allseas when using $\mu \propto F_n^{-1/3}$ for different three different PU hardnesses, and also tested under wet conditions. Plotted on the Y-axis is a variable named X, which encompasses all variables of the system. If the COF is perfectly predicted by $\mu \propto F_n^{-1/3}$, the variable X is a constant.

From Bhushan follows that when the normal force on the polyurethane pads is large enough, and the surface roughness is low, $A_r \sim A_a$ [5]. The polyurethane can be regarded as a single large asperity and $\mu \propto F_n^{-1/3}$. Previous slip test results from Allseas have been compared to this formula leading to figure 2.7. If the formula would fit the data perfectly, the line would be straight and horizontal. As can be seen, the formula does not fit the data perfectly. However, especially for the higher normal forces, where it is more likely that the $A_r \sim A_a$, the data presents fairly straight and horizontal lines. It should be noted that in the testing of figure 2.7, the flat pads were compressed against a round pipe with increasing force, which leads to a larger apparent area A_a. Due to the non-homogeneous distribution of pressure, it is not likely that a flat pad pressed against a round pipe can be regarded as simply a large single asperity. This is because the contact pressure at the sides of the contact patch is lower than that in the middle, meaning the pressure is not large enough for $A_r \sim A_a$. Material hardness, geometries, apparent area A_a, and likely other variables would have to be included in the formula of Bhushan in the case of a round pipe versus a flat pad.

2.1.3. Testing methods

Since it is hard to predict the coefficient of friction and to improve current formulas for polyurethane, testing is performed. Typically, scientific material testing is performed on a small scale, though this

might not always be the best choice. According to Blau [6], it is especially inadvisable to use values of polymer friction coefficients from small-scale experiments for the final design unless the test conditions were similar in nearly all aspects to those of the intended application. This is due to the nonlinear behaviour of polyurethane, which changes with every variable that is altered.

In the case of tensioner pads, for instance, the material bulges under compression. If one used a different geometry of material, this bulging on the sides could be different, the contact pressure could be different, and therefore the outcome of the small-scale experiment would be different. Scientific research on the application of polyurethane in tensioner pads is not widely available. Polyurethane is often used in situations where loads and, therefore, contact pressures are smaller than those found in tensioner pads.

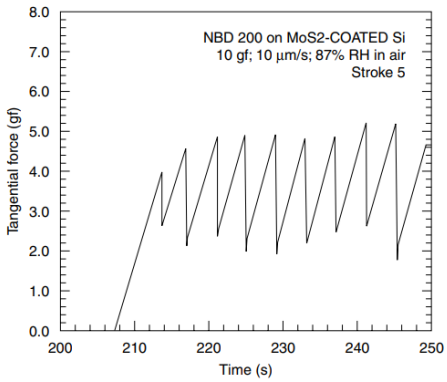

Figure 2.8: Stick-slip behaviour where the tangential force rises and is suddenly lost. This effect of sticking and rapidly slipping is repeated until one or more parameters of the system change. Figure from Blau [6]).

Most friction research found on polyurethane is about the kinetic COF. Commercial testing methods are widely available for kinetic friction. One reason could be that most testing is done for machinery, in which parts tend to move and experience kinetic friction. With this type of testing, lubricants can be applied to obtain low kinetic COF. This does not take away the need to know the static friction. When not using lubricants, it is important to know the difference between the static and kinetic COF. When this difference is large, stick-slip effects can occur. An example of stick-slip behaviour is shown in figure 2.8. Stick-slip behaviour, as its name suggests, is the effect when material first sticks due to the static COF. After the force becomes too large for the material to stick, it slips. Since the kinetic COF is much lower, it slips quickly until the material can regain traction and sticks with its static COF again. This process is repeated until some variable or multiple variables of the system change.

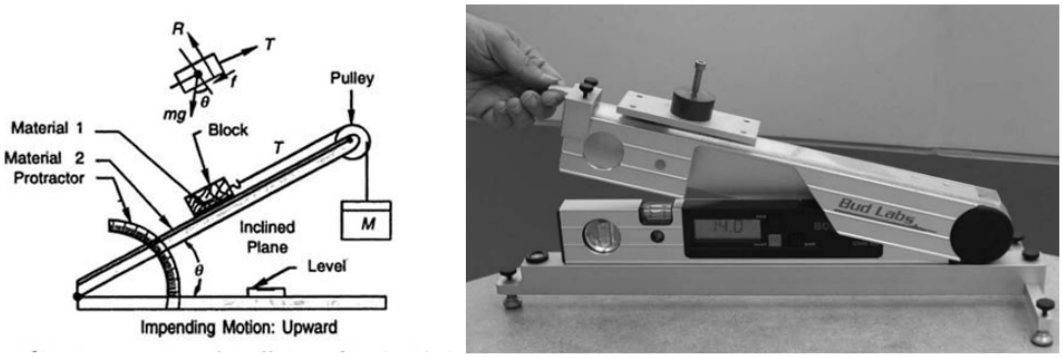

Figure 2.9: Schematic of inclined plane apparatus to test static friction and commercial apparatus [6])

For static friction testing, a very simple setup can be used to test the COF. The most simple test for static friction is the inclined plane apparatus from figure 2.9. This test is quickly reproducible and fairly accurate. One problem is that the normal forces on tension pads are in the order of tens of kilonewtons.

The large forces make static testing on an inclined plane apparatus impractical. The experiments could be scaled, but then it would be inadvisable again to use the exact numbers from the test for the true scale application.

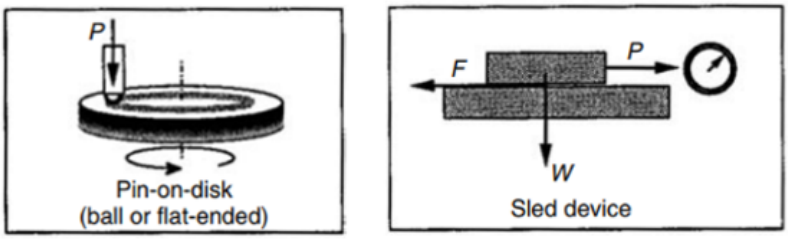

Figure 2.10: Schematics of commercially available sliding friction tests [6].

There are multiple testing methods for finding the kinetic friction coefficient. Research is often done with pin-on-disk tribometers, as seen in figure 2.10. In this test, a pin, usually made of steel, is pushed onto a disk of the material one wants to research. This disk of material spins around while testing, and the moment required to spin it is recorded. With the known force on the pin and its distance to the center of the disc, the sliding/ kinetic COF can be calculated.

There are a few reasons why the results from the pin-on-disk tests are not directly transferable to the case of tensioner pads. To simulate anything close to static friction, the spin speed of the disk should be very low. If, in this case, a steel pin is used on a polyurethane disk, the hysteresis effect, which will be elaborated on later, would play a large role in the deformation of the material and the friction. It is also possible to use a polyurethane pin to reduce the effect of hysteresis. The test would have to be performed on a steel disk. The disadvantage is that the results must still be scaled, which is inadvisable [6]. Moreover, the contact geometry of a round pin versus a flat plate is the exact opposite of the case of tensioner pads, where the nondeformable object is round, and the deformable polyurethane is flat. Most research published with pin-on-disk tribometers is concerned about kinetic friction or wear rather than static friction, and therefore out of the scope of this thesis.

The second manner of testing from figure 2.10 shows a device that tests a small piece of test material and forces it into a, usually steel again, surface. It is then pushed from side to side, and the force required to do so is recorded. This type of testing is more in line with the case of tensioner pads. The sled device can be used to test static friction, but generally, numbers for the kinetic friction are published using this method.

Exact values from kinetic friction tests are not suitable for research into tensioner pads since it would mean that a pipe slips, which should be prevented. Behavioural trends from kinetic friction tests can be used as guidance though. It is inadvisable to use values from any previous tests since it is highly likely that not all variables are similar.

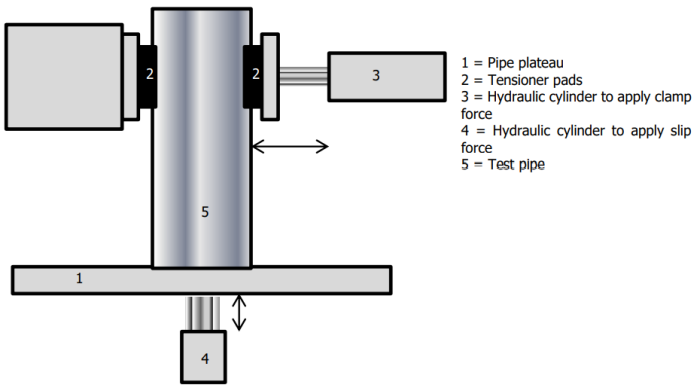

Figure 2.11: Schematic of slip test setup of Allseas.

To avoid inaccuracies due to scaling effects, Allseas has made a full-size testing machine to test their tensioner pads. In this test rig, one piece of the tensioner track, also known as a crosstie, is replicated. In figure 2.11, a schematic of the rig is shown. Tensioner pads are attached to the rig, and a test pipe is lowered into it by a crane. Then the hydraulic cylinder that produces the clamping force is actuated manually to the required hydraulic pressure. When this hydraulic pressure is reached, the second hydraulic cylinder is actuated. This cylinder pushes the pipe up to simulate pipe slip in the tensioners. From the hydraulic pressure data, a point is then chosen to represent static friction.

Figure 2.12: Slip test example to find the static coefficient of friction.

An example of the data log with the data plotted for clarity can be seen in figure 2.12. From the data log, the maximum hydraulic pressure of the upward-pushing cylinder can be extracted, illustrated in the figure with the red dotted lines with the μ_s on top. This value is believed to represent the point where static friction μ_s is lost, and the pipe starts slipping. From these tests, extracting the kinetic coefficient of friction μ_k is also possible. From the figure, it is clear that the hydraulic pressure stays quite constant during the slipping of the pipe, so in this case, a constant μ_k can be obtained.

Because of how the test setup works, pumping a constant hydraulic oil volume into the slip cylinder instead of gradually increasing hydraulic pressure usually causes the pipe to slip in the test rig. This slipping, however, does not mean the results are worthless. It is beneficial when the pipe starts slipping since the maximum value of the static coefficient of friction is not reached when the pipe does not slip. If the pipe does not slip, the exact μ_s is never reached, and it can only be estimated. Estimating this value is especially inconvenient because the pipe tends not to slip at the highest clamp forces the test rig can achieve. These clamp forces are most representative of the real tensioner forces. Therefore, if the pipe does not slip at the highest clamp forces, the real tensioner slip forces cannot be properly estimated. The upside of this is that when the pipe does not slip, the static coefficient of friction is always larger than when the pipe does slip, and the value is considered conservative.

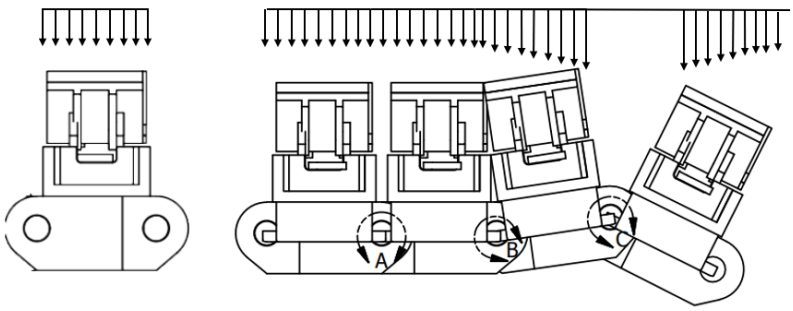

Figure 2.13: Distributed loads of the test rig on the left and a ship on the right.

There are advantages and disadvantages to the Allseas test rig. The major advantage is that full-scale tensioner pads and pipes can be used. This means no scaling effects have to be accounted for, and the results translate almost directly to the real tensioners. This means that the test bench is a valid way of testing different pad materials and geometries. It is also useful to test different pipe coatings to see which offers the most grip.

Another advantage of a full-scale test setup is that it is possible to test pads that have been used on ships for years. The effect of ageing of polyurethane, for example, can be tested, provided a baseline test was done with the pads when they were new.

There are also some downsides to testing with this test rig compared to a ship. One of them has to do with the fact that there is only one crosstie in the test rig, compared to dozens in the actual tensioners. A crosstie is a single piece of the track with the tensioner pads mounted on it. Because of the one crosstie that is unable to rotate in the test rig, the load in the pads is evenly distributed, as seen on the left in figure 2.13. In the tensioners on the ship, the crossties are part of a large chain, so they can rotate with respect to each other. In this case, the pressure on the pads is not necessarily evenly distributed since the crossties are not supported evenly by the rollers that support them. These rollers are hydraulically actuated, creating the clamping force between the tensioner and pipe. From figure 2.13, the load difference might not seem like a problem, but when considered in 3D, this means that the round pipe is pushed into the flat pad further, and the contact area increases significantly at the point of the highest pressure. The distributed load is elaborated on in chapter 4.

Another downside of the test rig is that testing is always performed statically, meaning the clamping and shear forces are constant. When the tensioners on the ship are activated, the tracks are not always stationary. This is because a ship is continuously subjected to wind and wave forces moving it. Especially the waves make the ship pitch and roll, leading to more or less tension in the pipe. These peaks in tension are softened by the tensioners that can pull the pipe in or let it loose. This creates a shear force in the pads that is not completely constant in time since the tensioners cannot react instantly to different conditions. Because the system is reacting to the conditions by reading the tension in the pipe, there is a small delay. This variation in the loading of the pads cannot easily be replicated in the test setup.

By far, the biggest downside of the full-scale setup is the instrumentation. Only the hydraulic pressures from the clamp and slip cylinders are logged in the test setup. More data is required to determine the static coefficient of friction accurately. Displacements should be accurately recorded, and instead of hydraulic pressures, load cells should be used to measure forces more accurately. Until the displacements and forces are measured, the test setup can only be used to make rough guesses about the kinetic coefficient of friction.

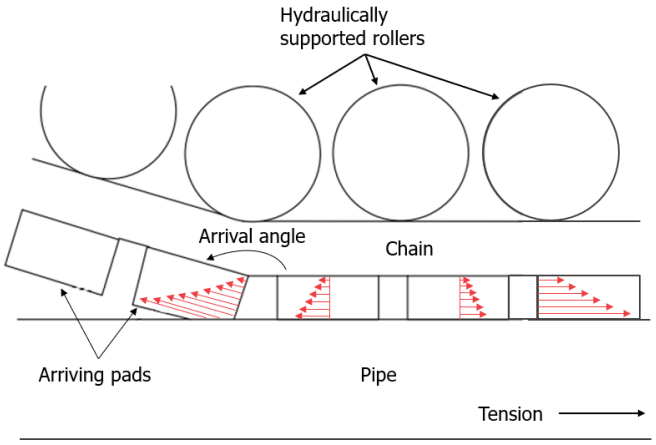

Figure 2.14: Arrival effect of pads with arrows indicating forces in the pads.

Another effect not translated from the tensioners to the test bench is one known at Allseas as the arrival effect. In the tensioners, every time the pads start to touch the pipe, they are subject to this

effect. The arrival effect, as shown in figure 2.14, owes its name to when the pad arrives at the pipe. When arriving at the pipe, it is always at an angle compared to the pipe. The chain of crossties with pads mounted on them should travel at the same speed as the pipe. However, since the pads have to rotate over the angle they come in at and they stick out a bit from the crosstie, their velocity is higher than that of the pipe. Because of this, the pads are sheared in the direction opposite to the direction of preference. The pads have to slip over the pipe for some distance in order to be sheared in the right direction to counter the tension in the pipe. In other words, the arrival effect has a detrimental effect on the overall tension capacity of a tensioner.

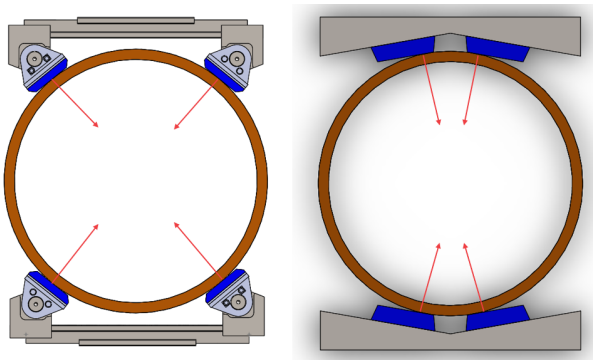

Figure 2.15: Difference in force distribution on a 40” pipe. On the left, the PS configuration. On the right, a more common configuration.

The arrival effect exists in many if not all, track-like tensioners, but it can be minimised in several ways. Most of these fixes have downsides as well. Firstly, the arrival angle can be minimised, but this would require either a longer tensioner or less travel for the hydraulic damping in the tensioners. It is also possible to reduce the height of the pads/pad holder combination. The disadvantage of this is when supporting larger pipe sizes; there is an increased chance of buckling the pipe in the tensioners since it is essentially clamped from the top and the bottom instead of from the sides. This effect is illustrated in figure 2.15 with a 40” pipe. This effect is increased when the pipe size is larger. There are more ways to reduce or even eliminate the arrival effect. The arrival effect is described in detail by Smit [20] and will not be further discussed in this report.

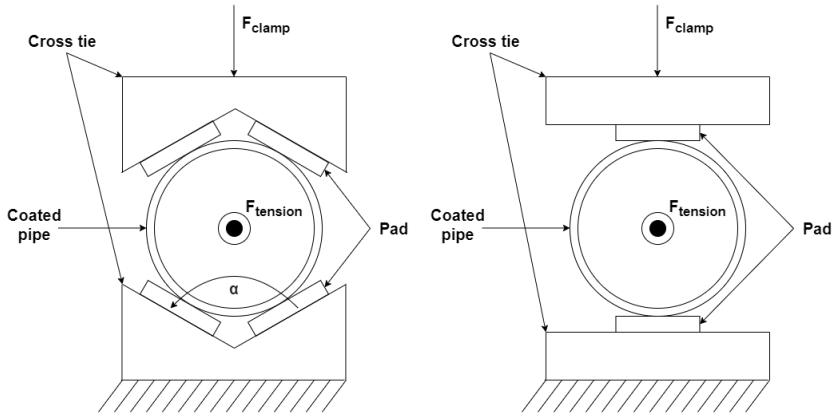

Figure 2.16: Slip test setup top view with left the setup with four pads, right the setup with two pads.

The last downside discussed in this report is that the clamp forces in the test rig do not fully approach the clamp forces of the tensioners. This problem can be solved partially by adjusting the test setup to use only two pads, as shown in figure 2.16 on the right. Using only two pads instead of four would almost double the normal force on the pads. At Allseas, every ship uses different tensioners and, therefore, different tensioner pads. The test rig currently can fit the pads of most ships. Tensioner pads are always placed some distance apart and at an angle on the crossties to reduce the circumferential

stress on the pipes, as in figure 2.16 on the left. The angle α of this is different for every ship, though this is not accounted for in the test rig, which has a fixed angle of 120 degrees.

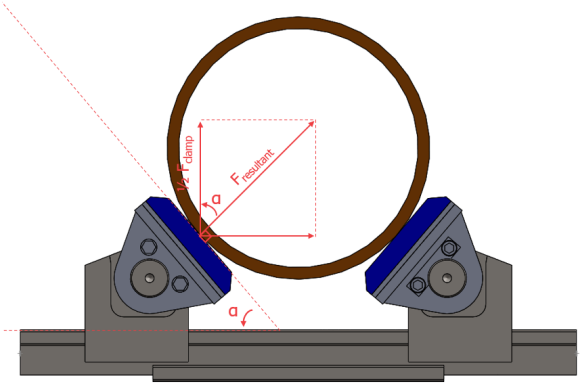

Figure 2.17: Force in swivelling pads broken down in components

The ship called the Pioneering Spirit that this report is primarily aimed at works in a different way. The angle α is not fixed in this case. Pads can swivel some degrees to position themselves at the most optimal angle to the pipe, as seen in figure 2.17. Not having a fixed angle reduces the forces not perpendicular to the tensioner pads. The figure shows that the resultant force, also known as normal force, is perfectly perpendicular to the pads, this is an important assumption, and it will be tested before other tests are performed.

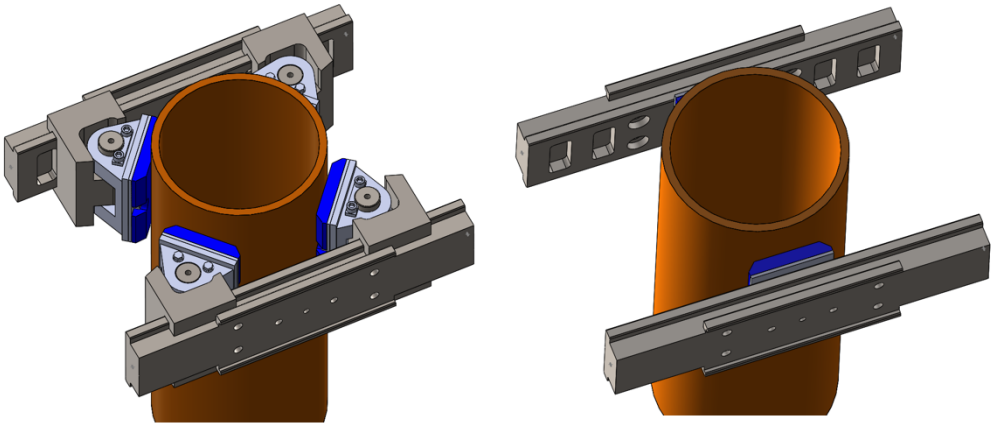

Figure 2.18: Two new setups with the new test crosstie that mimics the Pioneering Spirit tensioner setup

One way to counter the last disadvantage of the test setup not reaching the same forces as on the ship is to reduce the number of pads used in the setup from four to two, as mentioned before. The new crossties produced specifically for this project can mount just two pads instead of the four used normally. Using two pads means that the pads' normal forces will be perfectly perpendicular. To verify that the normal forces are perpendicular in normal operation, tests will be performed as mentioned above. The advantage of this system is that while not exactly doubled, the forces on the pads will increase significantly. With this two-pad setup, it is possible to exert forces on the pads comparable to the ones in normal operating conditions of the ship.

2.2. Normal force/ contact pressure

There are inconsistencies in which loading conditions are reported in the literature. Some researchers prefer to report the normal force or load, yet others prefer contact stress or contact pressure–velocity (PV) products. The PV product is a convenient metric for comparing the maximum load-carrying capacity of different polymeric bearing materials (i.e., PV limit). Sometimes, the apparent contact pressure (also called the nominal contact pressure) or the Hertzian elastic contact stress is reported. The apparent contact pressure is typically a macroscopic quantity: the applied load divided by the apparent contact area [6]. In this thesis, the normal force is used. The reason for using normal force instead of pressure is that the pressure could not be calculated due to an unknown contact surface area.

2.2.1. Asperity contact

Though equation 2.1 for Coulomb friction is correct for solids primarily, it is not as clear cut for elastomers like polyurethane. For elastomers or polymers, the coefficient of friction μ can depend on the normal force. When the contact pressure is high enough, the coefficient of friction decreases when the load/ normal force increases like $\mu \propto F_n^{-1/3}$ according to Maegawa [14]. The effect of decreasing COF for increasing normal force, and therefore contact pressure, can also be seen in previous friction testing performed by Allseas.

To understand why the coefficient of friction decreases when load increases, knowledge about asperities is required. When looking at materials at the micro-scale, it can be observed that they are never truly flat. At this scale, materials have small peaks of material called the asperity tips or peaks. As seen in figure 2.19, two contacting surfaces only touch at the asperity peaks. When the normal load on these surfaces increases, the asperities get deformed either elastically or plastically, creating the real contact area A_r that was briefly touched upon in section 2.1.2.

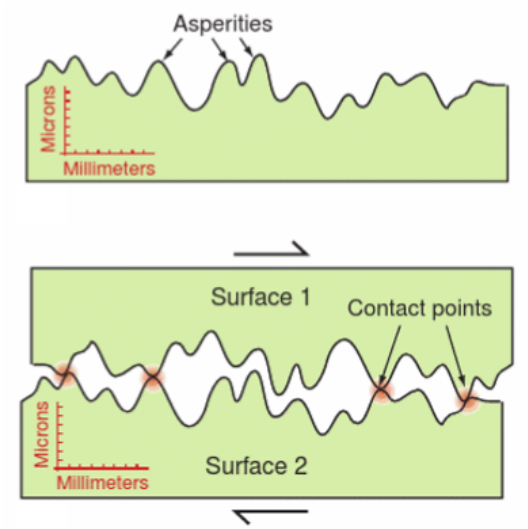

Figure 2.19: On top, the profile of a surface, magnified vertically. On the bottom, two surfaces in contact touching at asperities only. Figure from Ashby[2].

For solid materials like metals, the behaviour of asperities is predictable. By measuring the roughness of the material, the size and number of asperity peaks are known. In turn, it is then possible to predict when they will elastically or plastically deform depending on the material's yield strength. For polymers, this behaviour is hard to predict. Because polyurethanes are quite soft and incredibly resistant to strain, asperity peaks are not deforming plastically easily. When the normal force on the pads and contact pressure increases, the number of asperity peaks increases.

The main disadvantage of plastically deformed peaks is that material that broke off forms a layer between the polyurethane and its counterpart. This material prevents asperity peaks from reaching each other and works like a lubricant. It should be noted that some polymers create a boundary layer of lubricant by themselves when the material is compressed. For this reason, some polyurethanes can

be used in low-friction applications like implants.

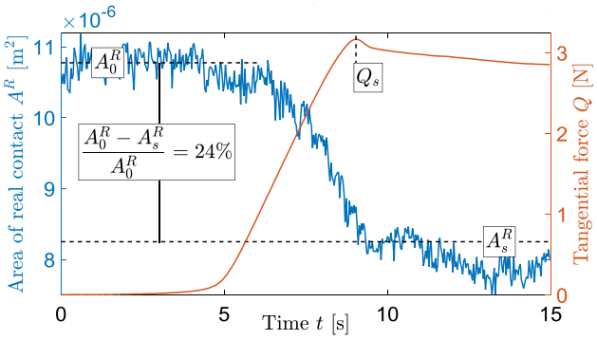

Figure 2.20: Evolution of A_r when the material is loaded in shear from Sahli [18].

Another part of asperity contact is creep, also known as geometric ageing of the polyurethane [18]. When the material is loaded for some time, the asperity contact, or real contact area A_r, seems to grow because the polyurethane is slowly deforming/settling under the load. In the research from Sahli, it seems that the creep effect is quickly lost when the material is loaded in shear, as shown in figure 2.20. The expectation is that softer materials are impacted more quickly by creep since they can deform more easily. If temperature influences hardness, it may also play an important role in the effect of creep.

Research has been done on kinetic sliding friction between a steel surface and a set of self-lubricating polymers by Quaglini [17]. In this article, the authors conclude that the real contact area A_r can equal the apparent contact area A_a at high contact pressure. This research is not directly comparable to the case of polyurethane since it was done on self-lubricating materials with a much higher hardness than that of polyurethane. However, the principle of the real contact area becoming as large as the apparent contact area does still apply. What can be stated is that in the case of flat tensioner pads versus a round pipe, the A_r will not equal A_a. Because of the geometry, the pressures in the middle of the pad will be larger, and A_r and A_a could be equal, but towards the sides, there is less contact pressure, and the apparent and real contact areas are no longer equal. More on this contact pressure distribution can be found in chapter 3.

An important factor in asperity contact is the surface roughness. The research of Jiang [13] found that for thermoplastic olefins, higher surface roughness leads to a lower surface coefficient of friction. The likely reason is that fewer asperities are in contact between the surfaces, leading to a smaller real contact area and, thus, lower COF. They also concluded that with increasing normal force, the friction levelled off for the different surface roughnesses tested. The levelling off might be because A_r approximates A_a, and asperity contact equalises.

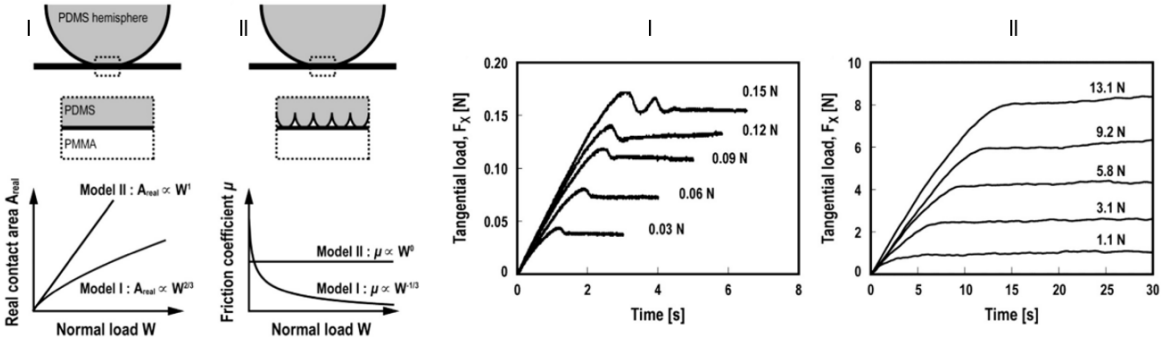

Figure 2.21: On the left, the relation between the experiments of Maegawa and the real contact area and COF, for I: a smooth hemisphere, and II: a rough hemisphere. On the right, time changes in tangential load F_x, on the left for a smooth polymer surface, and on the right for a rough polymer surface [14].

In the research of Maegawa [14], surface roughness is also tested. The setup tests smooth glass against a rough rubber, comparable to the case of polyurethane pads versus a smooth steel pipe. The results seem very similar to the experiments performed. Maegawa found two types of friction curves, shown in figure 2.21. The left curves are for a smooth polymer contact, where $A_r \sim A_a$. In this case, the friction followed the relationship of $\mu \propto F_n^{-1/3}$. In the right figure of 2.21, the rough contact relation was described by $\mu \propto F_n^0$.

2.2.2. Nonlinearity and impurities

It is clear that the behaviour of polyurethane is hard to predict. Ultimately the goal is to predict friction coefficients between polyurethane tensioner pads and different pipe coatings. These pipe coatings are often made of polypropylene, polyethylene or epoxy, aka polyepoxides. All those coatings are polymers and, therefore, behave nonlinearly in compression. It is hard to calculate how both polymers will interact with each other on a micro-scale, let alone to translate this to the macro scale. Moreover, most pipes have special rough coatings to try to improve the friction between pads and pipes. The coatings on these pipes are usually rough on a macro scale. One example of such a pipe would be where sand is blasted into the coating, leaving a rough surface. Deformation over these particles is large, and therefore plastic deformation is likely to occur, creating a lubrication layer between the pads and pipe, making predictions tricky.

Possible contaminants like water or grease can be tested on easily, while it might be harder to predict the effect of such impurities with friction models. Scratches or damaged coatings are not a rare occasion either, which means that predictions of COF from calculations are likely to be larger than in practice. Due to time constraints, this thesis is focused on the experimental side, and only simplified models for friction were developed.

2.2.3. Adhesion and deformation/ploughing

The main mechanisms that contribute to friction forces between polyurethane tensioner pads and pipes are adhesion and deformation. Adhesion is dependent on attractive molecular forces like van der Waal's forces. As mentioned in section 2.1.2, rubbery materials tend to show de-adhesion and re-adhesion behaviour in waves.

Deformation is an effect happening on both a macro and micro scale. On the micro-scale, it is the ploughing of the asperities. The asperities of the harder contacting material are ploughing through the softer material, dissipating energy and increasing friction.

The macro-scale deformation of rubbery materials leads to hysteresis losses. When the polyurethane is deformed, the material stores energy elastically. Not all energy is stored though. Some of the energy in deformation is dissipated as heat. This effect is called hysteresis. The dissipated energy increases friction. When the material is not loaded anymore, it will either fully or partly reform back to its original shape. When the material does not fully reform, the effect is known as residual strain. The effect of hysteresis was found to significantly affect friction during repeated testing.

Another example of macro-scale deformation is the deformation of the pads, leading to a larger contact area. Adhesion and deformation are very dependent on each other. When putting a shear force on a pad, the adhesive friction will deform the pad, for example. After the asperities then have deformed so much on the micro-scale that adhesion forces fail to hold on, the material will reorganise itself to close to its original state, allowing for re-adhesion, as was also shown in figure 2.6.

2.3. Hardness

2.3.1. Molecular difference

As mentioned in section 2.1, the hardness of polyurethane depends on the molecular formula of the material. Not only the ratio of soft segments to hard segments is important, but the crosslinking between the hard segments is so as well. Finally, the ends of the chains have an important role too. Where polyurethanes based on ethers do not have very reactive ends of the molecular chains, the polyurethanes based on esters react more, so they have a stronger bond.

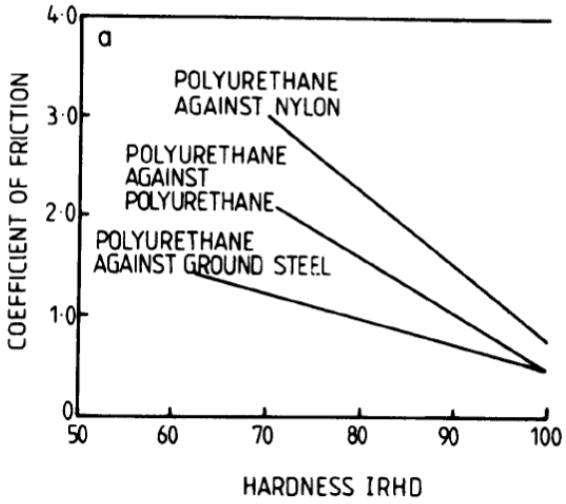

Figure 2.22: Relation between COF and hardness of polyurethanes on a chrome-plated brass surface with slip velocity of 2 cm/s. Figure from Wright [22].

There is a general thought that the softer the material is, the larger the coefficient of friction is. In his book Hepburn [11] even claims that the effect is linear like in figure 2.22. This is in disagreement with Allseas slip test research, where it is observed that sometimes harder materials have more grip than their softer counterparts, as shown in figure 2.23. There could be various factors that account for the observed differences. One of the explanations is that in the research of Wright [22], the normal force and, therefore, the contact pressure was very low. This trend is also seen in figure 2.23, where the softest material had the most grip at the lowest clamp force. It is, however, hard to claim that the effect is linear in this graph. Another explanation would be that the research from Wright [22] was published in 1969, and polyurethanes nowadays can have different coatings or different materials blended in to provide a better COF without necessarily impacting the hardness of the polyurethane. An example of incorporating different materials in the PU resin is shown in the research of Alberto [1], where graphene was used to alter the friction properties of PU without affecting hardness.

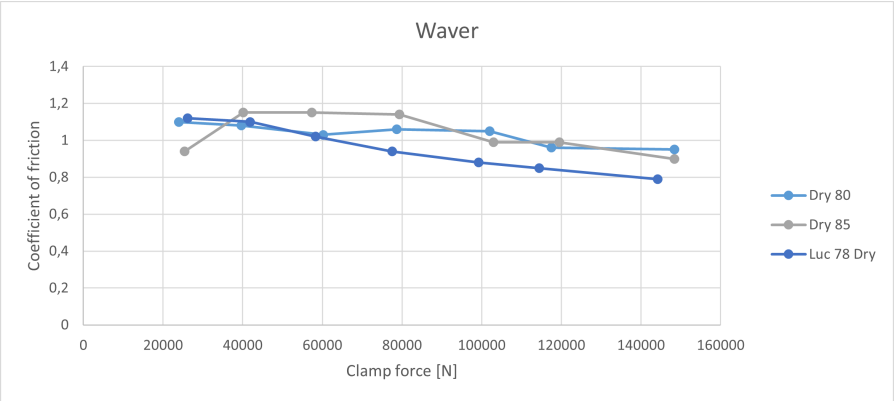

Figure 2.23: Relation between COF and normal force of materials with different hardness.

Another difference is that the research from Wright [22] in figure 2.22 is expressed against the hardness in International Rubber Hardness Degree (IRHD), while most other research regarding polyurethane is expressed in the Shore A or D hardness. Comparing the two testing methods is not useful since the testing methods differ [15]. Both testing methods compress the material locally with a durometer, a measuring device to measure hardness, but the geometry of the tips of the two durometers is different. The IRHD method uses a spherical durometer, whereas the Shore durometer has a truncated cone shape. The IRHD method even uses multiple tests for different hardnesses, which can differ by a fair margin compared to each other, see figure 2.24 on the left.

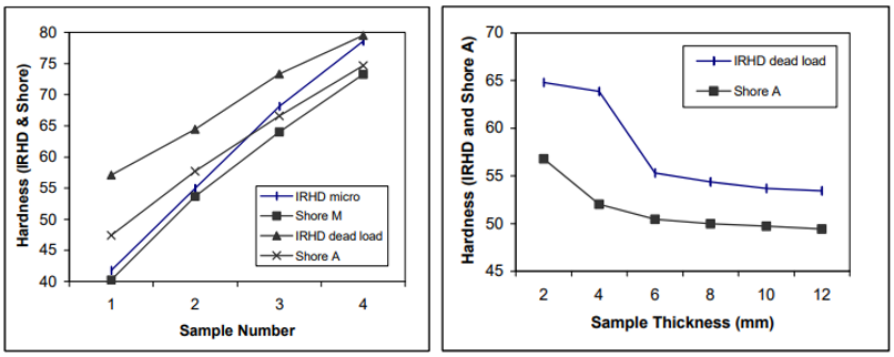

Figure 2.24: Shore A and IRHD testing compared. On the left, different methods on a 2mm thick sample are shown. The difference in hardness readings from Shore A and IRHD is depicted on the right. Figures from Morgans [15].

Another example of why the Shore and IRHD methods cannot be directly compared is because of the sample thickness. As shown in figure 2.24 on the right, the IRHD dead load test gives different results when measuring higher sample thicknesses compared to its regular 2-4mm sample thickness. This is because in higher sample thickness, the pressure in the material from the durometer is distributed more, and the perceived hardness is lower.

Though the reasons above explain why the Shore A and IRHD scales cannot be directly compared, it might be useful to provide a bit of a comparison between the two. The two scales are roughly similar to each other. They are at most of the range, around 5 points apart.

2.3.2. Tensile stress characteristics

Looking at figure 2.25, some observations can be made. At the lowest clamp force, the polyurethane with the lowest hardness seems to have the largest COF. For the softest material of Shore 78A hardness, the COF is roughly going down with increasing normal force. The material of Shore 80A that is a bit harder seems to have a peak at 60 kN normal force before the COF reduces with increasing normal force as well. The hardest polyurethane out of the three tested is the Shore 85A. This material shows a broader peak in its largest COF at a slightly larger normal force than the Shore 80A material.

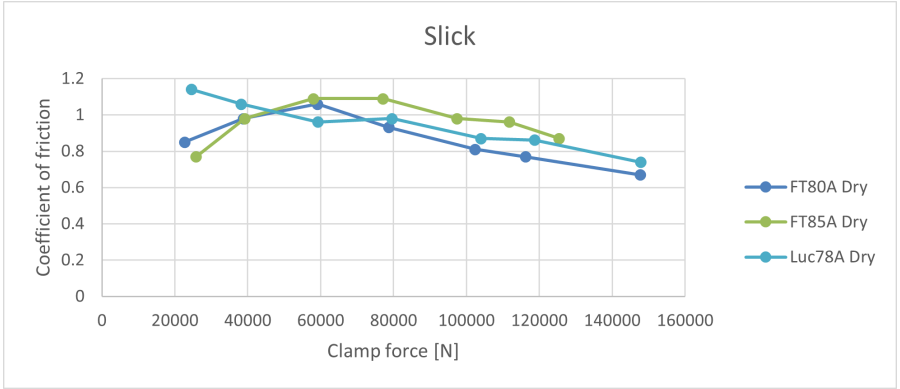

Figure 2.25: Relation between COF and normal force of materials with different hardness.

The differences of the materials in figure 2.25 can be explained by the difference in stress-strain curves for different hardness of materials. In figure 2.26, it is shown that the harder materials strain far less when subjected to the same tensile stress. For 10 Mpa of stress, the hardest Shore 85A material elongates around 135%, where the Shore 80A material is closer to 250% elongation, and the softest Shore 75A material is around 350% elongation.

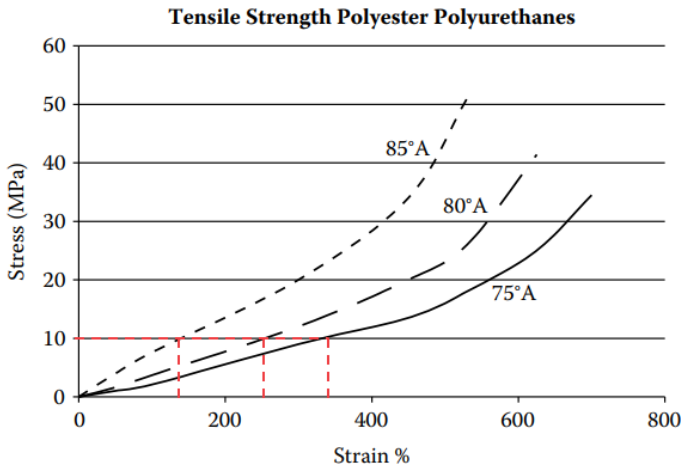

Figure 2.26: Stress-strain curves polyester polyurethanes of different hardnesses from Clemitson [9]

The broader peak for the hardest materials in figure 2.25, and this peak appearing at a larger normal force than its softer counterparts, can be explained by the surface area. The contact surface can increase significantly for softer materials, compared to harder materials at the same normal force. The peak is where the surface area is maximised for the softest materials. The pad only has a certain width, so there is a maximum surface area. After this maximum surface area is reached and the normal force still raises, the pressure in the material raises, which lowers the COF. The assumption, then, is that the whole surface of the pad is in contact with the pipe.

2.3.3. Compression stress characteristics

In the case of tensioner pads, the material is under compression and not in tension. In this case, the contact configuration is important. More information about the contact configuration can be found in section 2.4.

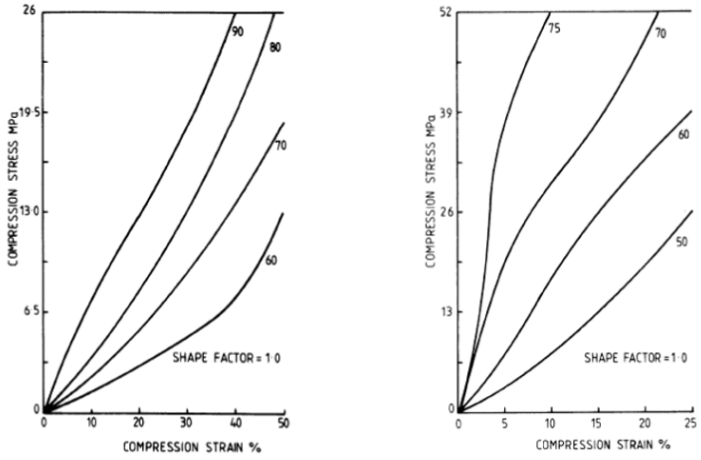

Figure 2.27: Compression-deflection characteristics of polyether urethane elastomers. On the left, elastomers from 60-90 IRHD hardness. On the right, elastomers from 50-75 Shore D hardness. Images from Wright [22].

Figure 2.27 shows that the harder the material is, the more it resists straining under compression. It

should be noted that, as before, no exact data can be used from the left figure because of the IRHD scale. That said, the figure does indicate a trend. The right figure expressed in the Shore D scale can be translated into the Shore A scale like in figure 2.28. The Shore D scale is used for harder materials than the Shore A scale. The only difference in the type of testing of the two is the type of durometer used. The Shore A tool uses a quite broad truncated cone shape, and the Shore D one uses a pointier shape, making it able to deform the harder materials.

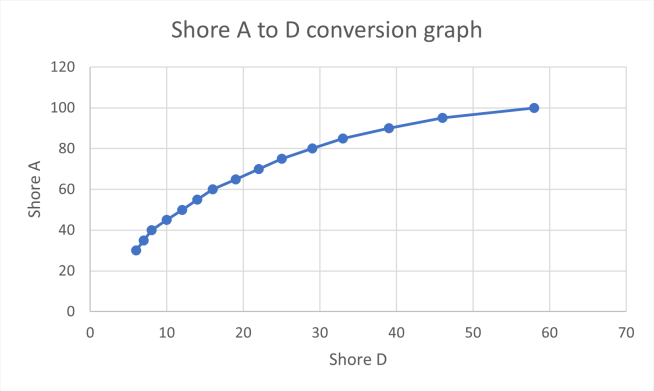

Figure 2.28: Conversion graph from Shore A to Shore D

One of the properties of polyurethane that makes it excellent in load-bearing conditions is the fact that it shows elastic behaviour for very high hardness variants. Most conventional elastomers have lost a considerable amount of elastic properties at a hardness of 75 IRHD and above [11].

2.3.4. Hardness and wear

One aspect that is not specifically addressed in this thesis is wear. Hardness and wear are dependent, though. It is generally thought that the harder a material is, the lower the wear is. This is not necessarily true, as seen from figure 2.29. In this figure, there are three distinct zones. In the first zone with polyurethanes softer than 75A Shore hardness wear is moderate. The middle zone B is the zone where wear is considered the lowest. Maybe surprisingly, the hardest polyurethanes wear the most. An explanation will be provided in section 2.5.

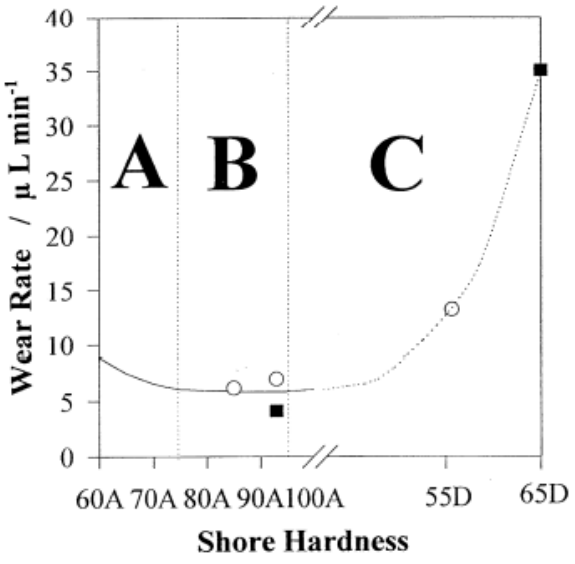

Figure 2.29: Approximate relation between wear rate and hardness for polyurethanes from Hill[12]

Abrasive Wear Comparisons

Material	Abrasion $mm^3.cm^{-2}$ (3.66 m)
Polyurethane 70 Shore A Ester	4.6
HD Polyethylene	6.7
UHMWPE	6.8
Nylon 66	7.5
PET	8.1
Polyurethane 80 Shore A Ester	9.0
Polypropylene	9.4
Polyurethane 80 Shore A Ether	10.1
Polycarbonate	11.8
Polyvinylidene fluoride	12.1
Polysulfone	12.5
Polyacetal	14.4

Figure 2.30: Abrasive wear comparison of different polymers from Clemitson [9]

In the book of Clemitson [9], a comparison is made between the abrasion wear of different types/ hardness polyurethanes, as well as other polymers, as seen in figure 2.30. The claim is also made that within the polyurethanes, the harder and tougher the material is, the more abrasion resistant it is, which contradicts the results from the figure. As mentioned before, though, wear is not further addressed in this thesis since it is hard to replicate the behaviour of pads in the tensioners at the current test setup.

2.4. Geometry

From previous friction testing with different pads at Allseas, it seems that the contact pressure between the polyurethane pads and the pipe needs to be reduced to increase the coefficient of friction. The contact pressure can be easily changed by altering the geometry of the pads and, therefore, the contact surface area between the pad and pipe. If one wants to increase the coefficient of friction, there are a few ways in which contact pressure reduction can be achieved.

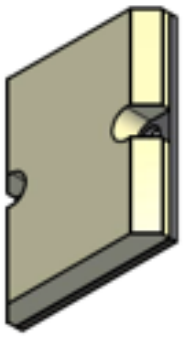

Figure 2.31: 3D representation of the current tensioner pad geometry

The most obvious way to reduce the contact pressure is to increase the pad surface area in contact with the pipe. The origin of the design of the current pads, shown in figure 2.31, is unknown; therefore, reasons for some of the design choices can only be guessed. The most likely reason for the shape is to create a single tensioner pad that could support the entire range of pipes from 6”-68” that the ship can lay. The disadvantage of designing a pad for a large variety of diameters is that the pad functions sufficiently on all different pipe sizes but likely never very well.

From the perspective of the pipe, pressure distribution or bending stresses on smaller pipes are small because the small pads support a large part of the pipe circumference. Larger diameter pipes will have peak pressures on relatively small areas of the pipe. The larger peak pressures, combined with the larger clamp forces required for larger diameter pipes because of their weight, could cause the pipe to buckle in the tensioners. From the perspective of the pads, the larger pipes are more beneficial at the moment since their larger curvature increases the size of the contact patch on the flat pads, whereas smaller pipes have a smaller contact patch.

To increase the contact surface area of the pads, it is suggested to make them curved to fit the pipes. The disadvantage is that if a single pad is still used for a large variety of pipe diameters, the pad must have a curvature similar to the 68” pipe. According to a research paper from Allseas, this slight curvature would still benefit all different pipe diameters because of the larger contact surface area.

Another way to increase the surface in contact with the pipe would be to maximise the pad width and length. In this case, there are some limitations to the overall dimensions. These limitations and their effect on the length and width of the pads will be further discussed in the design of the new pad in chapter 5.

For the geometry, not only the shape and dimensions of the contact area with the pipe are important, but also the thickness of the polyurethane layer and its shape. As seen in section 2.3, the thicker the material, the lower the perceived hardness due to stress distribution through the material. A thicker layer of polyurethane could lead to lower stress due to contact pressure.

Polyurethane is considered an incompressible material. It behaves very much like a liquid in its resistance to bulk hydrostatic compression, which is why its Poisson’s ratio is close to 0.5. According to Tsukinovsky[21], the Poisson’s ratio of 0.5 is valid for uncompressed polyurethane, but it can reduce to a value of 0.39 under shock compression. This value is closer to normal solids. In the case of the tensioner pads, the compression is not quick enough to be called shock compression, so a value of 0.5 seems right. The fact that PU is incompressible does not mean that the material cannot be

deformed but rather that the volume of the material stays the same when compressed. This is seen in experiments where the sides of the pad bulge out when it is compressed.

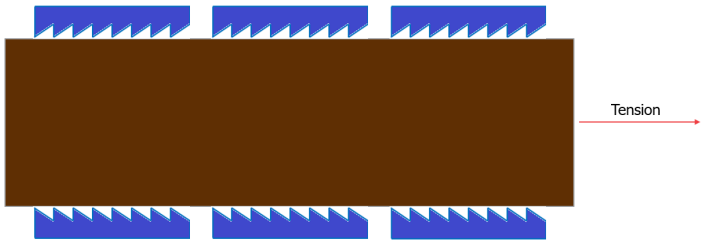

Figure 2.32: Example of directional pads with a sawtooth pattern.

An important part of the geometry is the pad's surface in contact with the pipes. The top of the pads can be formed in different shapes and roughness to help in the pursuit of high friction. Something that could very well help is a surface in the form of a saw-tooth that is directional in shape, like in figure 2.32. A large part of the friction generated in these pads would come from hysteresis. The problem with a design like this is wear. The sharp edges will be important for optimum grip, but since pressure and, therefore, stresses are at their largest at these places, wear will be prevalent, and performance will degrade quickly.

2.5. Temperature

The effect of temperature on material behaviour can be huge for the grip of a material. A good example of different grip at different temperatures are the soft slick tyres of racing cars or karts. When the tyres are cold, there is barely any grip, and it might feel like riding on ice. When the tyres warm up and are in the right temperature window, the grip is high, and speeds can go up.

From the book of Bhushan[5] follows that sliding velocity has a significant effect on friction. In this book, the claim is made that for viscoelastic materials, deformation due to an increase in temperature is equivalent to decreasing sliding velocities and vice versa. In other words, there is always a peak in the friction of PU. This peak is dependent on PU temperature and slip speed. When the temperature of the PU is higher, the peak is at a lower slip speed, and when the temperature is lower, the peak is at a higher slip speed. It could be that when sliding, the material heats up due to the dissipation of energy from friction. Sliding with more velocity dissipates more energy. So, the higher the temperature of the material, the lower the velocity has to be to heat the material to its optimum point. However, how much influence the temperature has on static friction remains to be seen.

Polyurethane is a good insulator. The material thermal conductivity of 0.1-0.3 W/m-K [9] is low compared to, for instance, steel, which has a thermal conductivity of approximately 45W/m-K. Polyurethane also has a specific heat capacity roughly four times larger than steel. These factors combined make it hard to heat the material from the outside. If one wants to heat polyurethane pads, it is recommended to heat them internally.

2.5.1. Polymer state

Polymers like polyurethane can be in different states depending on the temperature. There are the glassy state and the rubbery state. The state of the material depends on its glass transition temperature or the temperature at which the material changes from its glassy characteristics to its rubbery characteristics. Acrylic and polycarbonate are examples of materials with high glass transition temperatures and therefore being in a glassy state at room temperature. These materials are hard at room temperature and can be used to replace glass windows. An example of a material in the rubbery state would be polyisobutylene, also known as butyl or butyl rubber. This material is used for things like cleaning gloves. This material is very flexible and offers a high COF in its rubbery state.

The glass transition temperature of materials can be found by Dynamical Mechanical Analysis (DMA). DMA uses a machine to stretch and/or rotate the material at certain forces or amplitudes. It is also possible to control environmental temperatures. In this way, one can find the exact transition between the glassy and rubbery states.

The glass transition temperature in polyurethane is complicated. The material consists of hard and soft segments that have different transition temperatures on their own. Therefore, the glass transition temperature of the polyurethane depends on the ratio of soft and hard segments. Soft-segment glass transition temperatures are lower than hard-segment glass transition temperatures. When the material is mixed well, and the polymers are compatible, the polyurethane is expected to have only a single glass transition temperature. When this is not the case, one can find two glass transition temperatures in the material [16].

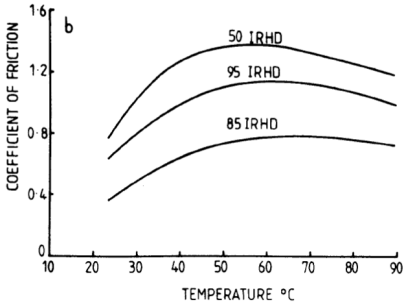

Figure 2.33: Relation between kinetic COF and temperature of polyurethanes on a chrome-plated brass surface with slip velocity of 1 cm/s. Figure from Wright [22].

In the rubbery state, the polyurethane has a higher COF than in the glassy state. Within this rubbery state, the COF is still dependent on the temperature. The higher the temperature, the softer the material will become due to the breakdown of crosslinking in the hard segments. According to figure 2.33 from [22], the kinetic COF can almost be doubled when the temperature is raised. The optimal temperature seems to be around 60°C. There are a few things to mention, though. First, Wright found a larger COF for 95 IRHD polyurethane than for 85 IRHD polyurethane. This contradicts the previous claims that the COF is linearly dependent on the hardness of the material. Secondly, this research was performed for sliding friction and did not necessarily predict static frictional behaviour. Also, the testing method is not clearly explained in the book. The testing method can influence the COF. Though the testing method is not clear, the test setup at Allseas to determine friction also uses sliding friction. The peak at 60°C might not be found in testing, but if friction can be doubled by changing temperature, it might be worth heating the polyurethane tensioner pads.

2.5.2. Drawbacks of heating

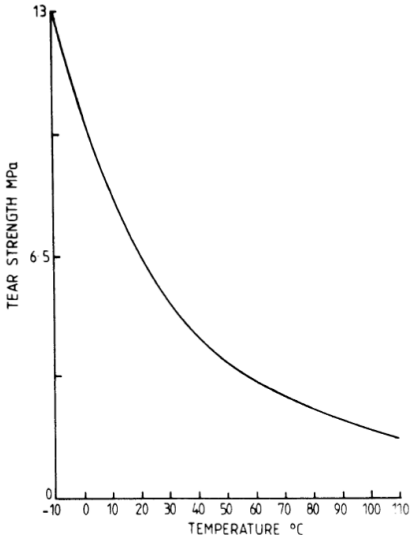

Figure 2.34: Relation between temperature and the tear strength of a typical polyurethane from Wright [22].

As mentioned before, the optimum material temperature could be around 60°C. The temperature should not exceed 70°C, though, since the mechanical properties of the PU weaken when temperatures rise. The influence of temperature on the tear strength can be seen in figure 2.34. The tear strength of the polyurethane roughly halves when heating it from 20°C to 60°C. It is, therefore, not recommended to heat the material much higher, even though the curve flattens. One of the suppliers of the polyurethane tensioner pads for Allseas recommends a maximum temperature of 70°C.

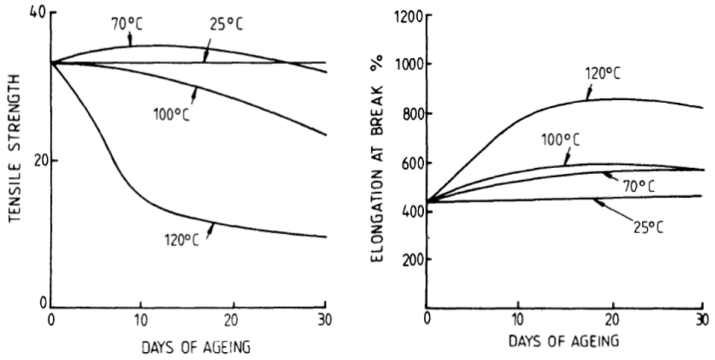

Figure 2.35: Effect of temperature on polyurethane properties. On the left, the effect on the tensile strength is shown. On the right, the effect on the elongation at break is shown. Figures from Wright [22].

When heated, polyurethane starts oxidising at a more rapid pace, like most metals. Polyester polyurethanes are considered more stable at higher temperatures than polyether-based polyurethanes. Above 80°C, there is a gradual permanent decrease in properties [11]. From research performed by Wright [22], the effect of different temperatures on ageing can be seen in figure 2.35. This figure shows that heating material below 70 °C affects the material properties. This impact is, however, considered insignificant. The tensile stress is not affected badly for 70°C, and the assumption is that for the lower temperature of 60°C, the effect will be negligible.

2.5.3. Effect of heat on wear

Heating affects the ageing of the material. Ageing, in turn, affects the wear properties of polyurethane. It is worth highlighting that this thesis is not about wear but rather about maximising friction performance. However, since the aim is to design something that might be used in practice, it is important to remember its presence. As it has already been established, heat influences the hardness of polyurethane. From section 2.3, it was found that softer polyurethanes do not necessarily wear faster than harder polyurethanes.

The reason the hardest polyurethanes, as seen in figure 2.29, wear the most is likely due to hysteresis. Because the harder polyurethanes have higher hysteresis, heat builds up relatively quickly, and the material softens greatly [12]. It is also claimed in the research of Hill [12] that in the middle region B of figure 2.29, the wear resistance of polyurethanes has been found to be almost independent of the temperature of the material.

The most prominent wear mode of polyurethane tensioner pads is likely to be abrasive wear. This can be tested with a rotating wheel like in the research of Capanidis [7], where abrasive wear of different polyurethane foams was tested.

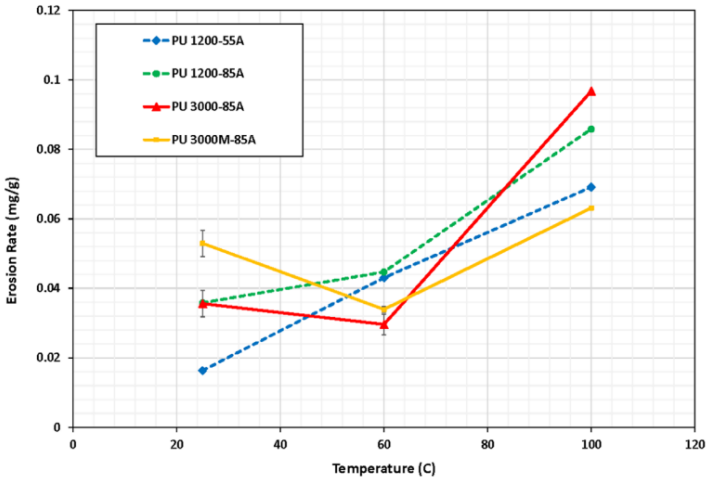

Figure 2.36: Erosion rate as a function of PU temperature from Ashrafizadeh [3].

Another way of testing the wear of polyurethane is with erosion testing. The research from Ashrafizadeh [3] gives a nice overview of how many contradictory papers have been submitted about the wear behaviour of polyurethanes. From their research, it can also be concluded that there is no clear relation between temperature, hardness, and wear of polyurethanes. For some samples, erosion wear is reduced from 20°C to 60°C, whereas others have increased as seen in figure 2.36. Noticeably, erosion is going up for all polyurethanes at 100°C. The latter is thought to be due to the mechanical breaking down of crosslinking in the molecules.

2.6. Summary literature

From the literature, it is found that various important variables influence the coefficient of friction. It was found that the asperity contact plays a large role in the COF. When the normal force leads to high contact pressure, the real surface area A_r in contact is similar to the apparent surface area A_a in contact. If $A_r \sim A_a$, the COF is likely to follow the relationship of $\mu \propto F_n^{-1/3}$.

For the hardness of the pads, it seems that softer polyurethanes generally provide more friction, but not necessarily since polyurethanes can have additives that influence friction. The hardness of polyurethane has a significant influence on the compression and tension stress-strain curves. In other words, softer pads deform more when the flat pads are compressed against a round pipe.

The geometry of the pads is important in the friction of the pads, but it is so because it influences the variables described above. By changing the shape of the pad surface in contact with the pipe, the size of the contact area is largely determined. The thickness of the pad further determines the size of the contact surface. When pads are thicker, the pressure distribution through the pads is better. The increased pressure distribution leads to a lower perceived hardness, as seen in figure 2.24, and a more conformal contact between pads and pipe. The larger contact area results in lower shear stresses and a higher COF.

There does seem to be an influence of temperature on the coefficient of friction, but its evidence is circumstantial. Temperature influences the hardness of the polyurethane, which in turn might influence the COF. Temperature has a negative influence on the mechanical properties of polyurethane. The tear strength of the material reduces at higher temperatures, and the ageing effect seems to increase at higher temperatures.

Essentially all variables summarised above are dependent on each other. It is difficult to single out the influence of a single variable in the case of flat tensioner pads compressed against a round pipe with the test setup at disposal.

3

Finite element analysis simulations

3.1. Introduction

To gain a better understanding of the pressure distribution in the polyurethane tensioner pads, and to find out what the influence of pad geometry on friction is, Finite Element Analysis (FEA) simulations were performed. In the FEA simulations, it is possible to include factors like the effect of temperature, pad hardness, and surface roughness. Only basic results were achieved with the software, and factors like temperature and surface roughness were not included due to a shortage of time. Some assumptions about the lower stresses in the pads with increased contact surface area were verified with the software, and therefore it was still a valuable tool in the design of a new pad. To include the majority of the work that has gone into this thesis, the finite element analysis simulations will be briefly touched upon.

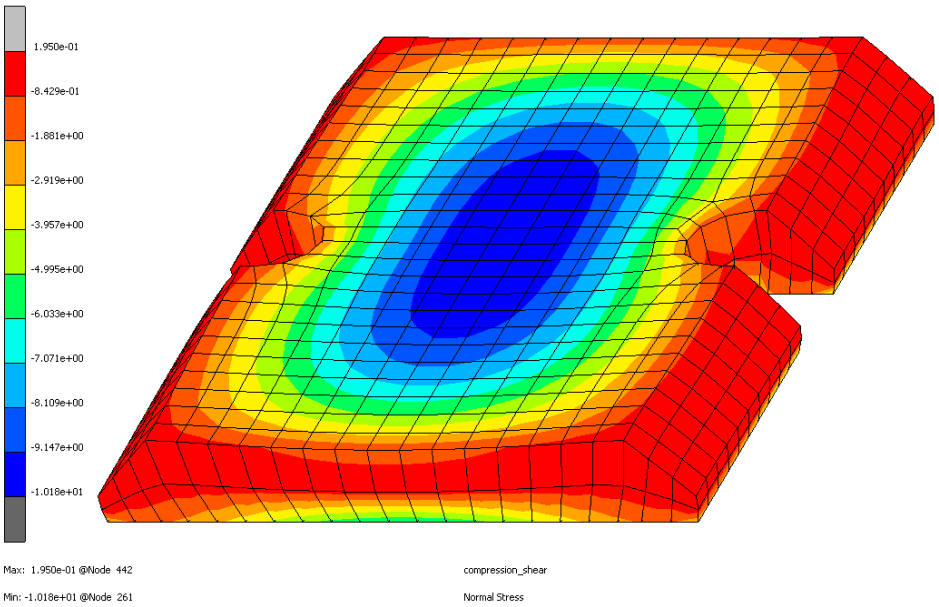

Figure 3.1: Course pad mesh loaded with normal force showing normal stress. This figure perfectly shows that stresses in the middle of the pad are larger than on the side where the material can bulge out, reducing stress.

The software used for the analysis was MSC Marc Mentat. This software is specialised in solving large deformations and dealing with nonlinear materials like polyurethane. Most info about building up the simulation for friction behaviour between pipe and pads was found in a past bachelor end project that some students performed at Allseas. The primary aim of this group was to find different shapes of

pads to see which would perform better. Their work could not be directly used because of the coarse meshes and an unrealistic pipe radius. In figure 3.1, one of the coarse meshes is shown. In this figure, the pad is loaded with a pipe with a diameter of 5 meters and a compression force of 20kN. The colour scale represents the normal stress in the material. Besides the fact that the results of this research were not necessarily useful, the structuring of the files was very helpful.

Models used in the FEA simulations were created in CAD software, in this case, Solidworks. An example of this is given in figure 3.2 where a 16” pipe is used against a current PS pad. The pipe was changed between 16” and 12” to have the same radius as the pipes used in the experiments in Heijningen, to keep variables as similar as possible.

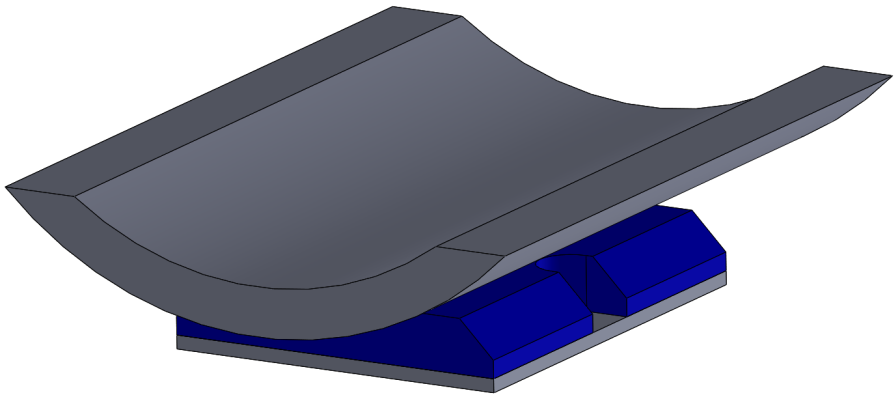

Figure 3.2: Original PS pad versus 16” pipe CAD model for MSC Marc Mentat.

To represent the polyurethane in the FEA simulations, the Arruda-Boyce model is used. Values for material properties are obtained from old internal reports of Allseas. These values were not validated through testing, so they might be inaccurate.

3.2. Results from FEA simulations of different pipes on the PS pad

The mesh size and time step can be reduced to obtain more accurate results in FEA simulations. The increase in accuracy comes with a drawback. Reduced mesh size and time step increase calculation time and file size massively. The impact of mesh size was one of the first things measured to see if a coarse mesh would be accurate enough. In Figure 3.3, three different meshes are shown. These are all loaded solely with the same normal force, not in shear. The reason for not loading the pads in shear was that experiments never validated the FEA simulations. Because of the lack of validation, the actual friction was unknown, and therefore a conservatively low Coulomb friction value of 0.3 was chosen. Since the friction is low, the shear stress in the pads is also low, and the pad deformation is likely to be smaller than in reality. Rather than showing the results of the pads in shear with their corresponding von Mises stresses, which were highly likely to be wrong, the choice was made to omit the results of the shear loading entirely. There is still shear present in the pads due to the normal loading and subsequent deformation of the pads, but its influence is comparatively small.

Another problem with the friction of the material in FEA is that the surfaces of materials are perfectly smooth. In reality, there are asperities as mentioned in section 2.2. These asperities can have a significant influence on the friction between materials. Since the asperities could not be correctly modelled in the short time span, it was omitted.

The stress plotted in all figures from this point on is the von Mises stress. Von Mises stress was chosen because it is a combination of stresses in different directions, like shear stress and normal stress. Arguably normal stress is the better stress to portray after loading the pads in shear was omitted, but due to time constraints, not all FEA simulations could be run again to obtain normal stress.

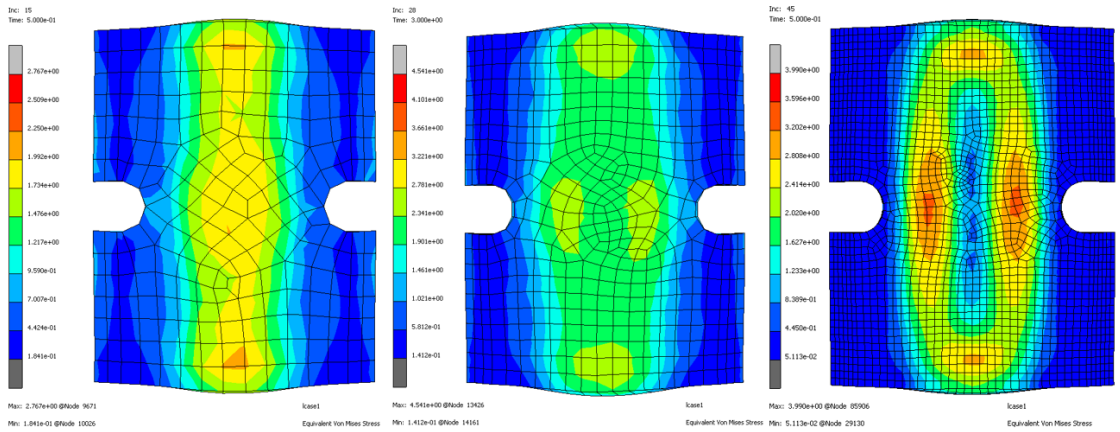

Figure 3.3: Influence of mesh size on accuracy in results. Mesh size from left to right, maximum 15mm, maximum 10mm and maximum 5mm. Other variables are unchanged. Warning, colours in different scales represent different numbers!

From left to right in figure 3.3, the maximum mesh size is 15 millimeter, 10 millimeter and 5 millimeter. The figure shows that the maximum von Mises stress differs significantly between the different meshes. Also, the increment or the number of steps necessary in a certain time in the simulation goes up from 15 for the most coarse mesh to triple that in the finest mesh. The time in the middle figure is different from the other two. Therefore the rate of loading is different. This does not matter since neither the polyurethane nor the pipe was given mass, so inertia effects are absent.

What cannot be seen from figure 3.3 is the time needed to calculate the simulations. Since the simulations were performed in 3D, the amount of elements in the third simulation is roughly $3^3 = 27$ times larger. This is not exactly true in practice since the 15mm and 5mm are maximum values, but it is not far off. What was also noticed was the increment increased by a factor of 3. These factors alone would make the simulation close to 90 times slower. In fact, the calculation took around 90 seconds for the 15mm mesh and over 8 hours for the 5mm mesh.

The problem of fine meshes taking longer to calculate can be reduced by using adaptive remeshing. In the time span of this thesis, that could not be fixed despite multiple efforts. Local adaptive remeshing effectively reduces the mesh size of elements that undergo large deformations. The advantage of this is that not the whole pad has to be remeshed, which would again lead to larger calculation times. Because adaptive remeshing was not performed, and the mesh size was coarse, the accuracy of the numbers is questionable. Looking at figure 3.3, it can be seen that it cannot be claimed that results have converged in the 5mm mesh. As with many things, though, trends should be observed rather than looking at exact numbers.

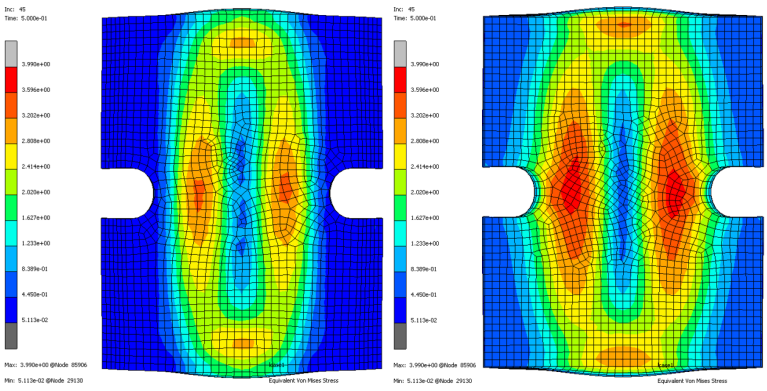

Figure 3.4: Von Mises stress of pad loaded with normal force. On the left, the front of the pad, and on the right, the back of the pad. Pad hardness of Shore 75A loaded with a 16” pipe.

Figure 3.4 shows the Von Mises stresses at the front and the back of the pad. One observation is

that the stresses at the back of the pads are larger than at the front. This could simply be an artifact of the way the material is glued firmly to the non-deformable backplate, whereas in real pads, the bonding might be able to stretch a bit. In any case, the target is to reduce these stresses as much as possible since more stress seems to lead to a lower coefficient of friction.

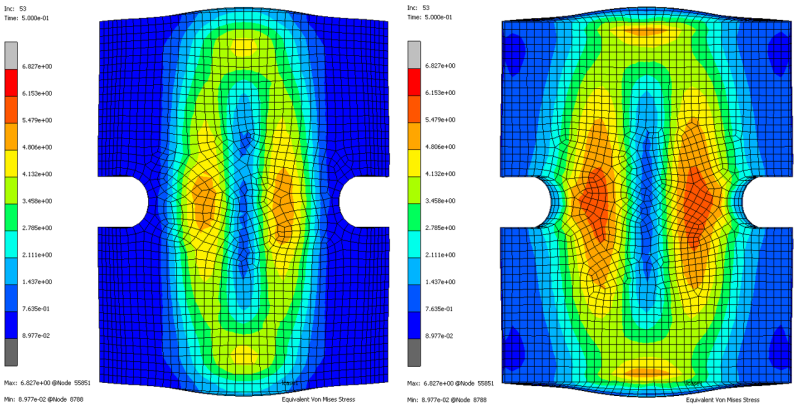

Figure 3.5: Von Mises stress of pad loaded with normal force. On the left is the front of the pad, and on the right is the back. Pads of hardness Shore 75A versus a 12” pipe.

The data from the FEA simulations that is still comparable is the Von Mises stress in the polyurethane under the same conditions. Figure 3.4 and 3.5 show the difference in loading the current PS pads with a 16” pipe and a 12” pipe, respectively. At first, the difference does not look large until a closer look is taken at the scale on the left-hand side of the figures. From this scale, it can be seen that stresses are roughly 50% higher for the case of the 12” pipe. Higher stress is expected since the 12” pipe will have a smaller contact surface, leading to higher pressure and more stress in the material. This is more significant because a relatively soft polyurethane is used in this case. When the polyurethane is harder, it deforms less, leading to a smaller contact area and higher pressure. Figure 3.6 illustrates the effect of softer versus harder pads.

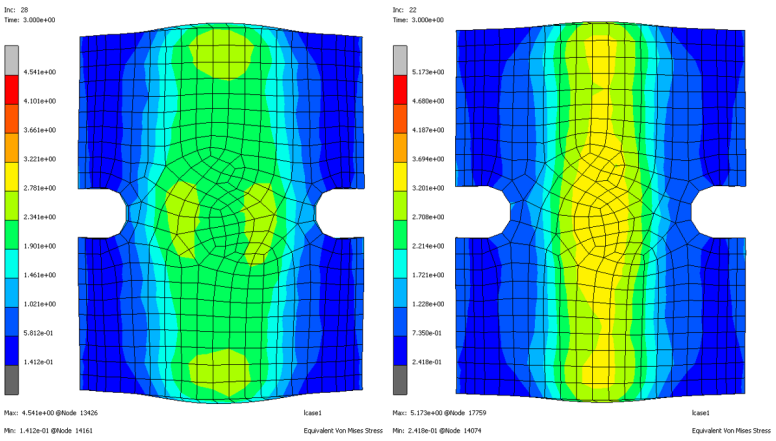

Figure 3.6: Von Mises stress of pad loaded with normal force. On the left, the front of the pad with 75A Shore hardness. On the right, the front of the pad with 90A Shore hardness. Both are loaded with the standard load and a 16” pipe.

3.3. Summary FEA simulations

In this chapter, the FEA simulations performed were explained. Though the software is powerful, it was not fully exploited. Meshes were too coarse to be converged, and results from shear loading were considered not good enough. Results from previous research were not accurate but were used as a guideline in designing a new pad. FEA simulations will be used to compare the von Mises stresses of the new pad designs to the current pads, and the results will be shown in chapter 5.

4

Baseline testing

4.1. Testing methodology

The tests were designed to answer the research question from chapter 1. First, the influence of normal force on the COF is tested by varying the test bench's hydraulic clamp pressure (HCP). The HCP is varied across most of the testing to see if the observed trends are reliable and meaningful results can be extracted.

The pad hardness is tested by using all four different pads on the two different pipes that were tested. From the two datasets, a conclusion can be drawn on whether hardness impacts the friction performance of the polyurethane tensioner pads.

The influence of pad geometry was not tested in baseline testing. Only one pad geometry was available and tested. Though the geometry was not tested in the test rig in Heijningen, some remarks can be made on performance of different geometries through the FEA simulations and from there, conclusions will be drawn.

The influence of pad temperature on friction is also tested. This is done by heating the pads in an oven to a target temperature and testing them at a predetermined HCP. Since the pads are cooling down quickly, testing the heated pads at all the different HCPs tested before was impossible. Therefore, no clear relation can be drawn between the contact pressure and temperature on the friction performance.

Next to properties concerning the polyurethane, some ambient factors are measured to see if they have any influence. The measured factors are the ambient temperature and the relative humidity. The relative humidity was not always measured, due to a lack of available equipment, as shown in figure 4.1.

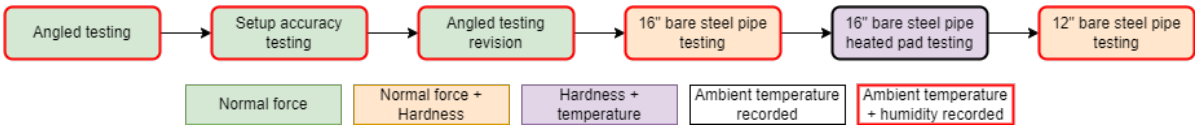

Figure 4.1: Testing flowchart with colour-coded objectives.

First, the slip test machine is prepared for the testing, after which all the tests are performed. Out of all testing, the most important tests and their use are depicted in figure 4.1. The figure shows that most of the testing was used to determine the influence of normal force on the pads, a large part of the testing was used to determine the friction of different hardness of pads, and a small part was used to determine the influence of temperature.

4.2. Preparations for baseline testing

From chapter 2, it was learned that to test accurately, it is vital to replicate the setup in the real tensioners as well as possible in the test setup. As stated before, the angle of the pads in its initial configuration of the test bench was 120 degrees, which is an angle that is not valid for the PS setup, where the pads can swivel and make angles between roughly 80 to 120 degrees. Therefore, the test setup first had to be modified.

To replicate the setup, original pad holders from the PS are used. These will make sure the pads can rotate. Next to rotating, the pads can also be adjusted in width to suit larger or smaller diameter pipes. After the correct width between the pad holders is chosen, the pad holders are fixed with fixation blocks. To mount the pad holders and fixation blocks to the slip test bench, a transition piece between the pad holders and the test bench was needed.

It was not feasible to mount real crossties of the tensioners to the test bench in Heijningen since they are both too heavy and not easily mounted to the machine. Therefore, the decision was made to machine new transition pieces that could be easily bolted to the existing setup on one side. The front and most of the sides of the transition piece are copied from the crossties of the PS tensioners. Only the back was changed to fit the test bench. This transition piece, from now on called a crosstie, can be seen in figure 4.2 on the left.

The crossties were designed with versatility in mind. Not only can the original pad holders from the PS be supported in multiple configurations, but there is also the possibility to mount single PS pads directly in the middle of the crosstie. With a relatively simple and thin transition plate, it is also possible to mount single pads from another Allseas vessel with a similar tensioner setup but a different geometry of polyurethane pads. There were two primary reasons for mounting single pads in the middle of the crosstie. The first reason was to reach larger clamping forces, as mentioned before. The heated pad testing was the second reason to mount a single pad in the middle of the crosstie. The original pads are tested at higher temperatures by heating them in an oven, mounting them on the test bench and performing the necessary tests. As soon as the pads leave the oven, they cool down. Therefore, the quicker one can mount the pads on the crosstie, the better. This is especially helpful when testing at higher temperatures because the larger the temperature difference between the pads and the environment is, the larger the heat flux is, and the quicker the pads will cool down.

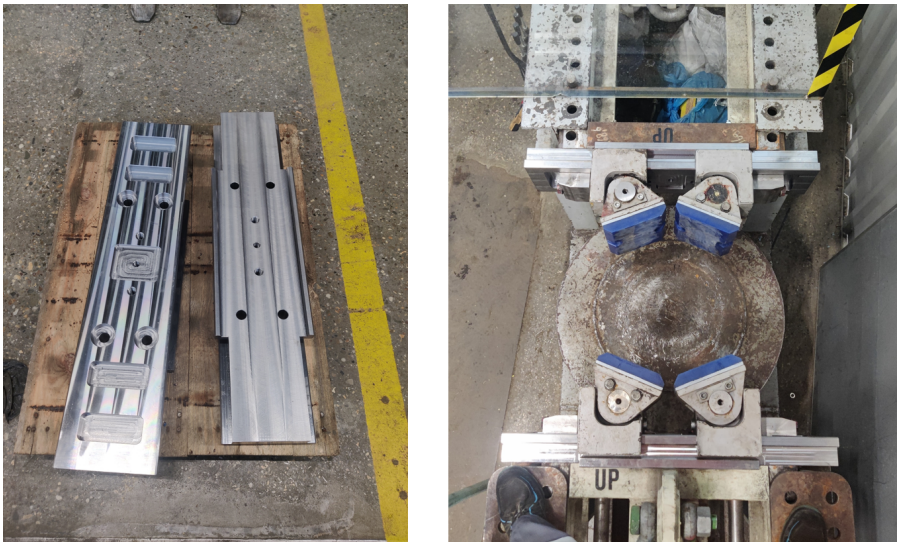

Figure 4.2: Pictures of the new crossties made to imitate the PS. On the left are the crossties after arrival. On the right are the installed crossties, complete with PS pad holders and pads.

After the crossties were produced, modifying the machine and, subsequently, testing could begin. Mounting the crossties was quite straightforward, and the result is shown in figure 4.2. There was an unforeseen minor issue. In the past, the slip test bench had been modified and was now asymmetrical.

This was never accounted for in the design, and the repercussion is that the position of the two crossties differs a few millimeters in height. Theoretically, this results in a small moment on the pipe when it is clamped down. It was chosen to neglect its effect since it would be counteracted by the pipe being supported by the platform, which also likely creates a small moment.

4.2.1. Slip speed variation

Before the bulk of testing was started, the hydraulic oil flow volume of the slip cylinder, thus the slip speed of the test setup, was adjusted to see if it made any difference. From section 2.5, it seemed that there was a correlation between temperature and friction. Since almost all energy needed to slip the pipe through the pads in the experiment is converted into heat, the presumption was that the higher the slip speeds are, the more this produced heat influences the results. This effect would be increased because the thermal conductivity of polyurethane is similar to many rubbers and only around 0.1-0.3W/mK [9]. This means that the heat generated due to friction would quickly heat the surface and, therefore, potentially significantly influence the frictional behaviour of the material. This effect would be partially counteracted by using a steel test pipe, which acts like a heat sink thanks to its large mass and good thermal conductivity.

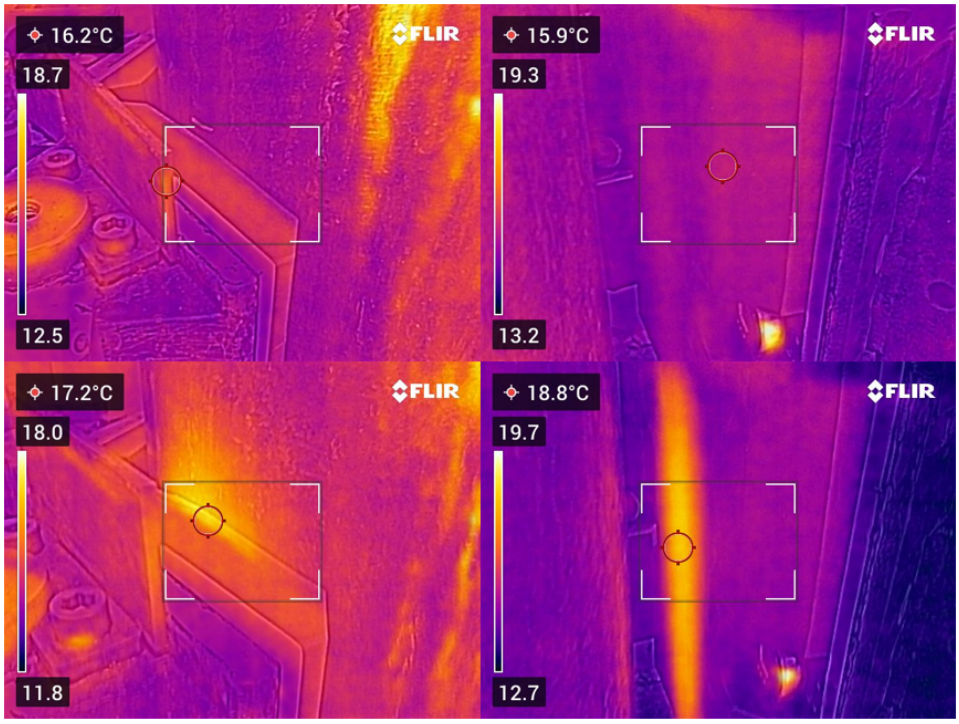

Figure 4.3: Left to right upper: thermal pictures during the slow test and after the slow test, left to right lower: thermal pictures during and after the fast test.

It is hard to measure the surface temperature of the polyurethane in contact with the steel pipe. Most methods to measure the surface temperature either influence the surface that has to be measured, or they are too inaccurate to measure the thin surface layer that is influenced by temperature, also known as the flash temperature [5]. The decision was made to use a thermal camera to inspect the surface for temperature changes. This method is far from accurate, nor is it able to measure the contact surface while sliding, but it was the best method available at the time. The results from the thermal camera are shown in figure 4.3. It can be seen that in the slow testing, where slip speeds are roughly 1mm/s, the execution of a single test does not show a significant rise in the surface temperature according to the thermal images. The quicker slip test of roughly 6mm/s shows an obvious rise in temperature, both during and after testing. This effect will be enlarged by the fact that usually multiple tests are performed in a short amount of time. Therefore the temperature will rise significantly and potentially influence results.

The tests in figure 4.3 were tested at relatively low clamp forces. When testing at higher hydraulic clamp forces, pushing the pipe through the pads takes more energy. This means that more heat is dissipated to the pads, possibly influencing the polyurethane more. This was considered another undesirable variable; therefore, all testing was performed at the slower slip speed.

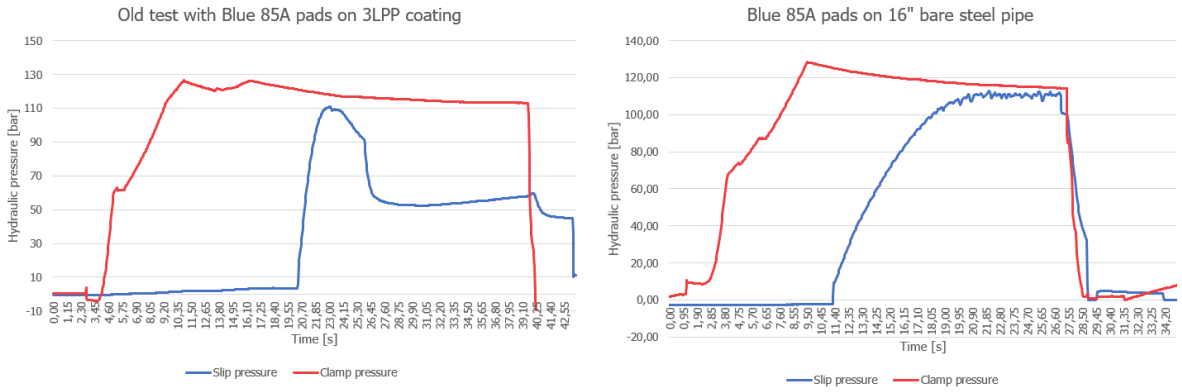

Figure 4.4: On the left, an old slip test example. On the right one with the current slip speed.

Next to tests taking longer, there is another downside to testing at a lower slip speed. At higher slip speeds, the graph often shows a clear peak in the slip test pressure like on the left in figure 4.4. The top of this peak was used to represent the COF. The value of the COF at the peak could be used to represent the static COF. From section 2.5, especially figure 2.33, where a graph is shown of the COF at different temperatures, the presumption grew that the peak in friction seen in figure 4.4 on the left could be down to the material heating up on the surface, and therefore reaching its optimal temperature for friction. After this optimal point is reached, the polyurethane possibly overheats and friction is reduced. When testing at the lower slip speeds, the graph often has no peak like on the right in figure 4.4. The downside is that the lack of a clear peak makes it harder to assign a single representative value for the entire graph.

One thing to note is that the way of testing is fundamentally different to what happens in the tensioners. In the tensioners, the polyurethane barely slips on the pipe and, therefore, will not significantly heat up from anything other than hysteresis, which is believed to have a minor effect in raising the temperature. In the test bench, the material slips and heats up, and then from the curve of slipping, a point that is supposed to represent the COF is chosen.

4.3. Angled testing

After the modifications of the test setup were completed, angled testing could commence. As explained in section 4.1, the angled tests were the first tests where the surface pressure effect on friction was recorded. This was, however, not the primary aim of the angled tests. The primary aim was to find out if it could be validated that the clamping force is always perpendicular to the pads, so the 2-pad setup, shown in figure 4.5, could be used.

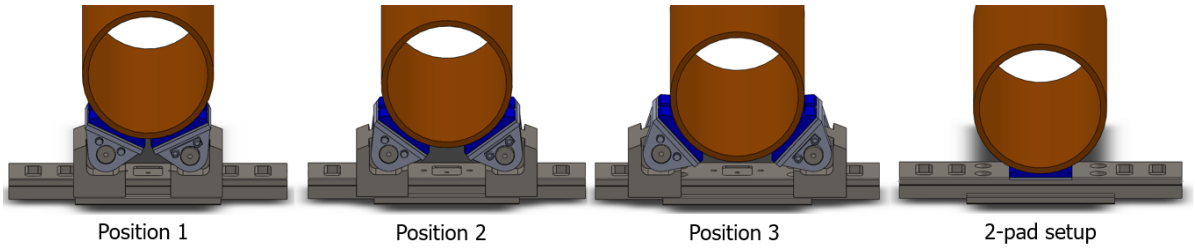

Figure 4.5: Different setups possible with new crosstie and 16" pipe.

To increase the clamp forces in the test setup, approaching the clamp forces in the tensioners, it was decided to use only one pad on each side of the pipe, leading to the 2-pad setup. Depending on the angle of the pads against the pipe, this would lead to roughly 29-88% higher clamp forces following from formula 4.1.

$$F_{\text{pad}} = \frac{F_{tb,clamp}}{N * \cos \alpha} \tag{4.1}$$

Where $F_{tb,clamp}$ is the test bench clamp force, and N is the number of pads per crosstie. The angle α is roughly between 20-50 degrees.

Equation 4.1 is only valid when the pad's normal force is perpendicular to the pad. When testing with two pads, the normal force is perpendicular, but this needed to be validated for the pads at an angle. To do this, a simple test was designed. Because the pad holders can be shifted into different locations, it is possible to test on a 16-inch pipe with the pad holders in three different positions. The positions are shown in figure 4.5, where the angle of the pads gets steeper for each subsequent position. The fourth position that can be tested is where the pad holders are removed, and only the two pads are mounted to the crossties.

The angles that the pads would make versus the pipe were estimated in CAD software. This estimation was done without deformation of the pads, so in practice, the angle would always be smaller because of the rotation of the pads due to indentation. The actual angles that the pads made with respect to the crossties in experiments would have to be measured every time.

Calculations were made to determine what the pads' normal forces were in the tensioners on board the ship. These normal forces would then be replicated in the test bench for the different pad angles, as precise as possible. When the pad angles increase, normal forces on the pads will increase when the pressure in the hydraulic clamp cylinder stays equal. Therefore, altering HCP to achieve the same normal forces on the pads is necessary. When the normal forces on the pads are similar, and the force is, in fact, perpendicular to the pads, the force it would take to slip the pipe through the pads should also be similar. If the slip forces are not similar, the assumption that normal forces on the pads are perpendicular might not be true.

The full table of hydraulic clamp pressures in different positions is represented in figure 4.6. A large range of normal forces on the pads expressed in metric tonnes is tested. As seen from the figure, the larger the angle of the pads, the smaller the hydraulic pressure in the clamp cylinder must be to achieve the same force in the pads. The hydraulic pressures were rounded to 5 bars differences to make them more achievable in testing. Some cells are coloured red, which indicates that the test setup cannot supply the required hydraulic pressure, so the experiment cannot be carried out. Other tests that were not carried out are the ones with less than four metric tonnes (mT) of normal force on the pads since it is unrealistic that in the tensioners, normal forces on the pads are smaller than 4 mT.

Force on pads [mT]	Position 1: 25 deg [bar]	Suggested pressure [bar]	Position 2: 36.5 deg [bar]	Suggested pressure [bar]	Position 3: 48.5 deg [bar]	Suggested pressure [bar]	2-pad setup [bar]	Suggested pressure [bar]
3,0	67,92	70	60,24	60	49,66	50	37,47	35
3,5	79,24		70,28		57,94		43,72	
4,0	90,56	90	80,32	80	66,21	65	49,96	50
4,5	101,88		90,37		74,49		56,21	
5,0	113,20	115	100,41	100	82,76	85	62,45	60
5,5	124,52		110,45		91,04		68,70	
6,0	135,84	135	120,49	120	99,32	100	74,94	75
6,5	147,16		130,53		107,59		81,19	
7,0	158,48	160	140,57	140	115,87	115	87,43	85
7,5	169,80		150,61		124,15		93,68	
8,0	181,12	180	160,65	160	132,42	130	99,92	100
8,5	192,44		170,69		140,70		106,17	
9,0	203,76	205	180,73	180	148,98	150	112,41	110
9,5	215,08		190,77		157,25		118,66	
10,0	226,40	225	200,81	200	165,53	165	124,90	125
10,5	237,72		210,85		173,81		131,15	
11,0	249,04	250	220,89	220	182,08	180	137,40	135
11,5	260,37		230,93		190,36		143,64	
12,0	271,69	270	240,97	240	198,63	200	149,89	150
12,5	283,01		251,01		206,91		156,13	
13,0	294,33	295	261,05	260	215,19	215	162,38	160
13,5	305,65		271,10		223,46		168,62	
14,0	316,97	315	281,14	280	231,74	230	174,87	175
14,5	328,29		291,18		240,02		181,11	
15,0	339,61	340	301,22	300	248,29	250	187,36	185

Figure 4.6: Method of determining hydraulic clamp pressures for different positions.

As mentioned, the actual angle of the pads was measured after clamping the pipe every time. This angle was measured on a single pad, and the assumption was made that all the pads would make the same angle with respect to the crossties. After every test, the pads were reset to the estimated pad angles from CAD since that was the point of first contact. Resetting the angles was a very time-consuming job, and one could argue that it is inaccurate. At one point in time, all the pads' angles with respect to the crossties were measured to see if the angles were significantly off. In this case, the angles of the other pads were within 0.3 degrees of the one that was measured every time, and therefore the influences of different angles from other pads were neglected.

Figure 4.7: Example of pipe surface suspended from the table that provides the slip force.

To keep testing results accurate and to change as few variables as possible, all angled tests are performed on the same test 16" bare steel test pipe with the same 85A Shore hardness pads. The pipe was supposed to be as smooth as possible, but since pipe storage is outside, the pipe in question had been exposed to rainfall for quite a while, so the pipe was covered with a thick layer of rust. To make it as smooth as possible, a good effort was made with an angle grinder and flap discs to remove all rust from the pipe. Since the pipe had been exposed for a while, the rust had set in quite deep, and it was not possible to make the pipe as smooth as originally intended. It was not attempted to measure the surface roughness because the surface was not evenly affected by the oxidisation. An example of the pipe surface can be seen in figure 4.7. Coincidentally the surface of 85A Shore hardness set of

polyurethane tensioner pads had previously been roughened as well since the belief at the time was that roughing the pads would yield more grip on the pipe. This might have been because pads were never cleaned after manufacturing and still had the release agent on them that was needed to remove them from their moulds after pouring. The assumption was made that, though the piece of pipe and the pads were flawed, they would be flawed for all tests, and the data comparing different angles would still be accurate enough to observe trends from.

In hindsight, this test was flawed from the start since the loading of the pads is fundamentally different between the test setup and the tensioners. In the test setup, the pads first touch the pipe over their complete length. When the hydraulic clamp pressure is increased, the pads start to deform and reduce in thickness. This reduction in thickness leads to an increasing angle α and a possible non-perpendicular normal force on the pads. The non-perpendicular normal force leads to a larger shear force and, therefore, lower friction [18]. In the tensioners, this is not a problem since the pads arrive at the pipe at an arrival angle. As mentioned in section 2.1.3, this arrival angle leads to the arrival effect. It also means that the pads make first contact with the pipe at a single point rather than a line contact. The pads are then loaded from this single point, where friction prevents the pads from rotating, keeping normal forces perpendicular to the pads.

Figure 4.8: Test bench inner frame painted white, outer frame bare steel/painted grey.

Though flawed, these tests had significant value since they showed a shortcoming of the test setup, which will be explained later. As observable from figure 4.5, the further the pad holders are spread apart, and the larger angle α is, the closer the pipe comes to the crosstie. Since there is limited travel in the hydraulic cylinder, the test bench can be adjusted to accommodate larger or smaller pipes by moving inner frames outward or inward on both sides. The inner and outer frames can be seen from the top on the right of figure 4.2 and more clearly from the side in figure 4.8. The inner frame is connected to the outer one through the holes with pins, as shown in figure 4.8.

4.3.1. Angled testing results

As mentioned before, the data collected from the slip tests is hydraulic pressure from both the clamp and the slip cylinder. Both are measured at a rate of 20 Hz. This data is plotted, and a single representative point in time is chosen, as seen in figure 4.9. The position of the representative point in time is chosen in the following manner. The pad is sheared when slip force is applied, resulting in the linear increase of hydraulic slip pressure at the start. When the pad's grip on the pipe is lost, the hydraulic slip pressure will not rise linearly, and the increase in pressure starts to reduce. The exact point where slipping starts cannot be retrieved from the hydraulic pressures. The assumption is that static friction is lost after the linear rise of hydraulic slip pressure stops, and some point curve is chosen as the representative point.

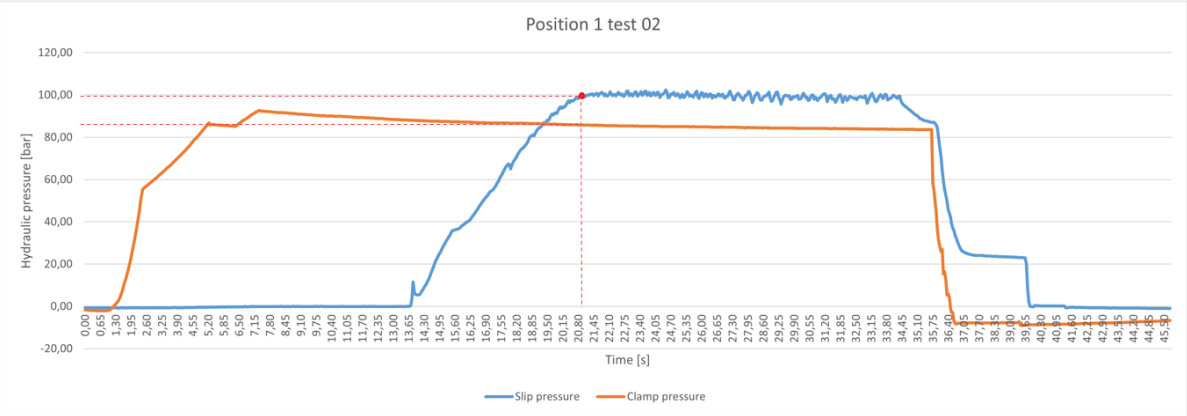

Figure 4.9: Graph of one of the first tests with the chosen representative point as a red dot.

At the representative point, the hydraulic slip pressure is converted into a force. Then, the force of gravity due to the mass of the pipe and the plateau it is placed on is subtracted. The hydraulic clamp pressure is also converted into a force, taking into account the measured pad angle. In the end, the slip force is divided by the clamp force leading to the coefficient of friction. This method is subjective since no repeatable logic is used in determining the precise point chosen from the graph. However, some trends can be observed from the plotted points.

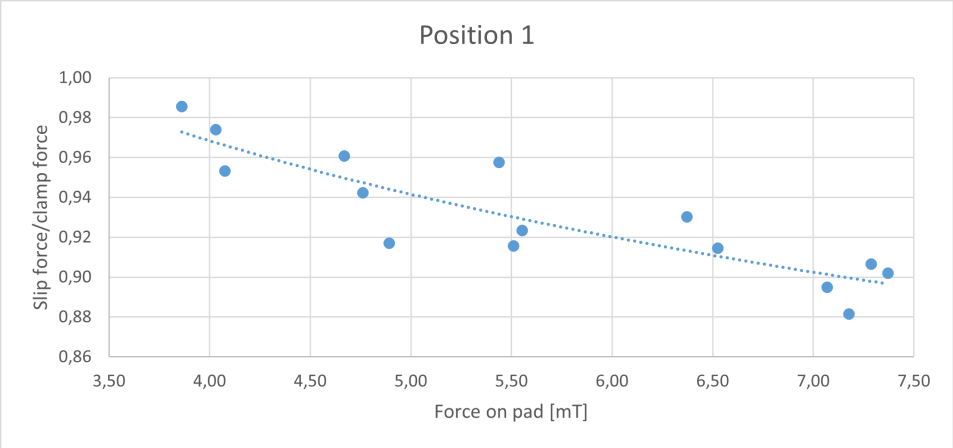

Figure 4.10: Data points from different graphs. Each dot represents a representative point from a graph out of a single experiment

From figure 4.6, it follows that for position 1, there are six different hydraulic clamp pressures to run tests at. Given that normal forces on the pads smaller than 4 mT were unrealistic, five HCPs remain to be tested. For repeatability, there are three tests at every distinct HCP, leading to a total of 15 tests for position 1. Figure 4.10 shows the first results from testing. Each dot in this graph is a representative point in a graph from the raw data as shown in figure 4.9. On the X-axis, the normal force on the pads is plotted, which was predetermined to be at values from figure 4.6. This plot shows that where the intended normal forces on the pads were 4,5,6,7 and 8 mT, these normal forces were not reached. This is because of a loss in hydraulic clamp pressure due to a leak. Though the exact target clamp forces were not reached, the points do show some groups, except for the highest hydraulic clamp pressures, which shows that the machine is operated manually and not automatically, leading to a larger spread in normal force. On the Y-axis of the figure, the slip force divided by clamp force is shown. This is essentially the same as the coefficient of friction μ from equation 2.1 for Coulomb friction.

Through the representative points in figure 4.10, a power trendline is drawn to see whether it would be near the value of $\mu \propto F_n^{-1/3}$ seen before in the book of Bhushan [5], but it is more like $\mu \propto F_n^{-1/8}$ in this case. A linear trendline would be as good of a fit for this graph, suggesting that the test results are

different from previous testing at Allseas and the values from Bhushan. The trend that can be obtained from this graph is that the coefficient of friction decreases with increasing normal force on the pads.

The same graph as that in figure 4.10 was made for the other two angled positions and the 2-pad setup. Instead of showing all these plots individually, they were plotted all together since the results are directly comparable. The resulting graphs can be seen in figure 4.11.

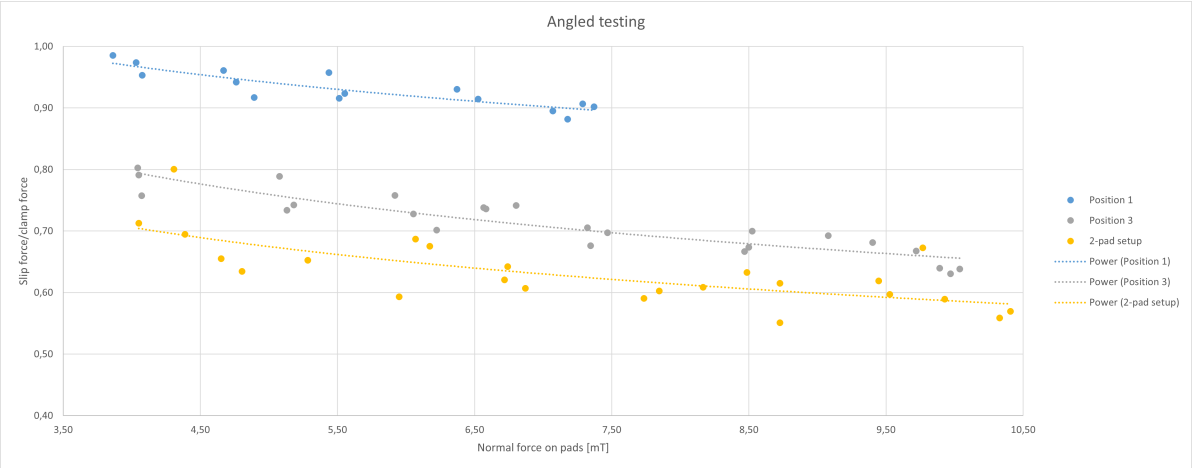

Figure 4.11: Data points from different graphs and different pad positions with trendlines

A few results can be extracted from figure 4.11. First of all, every trendline follows roughly the same direction. What can also be seen is that the COF is very dependent on the different positions, while this test was assumed to show that all different positions yielded roughly the same COF. The difference in COF between the data sets was too large to be neglected. Another thing to notice is that the results from position 2 are missing from the figure. This is because a software error resulted in a data set so different from the rest of the sets that it was deemed unreliable and therefore discarded.

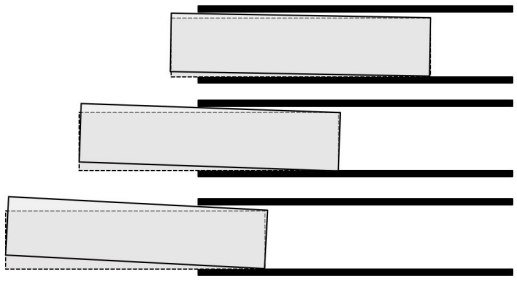

Figure 4.12: Simplified representation of inner and outer frames and influence of frame extension on the angle between the frames. Top angle 1°, middle 2°, and bottom one 3°.

It was found that the data sets for the different angled positions in figure 4.11 were far apart in terms of COF because of play in the machine. Every time a new position was tested, the pad holders were spaced further apart, decreasing the distance between the crossties. As mentioned before, the slip test bench works with inner and outer frames. To clamp the pipe in different positions, the inner frames can be shifted inward and outward. Every new position needed a shift of either one or both frames. There was more than a millimeter of play in between the inner and outer frames. Since the inner frame is shorter than the outer frame and the amount of space between the frames is equal, the more the inner frame is extended from the outer frame, the more of an angle it will make. An exaggerated example is shown in figure 4.12 on how the spacing between the frames can greatly influence the angle of the inner frames. Next to the play between the frames, the slip test machine was also bending at some places, increasing the angles of the pads with respect to the pipe.

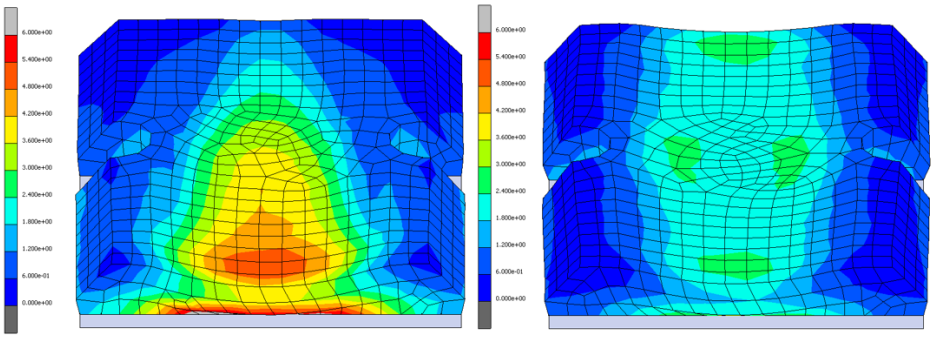

Figure 4.13: FEA simulation results of a PS pad 90A Shore hardness loaded with a 16” pipe at 1.5°angle compared to the same pad and pipe without distributed load.

The angle increasing between the frames poses a problem because it leads to a distributed load, as briefly touched upon in section 2.1.3. From a practical point of view, the angle of the pads is another variable that should be eliminated. Research from Ben-David shows that testing with even small angles of 0.01°can influence stresses and friction in material significantly [4]. The research of Ben-David was done versus a harder material than polyurethane, but results might be comparable when loading in more significant angles. To illustrate the effect of a small angle, FEA was used to create the results in figure 4.13. The situation depicted in the figure shows what happens when a 16” pipe is pushed into a hard pad at a 1.5°angle. Noticeably, the bottom of the pad is heavily deformed, while the top is almost untouched. The contact area is shaped like a cone. The pressure in the material at the bottom is also much higher than that at the top. When putting a distributed load on a pad, the total contact area is smaller than when loading it perpendicularly. The assumption is that because of the smaller contact area and the higher contact pressure, the COF is lower when the pad is loaded at an angle. In a later experiment, it was attempted to validate this theory, but due to the slip test machine reaching its limits, no conclusive results were achieved.

4.3.2. Conclusions angled testing

From the first attempt of angled testing, it is only possible to compare the friction of the polyurethane at different normal forces on the pads, leading to different contact pressures. The exact contact pressures in the polyurethane were not calculated since the vertical angles of pads with respect to the pipe and the contact area were unknown, but it can be seen from the results that with larger normal forces on the pad, the COF is declining. Whether this effect is purely down to the distributed load on the pads due to the play between the frames and the deformations of the machines will be determined in other tests.

4.4. Setup accuracy testing

In the previous section, a slip test was shown in figure 4.9. What is noticed is that the hydraulic clamp pressure is reducing over time. The pressure loss is created by a leak in the hydraulic clamping circuit. The leak is worse at higher HCP and creates uncertainty about the normal force on the pads. Namely, the inner frame of the slip test machine is tilted in the outer frame when applying slip force, as shown in figure 4.12. When the hydraulic clamp pressure declines, the inner frame is assumed to move back further into the outer frame, reducing the normal force on the pads. However, it was unclear whether the inner frame was still able to slide back further into the outer frame or whether is it stuck in place due to friction in the tilted configuration. If the frame is stuck, it leads to an overestimation of all COF since the COF is determined as a certain point in the hydraulic slip pressure, divided by its hydraulic clamp pressure at the same point in time instead of at the maximum clamp force.

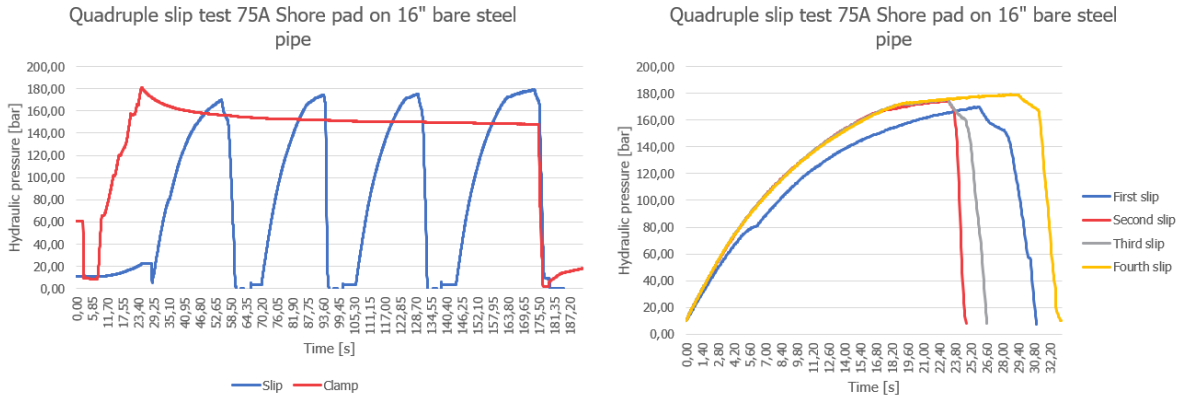

Figure 4.14: Multiple slips in a row, with on the left the entire test sequence, and on the right the slip pressure curves compared.

Two experiments were designed to determine if the machine's inner frame was stuck. In the first test, hydraulic slip pressure is applied and released multiple times in a row. Clamp force is applied, and slipping is commenced. After the slip pressure is applied for a while, pressure is released until the pipe is suspended from the slip platform. This will ensure there is no longer a moment on the inner frame, possibly causing it to stick to the outer frame due to friction. Once the pipe is suspended, slip pressure is reapplied until the pipe slips again, after which it is released, and so on, until the slip cylinder is at the limit of its range. Three tests were run like this, of which the results of one are shown in figure 4.14 on the left. If the hydraulic pressure drops, but the frame sticks, then the first test was performed at a higher clamp force and, therefore, would result in higher hydraulic slip pressures. The figure shows that the inner frame did not stick to the outer frame since the slip force did not reduce. On the contrary, when the hydraulic slip pressure graphs were compared in figure 4.14 on the right, it was found that the slip force only increased. This lower slip force is likely caused by hysteresis, an effect explained further in section 4.6.

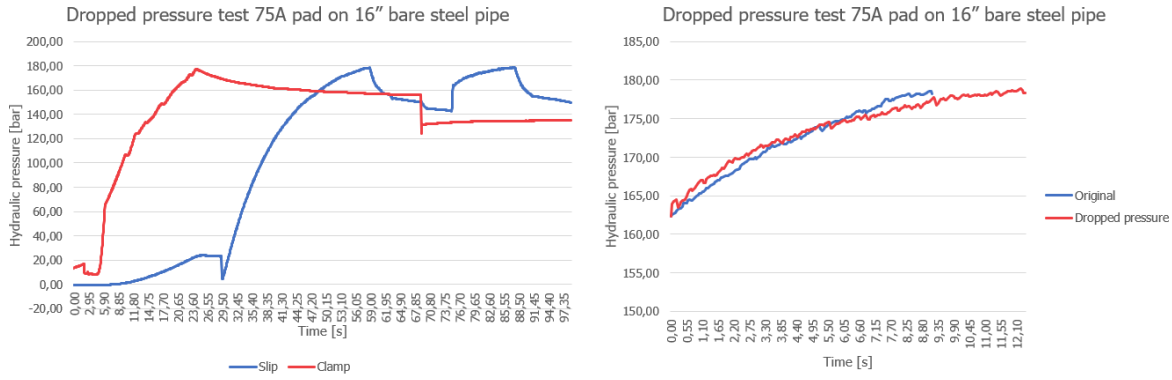

Figure 4.15: Test where the HPC was released briefly to see if the inner frame of the machine was able to move in the outer frame. On the left, the entire set of data is shown. On the right, the hydraulic slip pressure curve comparison is shown.

The result of the second experiment, performed to find out if the machine's inner frame was stuck in the outer frame, is shown in figure 4.15. Testing starts with applying HCP and then hydraulic slip pressure, as in all experiments. When the maximum hydraulic slip pressure is reached, the HCP is released briefly to see if the frame moves. The graphs in figure 4.15 show that the hydraulic pressure drop is roughly 25 bar, similar to the pressure drop over time at higher HCP tests. The result was that the hydraulic piston visibly moved. Therefore, it is improbable for the frame to have been stuck due to friction under shear load. On the right in figure 4.15, it is shown that the dropped pressure also yielded lower slip force than the curve with higher HCP. The difference between the two curves is mainly that the dropped pressure test ran longer, therefore, reaching a similar slip force.

4.4.1. Conclusions setup accuracy testing

With the results of these two experiments, it was concluded that the inner frame of the slip test machine did not stick to the outer frame, and the hydraulic clamp pressure chosen at the same point in time as the hydraulic slip pressure was indeed accurate. Testing can continue without adjustments on the hydraulics of the slip test machine.

4.5. Angled testing revision

All angled tests were redone after the slip test machine was altered. The amount of play between the inner and outer frames of the machine was reduced, and the outer frame of the hydraulically actuated side of the machine was reinforced. The results from the second set of angled tests are shown in figure 4.16. This graph shows the same as the one in figure 4.11, so each dot in the graph is a representative point of a complete graph from raw data. The normal force on the pads is shown on the X-axis, and the COF is shown on the Y-axis.

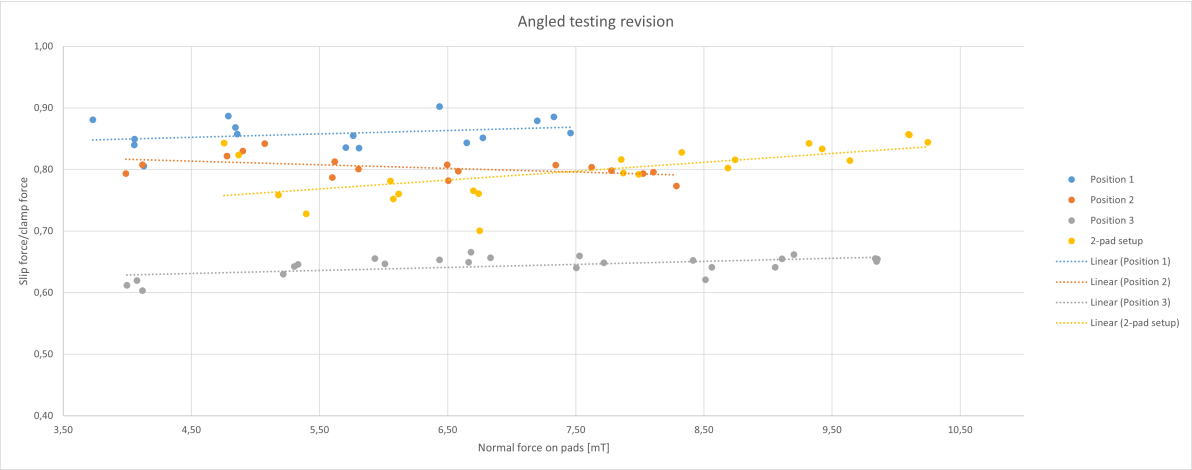

Figure 4.16: Data points from different graphs and different pad positions with trendlines

A few things from the results in figure 4.16 are noticeable. Firstly the data sets of position 1, position 2, and the 2-pad setup are much closer together than before. The sole outlier is the data set of position 3. Secondly, the friction does not seem to go down with increasing force on pads for most data sets. If anything, most go up.

Compared to the previous results of angled testing, the coefficient of friction of the position 1 data is lower than the previous results. An explanation could be that these tests were performed on different days, and friction was different due to ambient factors. The temperature was similar on both days, but the humidity was significantly lower, from roughly 60% down to 45% for the position 1 tests. Another thing that would have contributed is the angle of the pads. This time sheet metal brackets were made to easily preset the angles of the pads instead of resetting the angle with an angle measuring tool. This worked well, but a small mistake was made in the design, causing the angle to be off by roughly 1°compared to the first set of angled testing. The 1°extra offset leads to a less perpendicular force, which leads to a sideways shear in the material, and therefore the COF is slightly lower.

The data of position 2 cannot be compared to the previous data that was corrupted. It can be compared to the rest of the data in the second attempt of angled testing, though. This data set is the only one that does not show a rising trendline. The reason for the very small decrease in COF could be down to measurement errors.

For the data of position 3, one variable changed compared to the other data sets, which is solely applicable to the data set of position 3. From CAD, the estimated pad angle was supposed to be around 48.5 degrees, where its maximum rotation angle was 50 degrees. This was already a small angle that the pad was left to rotate. In practice, it turned out that a thick coating layer over the steel further restricted the angle to 49 degrees. Because of the geometry, this position is also where the angle changes the most when compressing the pads. This led to the pads hitting the maximum angle they could reach. An attempt was made to preset the angle to 43 degrees to see if the angle would stay below 48.5 degrees, but still, it reached its maximum angle in the experiment. Therefore, the pads were left positioned at their maximum angle of around 49 degrees. This does mean that the polyurethane pads are sheared to the side when compressed and then sheared lengthwise when commencing the slipping phase of the experiment. Loading material in shear decreases the real contact area A_r and,

therefore, static friction, as found from the research of Sahli [18]. The shearing in two directions leads to larger overall shear and less grip.

The difference between the trendlines between data for position 1 and that of position 2, and the 2-pad setup can also be explained by the difference in relative humidity. Where the relative humidity was around 45% for the tests of position 1, it dropped to 30-33% respectively for the rest of the tests. Without this drop in humidity, it is possible that the trendlines would be closer together.

As mentioned before, the second thing that stood out was how all values seemed to stay equal or even increase with increasing normal force. This was unexpected since the first set of angled tests showed a downward trend in COF, and all other slip test data from Allseas showed similar trends of decreasing COF with increasing normal force on pads. The machine's improvements seem to affect the results significantly, and the decreasing COF could be largely explained by the distributed load on the pads, as shown in figure 4.13. From video footage, it can be seen that there is still deformation in the test machine. It was later tested that the pads can still make an angle of roughly 0.5°with respect to the pipe, leading to a distributed load. This angle strongly depends on the pad's normal force, the slip force, and the coefficient of friction of the pad.

4.5.1. Conclusions angled testing revision

From the data of the second run of angled testing, it was found that the machine improvements influenced the results greatly. The COF is still dependent on the normal force on the pads but is now increasing instead of decreasing with increasing normal force on the pads. This does not necessarily mean that the COF increases with increased contact pressure on the pads since the contact surface area of the pads also increases with increasing normal force on the pads due to the contact configuration. It could be that the contact surface area increases more quickly than a decrease in COF due to increasing contact pressure, and therefore the overall COF still rises with increased normal force on the pads.

The data from the different positions of the pads was also much closer together than before, and small differences can be at least partly explained by a difference in relative humidity. Lastly, it was observed that the pads were sheared both horizontally and vertically for the position 3 data. The summation of shear led to significantly lower values in friction.

Most importantly, the angled tests confirmed that normal forces are indeed perpendicular to the pads, if not very close. It is, therefore, not unrealistic to proceed with testing with only two pads in the 2-pad setup. From this point on, all testing is performed with only two pads to operate at higher normal forces on the pads.

4.6. 16” bare steel pipe testing

Testing with the 2-pad setup required a new set of values for the hydraulic clamp pressure. In the previous angled testing, the maximum HCP of the slip test machine was not reached in order to compare the results with the angled pads. New test matrices were produced where the HCP of the test setup was maximised and easily compared to the hydraulic clamp pressures in the tensioners.

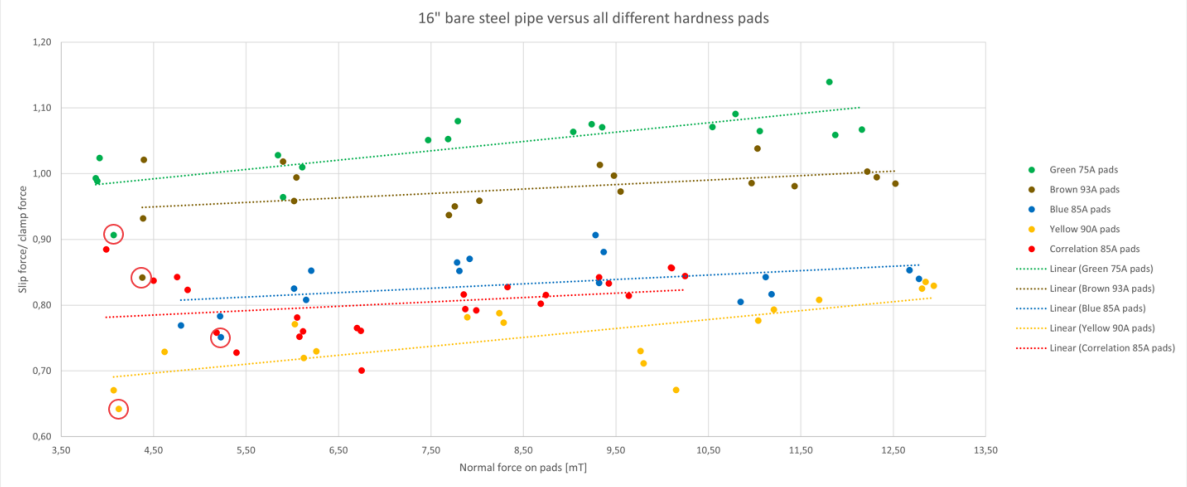

Figure 4.17: Slip test results for all different hardness pads versus a 16” bare steel pipe. The red circles indicate every first test of the different pads.

The results from all different hardness of pads testing versus the 16” bare steel pipe can be seen in figure 4.17. This figure shows roughly the same trend as the angled testing, where the coefficient of friction increases with increasing force on the pads. Next to all data from the tests from different hardness pads portrayed in the figure, the 2-pad setup data from the angled testing revision set is plotted in the figure as correlation data. Though the individual representative points of the correlation data are spread relatively far apart, the trendlines seem to correlate well. Overall the COF of the correlation data is lower than that of the more recent tests. The difference can again be at least partly explained by the difference in relative humidity, where the correlation tests were performed at 33% relative humidity and the new tests at 41% relative humidity.

What is noticed is that the coefficient of friction does seem to depend on the hardness of the pads. Apart from the hardest brown 93A Shore hardness pads, the friction decreases with the increasing hardness of the pads. The decrease of friction with an increase in the hardness of pads is what was also seen in section 2.3 at the lower clamp forces of prior slip tests performed at Allseas. The decrease in friction with increasing polyurethane hardness was also found in chapter 2. These tests seem to confirm the theory. A reason for the hardest pads performing second best could be that this polyurethane molecular formula is optimised for friction. Research from Alberto, discussed in section 2.3, seems to indicate that polyurethanes can have additives that increase the friction of the material without necessarily influencing its hardness.

Some observations were also made during testing versus the 16” bare steel pipe. The order of testing is from the smallest normal forces on the pads towards the largest normal forces on the pads. The first test or set of tests generally seems to yield a lower COF than the rest of the tests. The first test of every different hardness pad is indicated with a red circle in figure 4.17. The exact reason for this is most likely caused by hysteresis or stress softening. The effect of hysteresis was researched by Yang [24], where it was found that in cyclic loading, the material deforms more after repeated loading. The increase in deformation, or decrease of hardness, leads to a higher coefficient of friction, as seen in the experiments on the 16” bare steel pipe.

Figure 4.18: Photo's of brown 93A Shore pad damage, left photo halfway through the test sequence, middle one after roughly three-quarters of the tests and right photo after the test.

Another observation regarding the hardest pad of the four was that although it provided excellent friction numbers, it was slowly tearing up. The effect was noticed halfway through the tests for this pad and closely monitored from then. The expectation was that as soon as the pad is breaking down and some material let go, this material would roll up and act as a lubricant. To see this effect, the material that came off the pad was not wiped off on purpose, but the pads did not show such behaviour. The damage contour shows that there was a distributed load on the pads, indicating that not all play was eliminated from the slip test machine. The damage is formed in the same cone shape, though less sharp, as that of the FEA simulation of distributed load in figure 4.13. There are multiple explanations for the damage to this pad. One explanation was already mentioned in the literature in section 2.3, showing that perhaps counterintuitively, harder polyurethanes can wear faster than softer polyurethanes. Another explanation is that these pads might be very old and wear more quickly due to aged polyurethane.

4.6.1. Conclusions 16" bare steel testing

The tests on the 16" bare steel were designed to determine the influence on the friction of both the normal force and the pad hardness. As seen in the prior angled tests, the COF went up with increasing normal force on the pads for all pads. Since the contact surface area increases at higher normal forces on the pads, it is incorrect to claim that the COF of polyurethane increases with increasing contact pressure. At some pressure, the apparent contact area A_a is equal to the real contact area A_r, but due to the pads and pipe, this will never fully be the case since contact pressure at the edges of the contact surface area is lower than in the middle.

From the tests on 16" bare steel, it also seems that pad hardness significantly influences the COF. From these tests, it cannot be concluded why hardness has an influence. It can be because the apparent contact area A_a is larger for the softer pads, or the real contact area A_r is larger. Most likely, it is a combination of the two contact areas.

The last conclusion is that both hysteresis and humidity likely greatly affect friction. The hysteresis effect quickly disappears when doing multiple tests in a row. The effect of humidity seems to be influential in all experiments.

4.7. 16” bare steel pipe heated pad testing

The heating of pads to gain insight into the effect on the coefficient of friction was a large part of this research. As mentioned in section 2.5, polyurethane is a good insulator. To perform tests with heated pads, it would be convenient to heat pads from within. Since heating pads from within is not easy, it had to be validated that temperature significantly influences polyurethane’s friction performance. Testing of polyurethane was split up over multiple days since it was time-consuming. A flowchart with the testing order and recorded ambient factors can be seen in figure 4.19.

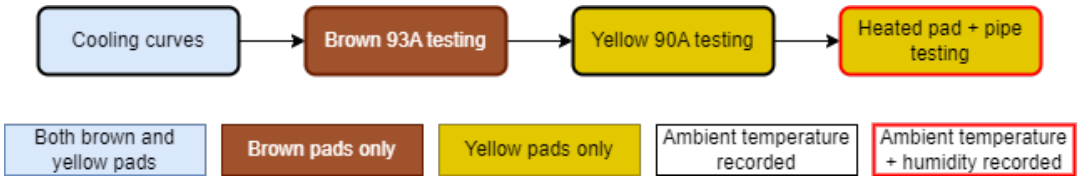

Figure 4.19: Heated pad testing flowchart with ambient factors recorded.

4.7.1. Heated pads cooling curves

It was decided to modify two pads for heated pad testing, namely the yellow 90A Shore hardness pad and the brown 93A Shore hardness pad. The two hardest pads were used since the brown pad was first believed to have a lower hardness. Testing two pads at different hardness would possibly yield different test results. These pads were machined to fit three thermocouples each, both for redundancy and to determine the difference between the core and surface temperature of the pads. The thermocouple distances from the top contact surface of the pads were approximately 1mm, 5mm and 15mm. To make measurements accurate, all thermocouples were placed exactly in the middle of the pad across the width, directly under the surface that would be loaded.

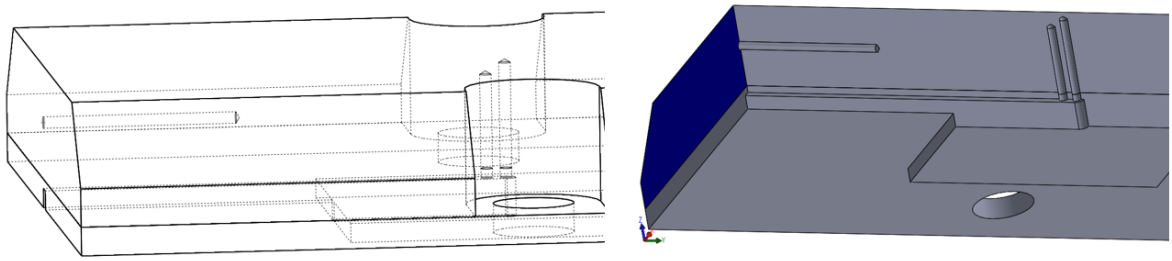

Figure 4.20: Machined parts of the pads where thermocouples are placed at 1mm, 5mm and 15mm from the surface. The figures show the vertical configuration of the thermocouples 1mm and 5mm below the surface and the horizontal configuration of the 15mm below the surface thermocouple.

Modifying a pad in any way alters its behaviour under compression and shearing. Therefore, care was taken to minimise the amount of material that was machined. Because of this, the thermocouples that would sit 1mm and 5mm below the surface were mounted vertically from the back of the pads. The thermocouples placed 15mm from the surface were considered less influential on the deformation of the pad and were mounted horizontally from the side of the pads. The other two thermocouples were mounted vertically. The material that was machined and thermocouple positioning is shown in figure 4.20.

To make the thermocouples function, the ends of the thermocouples were spot welded together. They were tested in boiling water to validate that the welding of the ends did not influence the accuracy of the thermocouples. From figure 4.21 on the right, it can be seen that the temperatures of the thermocouples were all within 1°C, which was accurate enough for a proof of concept.

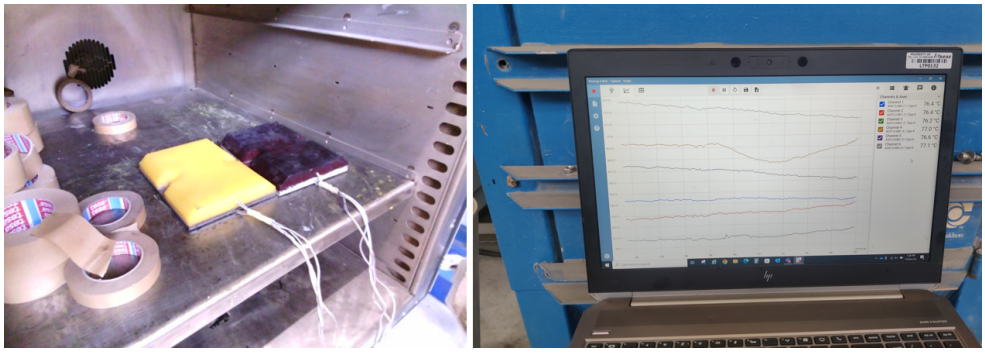

Figure 4.21: On the left, the brown pads in the oven are getting up to temperature. On the right, the temperatures of two sets of pads in the oven.

The first test with the pads with thermocouples was cooling down from high to ambient temperature while recording the temperatures. The cooling curves that were gathered were used to see how long the polyurethane would stay warm at different temperatures. These cooling curves then gave a rough estimation of how much time there was to mount the pads on the crossties and test them at different temperatures. Together with some material properties, an estimate was made of how much power was necessary to keep the pads warm at different temperatures.

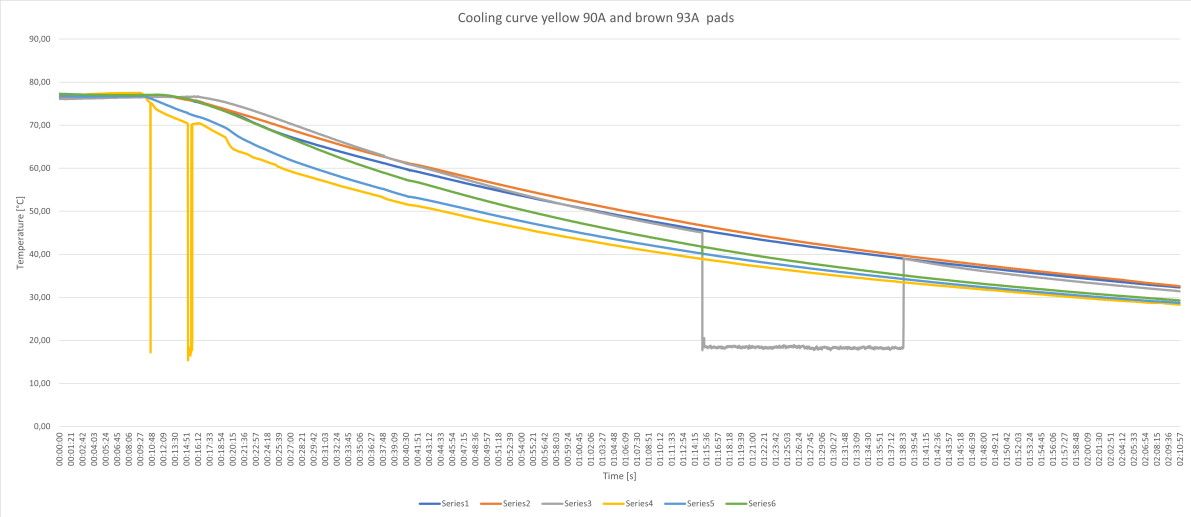

Figure 4.22: Thermocouple data of cooling pads in ambient air from around 75-30°C.

Figure 4.22 shows the results from cooling down the pads. The signals from the thermocouples were not always perfect. The changes made to the brown pad worked out better than those on the yellow pad. The suspicion was that on the yellow pad, the thermocouples were not all reaching their target depth in the pad.

Looking at the data per pad from figure 4.22, it shows that the brown pad its thermocouples showed the correct data. The sensor closest to the surface, in contact with the colder ambient air, consistently had the lowest temperature reading, while the sensor the furthest away from the surface had the highest reading. Apart from a dropped signal around 15 minutes into the dataset for the sensor closest to the surface, the sensor data was satisfactory. The yellow pad its thermocouples showed some unexpected signals. There was no gradual temperature drop when the sensors were closer to the surface. The signal from the sensor furthest from the surface also dropped out during the cooling curve data recording. This data confirmed that the sensors were most likely not installed correctly and that the spot weld on the sensor 15mm below the surface was not flawless. As a cooling curve, the data from the yellow pad was still useful, but the slip testing might be better performed with the brown pad for thermal accuracy.

4.7.2. Heated pad testing brown 93A Shore hardness

So far, all tests have been done on a whole range of different HCPs. Since the entire test schedule could not be tested for the target temperatures, it was decided to choose a HCP of 100 bar to test with. This pressure was chosen since it is quick and easily achieved on the test setup, as well as being representative of forces on pads in tensioners. The target temperatures were chosen as multiples of 10°C ranging from 20-70°C. These values were chosen like this since from section 2.5 the maximum temperature for the pads in use is around 70°C, and the optimum was suggested to be around 60°C.

Earlier, an attempt was made to perform heated pad testing, but the test schedule was not finished, and the results from the tests were inconclusive. Contrary to the earlier attempt of heated pad testing, the pads were heated to a little over 70°C to test from the highest to the lowest temperatures. Since the temperature difference, also known as ΔT, between the pad and the surroundings is largest at the highest pad temperatures, it cools down most quickly at this temperature. This requires short testing times at the highest temperatures and leaves more time for testing when the pad cools down. Because of this extra time, it was also decided to do some tests at 150 bar HCP. Because of the declining temperatures, finishing three tests for every temperature at 150 bar was not always possible.

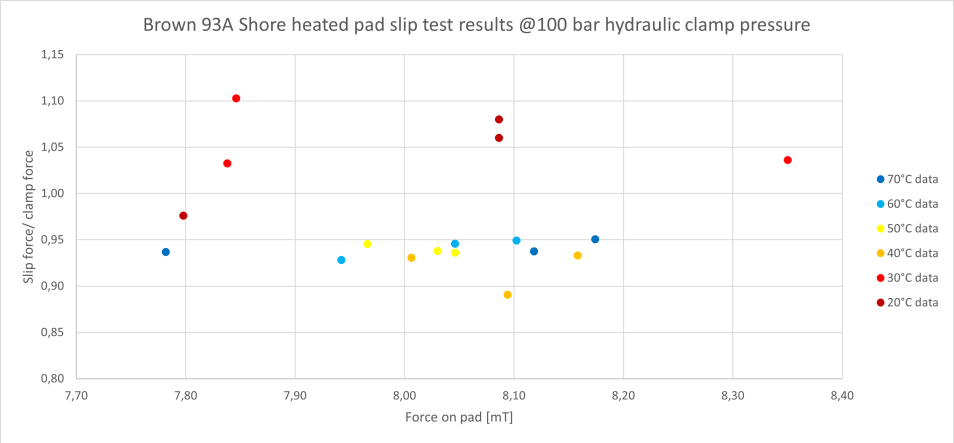

Figure 4.23: Brown 93A Shore hardness pads at various temperatures tested against 16” bare steel pipe at 100 bar HCP.

The heated brown pad testing results at 100 bar HCP are displayed in figure 4.23. From the testing with these pads, it was clear that temperature did have an influence. The peak was not found at 60°C as suggested in the literature, but rather between 20-30°C. The higher temperatures seem to have a narrow spread in COF, compared to the peak in COF around the values for 20 and 30°C.

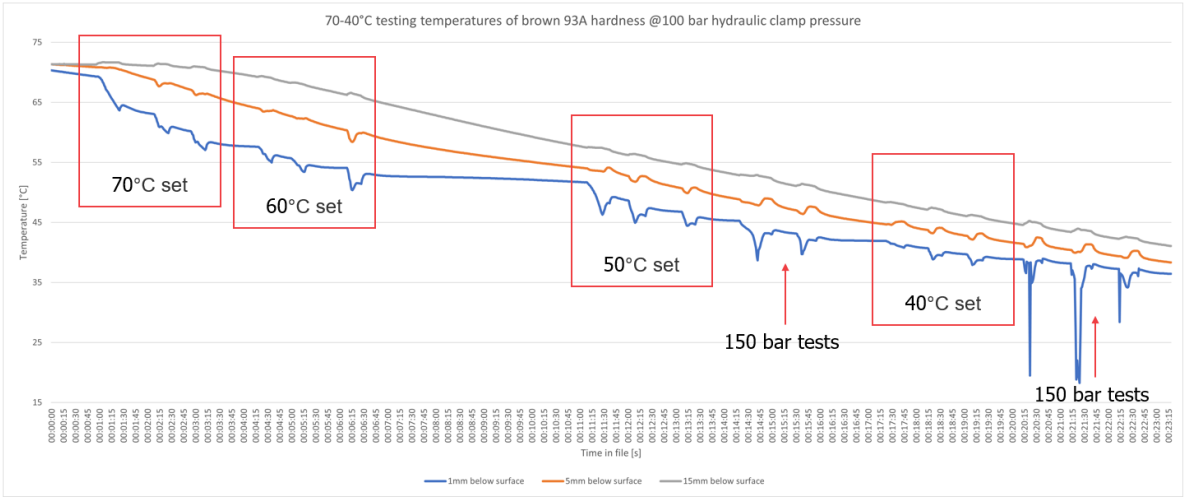

Figure 4.24: Brown 93A Shore hardness pads temperature data tested against 16” bare steel pipe at 100 bar HCP.

As mentioned before, it is hard to determine the temperature of the pads with multiple thermocouples attached. The temperature recording is shown in figure 4.24. Here one can observe that the temperature close to the surface of the polyurethane can differ significantly from the core temperature because the material is such a good insulator. It was, therefore, hard to determine when the different tests should be performed. In the end, there was not much difference in testing from 40-70°C, so the exact temperatures did not matter. An assumption was that the material would heat up while slipping, but no such effect was visible in the data from the thermocouples. The material could still heat up at the surface, but the thermocouples were not accurate enough to measure the phenomenon.

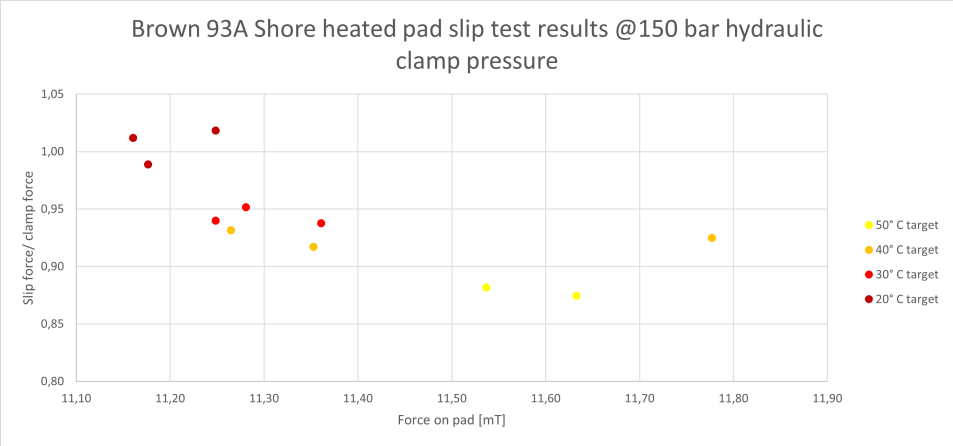

Figure 4.25: Brown 93A Shore hardness pads at various temperatures tested against 16" bare steel pipe at 150 bar HCP.

Tests were also performed at 150 bar HCP. This data set is incomplete since not all tests could be performed in time at high temperatures. The results are shown in figure 4.25. What can be seen in the data is that the friction seems to decrease with an increase in temperature.

4.7.3. Heated pad testing yellow 90A Shore hardness

The yellow 90A Shore hardness pads were tested next. Similar to the brown pads, slip tests were performed at 100 bar HCP and, where possible, at 150 bar HCP. This led to an incomplete data set for the 150 bar HCP, like the ones in figure 4.25 in the case of the brown pads. For this reason, the pads were reheated after being cooled down to 20°C, and all experiments of the 100 bar and most of the testing at 150 bar had been performed. After reheating, the gaps in the 150-bar experiments were filled.

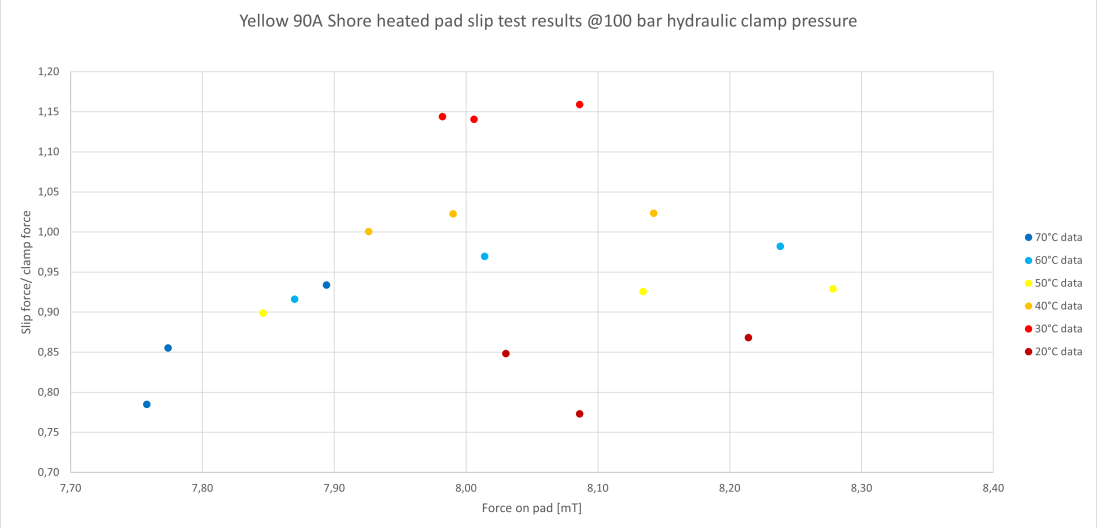

Figure 4.26: Yellow 90A Shore hardness pads at various temperatures tested against 16" bare steel pipe at 100 bar HCP.

The results of the heated slip testing at 100 bar HCP are shown in figure 4.26. The friction of the set of tests at 30°C is significantly higher than the friction at other temperatures. Again, there seems to be an optimum in friction at a certain temperature. Where the optimum for the brown pads was somewhere between 20-30°C, the optimum for the slightly softer yellow pads seems to be around 30°C. As with the brown pads, friction seems to drop with increasing temperature, though there is a larger spread in the data.

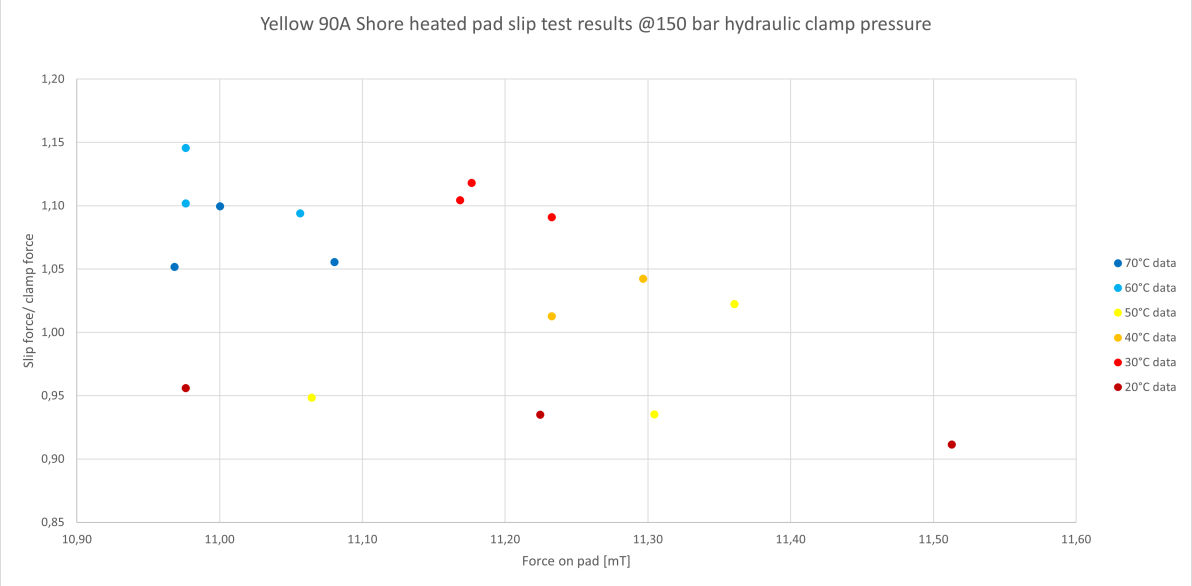

Figure 4.27: Yellow 90A Shore hardness pads at various temperatures tested against 16” bare steel pipe at 150 bar HCP.

By reheating the pads, the full test schedule was also completed for the yellow pads at 150 bar hydraulic clamp pressure to see if there were any significant differences. The results of these tests are portrayed in figure 4.27. From this data, it seems that there is not only a peak in friction at the 30°C mark, found in testing at 100 bar HCP too, but also around the 60-70°C area as found in the literature.

The results that were achieved from the heated pad testing are not entirely accurate since there are important variables of influence, like the pipe temperature. While it is accurate that the pipe was not heated, since it is not heated while laying pipe offshore, the pipe is heating up in repeated testing, thanks to the warm pads. To counter this effect, the pipe was turned to test on a colder surface again. The pipe turning was not noted down, though, so its influence cannot be tracked.

From the start, it was clear that exact friction numbers would not be found with these tests. Cooling of the pads and warming up of the pipe are two continually changing variables that are believed to be of too much influence. The purpose of these tests was to find if heat influenced the friction of polyurethane, which seems to be proven. To further check this influence and to eliminate one variable, namely the warming up of the pipe, it was decided to do more testing with heated pads on a heated pipe.

4.7.4. Heated pad + pipe testing

The last set of heated tests was performed with heated pads from the oven versus a heated pipe. While it is not realistic that pipes would be heated up to increase friction during pipe-lay, the tests were performed to see what kind of influence the heated pipe would have on the COF of the system. As an added benefit, it prevents the pads from cooling down as quickly as testing on a cold pipe. There were some significant drawbacks to heating the pipe, though. The heating of the pipe was done with a torch, which is not very accurate. Another drawback was that the temperature of the pipe was measured with a single thermocouple in the middle of the pipe in between the two pads. Hence, the pipe temperature in contact is not necessarily accurate because of the distance between the thermocouple and the pads.

Since this round of testing depended on the temperatures of both the pads and the pipes, the schedule of testing at 70-20°C in steps of 10°C was scrapped. Instead, the choice was made to start with

continuous testing and, later, when temperatures dropped less quickly, to return to sets at certain ranges.

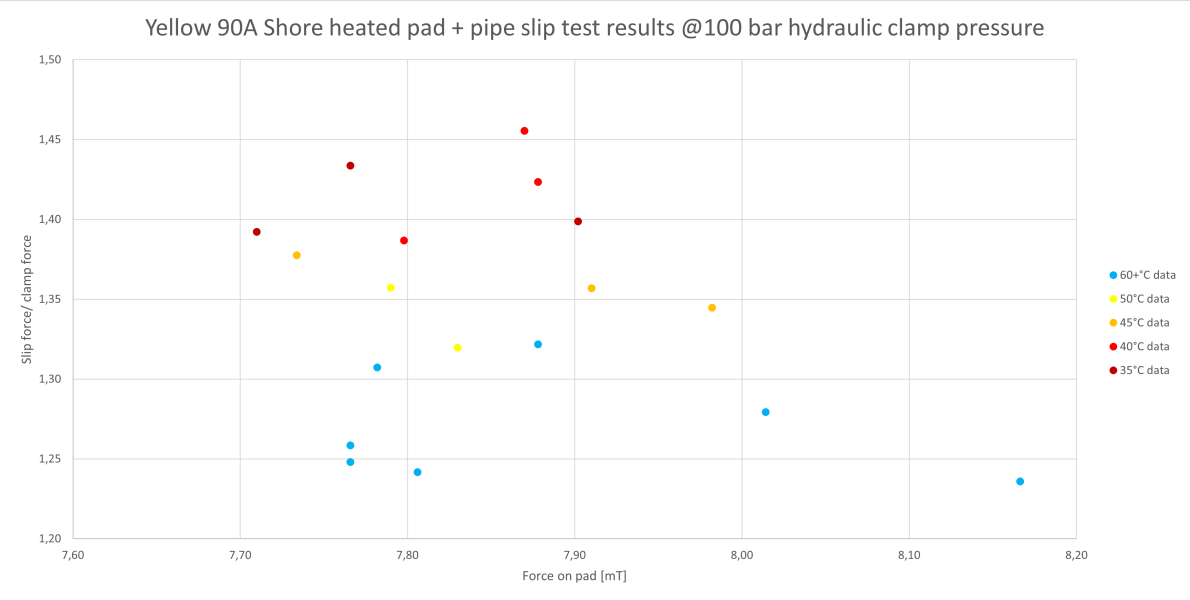

Figure 4.28: Yellow 90A Shore hardness pads at various temperatures tested against a heated 16” bare steel pipe at 100 bar HCP.

The results from slip testing with heated pads and pipe are shown in figure 4.28. The COF of the experiments performed around 35-40°C seems the largest. Furthermore, all values found for the COF are way than before in any heated testing, though this could be due to the ambient humidity being high. Therefore instead of looking at the numbers, one should look at the general trend in friction. By now, there is enough evidence that heating the pads could prove useful, and the new test pads should be fitted with internal heating.

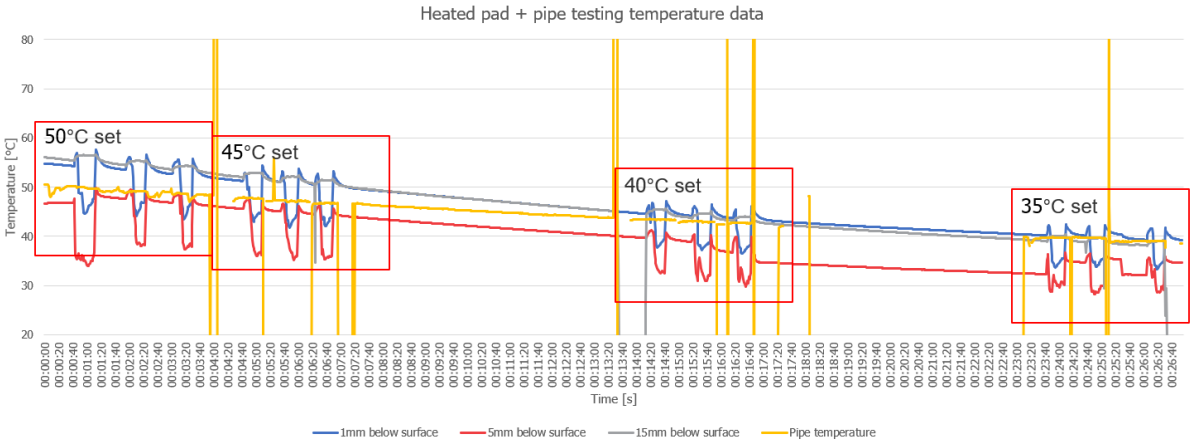

Figure 4.29: Yellow 90A Shore hardness pads temperature data tested against a heated 16” bare steel pipe at 100 bar HCP.

The data from the thermocouples is shown in figure 4.29. What is seen is that when there is more sensor data available, it is not necessarily easier to assign a specific temperature to the slip test. What can also be seen from the figure is the frequently lost signal of the sensor on the pipe. One of the leads was burned off during the pipe heating, causing the noise. Data from the pipe is also likely not very accurate. An effort was made to heat the pipe evenly, but it is likely that there could be a 10 °C between different parts of the pipe.

4.7.5. Conclusions 16” bare steel pipe heated pad testing

The experiments of this section were designed to find out if there was an influence of temperature on the coefficient of friction. The tests were done with two different pads to see if the hardness of the pads had an influence.

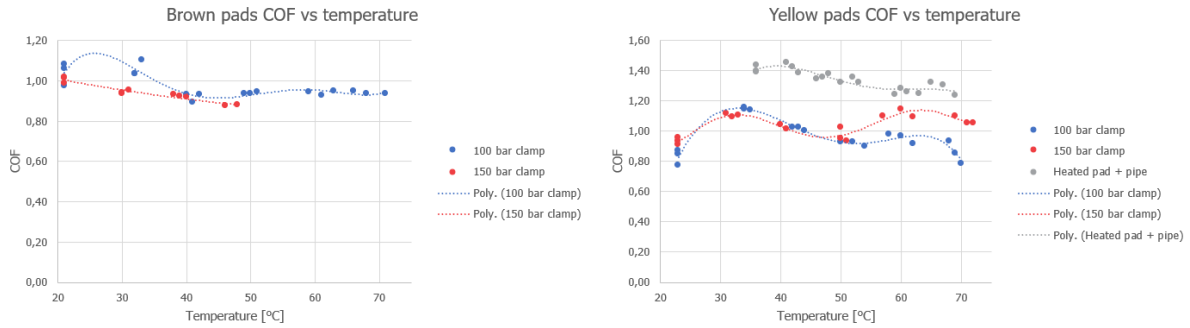

Figure 4.30: Graphs with the coefficient of friction for different temperatures. On the left, the graph for the brown 93A pads. On the right, the graph for the yellow 90A pads.

The test results at different temperatures are put together in figure 4.30. For the brown 93A Shore hardness pads, as seen on the left in figure 4.30, there was a peak in friction between 20-30°C at 100 bar HCP. The data for the tests at 150 bar HCP were inconclusive as it was not finished, but the lower temperature seems to be where the peak is. For the yellow 90A Shore hardness pads, two peaks are seen in figure 4.30 on the right. In all three data sets, the double peaks seem to be present.

The data shows that there is an influence of temperature on the coefficient of friction. Pads with internal heating are designed and will be produced to more accurately find the relation between temperature and friction in polyurethane.

4.8. 12” bare steel pipe testing

Testing on a 12” bare steel pipe was performed to find if the pad friction would change compared to the 16” pipe. Because of the smaller radius of the 12” pipe compared to the 16” pipe, the surface area of contact between the pad and pipe is smaller, leading to higher contact pressures for similar normal force on the pads. To accurately test the effect of only the pipe radius, all variables should remain roughly the same except for the pipe radius. However, keeping variables similar was not achieved. The previous 16” bare steel pipe was oxidised severely. A grinder with a flap disc was used to make the surface as smooth as possible. Grinding the surface did not yield the most consistent surface, so in the case of the 12” pipe, it was decided to use sandblasting to achieve a more consistent surface. The results are shown in figure 4.31. Though the surface was consistent, it was also incredibly rough, reminiscent of coarse sandpaper.

Figure 4.31: Sandblasted surface of 12” pipe.

Testing on the coarse surface of the 12” bare steel pipe was not comparable to the 16” pipe since the surface was much rougher. The 12” bare steel pipe was the last pipe to be tested, which was a good thing. Most of the pads were wearing quickly on the rough surface, which would have made testing after the 12” bare steel pipe difficult to correlate.

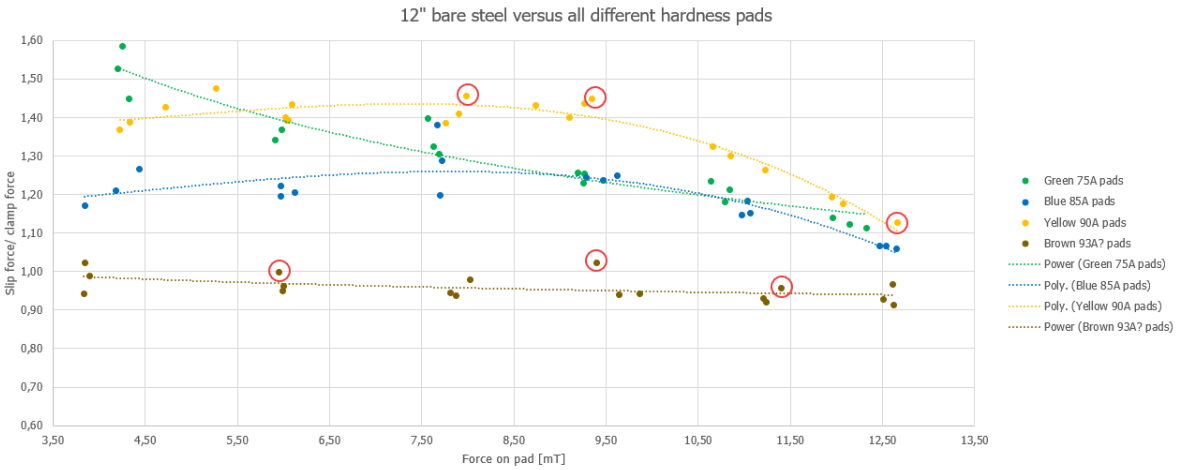

Figure 4.32: Slip test results for all different hardness pads versus a 12” bare steel pipe. Points within red circles are after a pad and pipe wipe.

The 12” pipe testing results are shown in figure 4.32. None of the pads seem to follow the same trendline. Out of the different pads, the hardest brown pads behave most like what was seen before. The second hardest yellow pads trendline is stable until the highest normal forces on the pads are reached, where the COF drops. The drop in COF is not solely down to the pads. The slip test machine

was at its peak of hydraulic pressure that could be supplied. The COF reduces since the hydraulic clamp pressure was increased, but the hydraulic slip pressure could not be increased.

The softest green pads were losing friction rapidly. This could be explained by the coarse surface of the 12” pipe. It was mentioned before that when material comes off the polyurethane, it could roll up and act as a lubricant between the pipe and the polyurethane tensioner pads. The suspicion of the loose material acting like a lubricant is reinforced by the fact that the COF was increased almost every time the pipe was wiped before a test. Wiping of the pipe and pads before testing is shown in red circles in figure 4.32. Accidentally it was not noted when the green and blue pads were wiped.

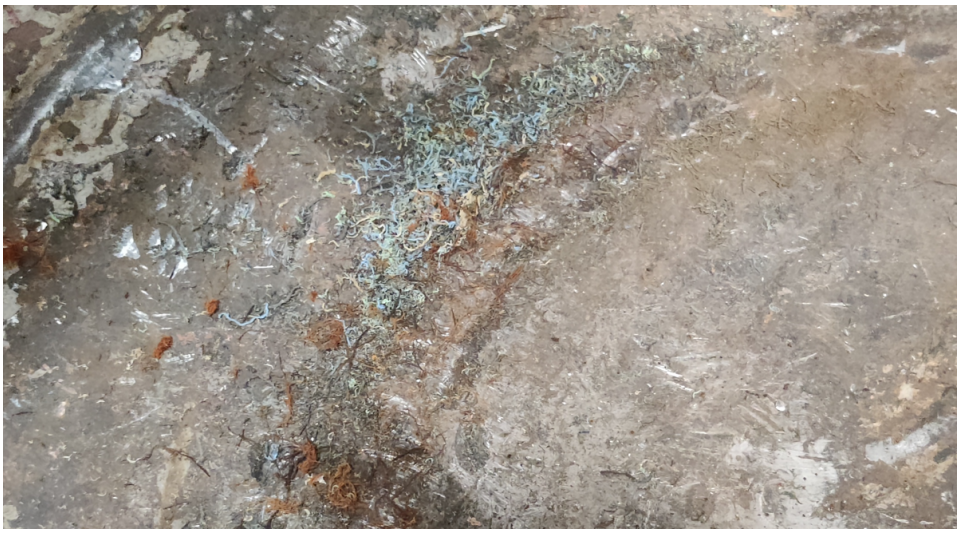

Figure 4.33: Aftermath of testing on the sandblasted 12” bare steel pipe.

In figure 4.33, the pipe plateau is shown below the pads after testing. In the figure, lots of polyurethane debris can be seen. The figure shows that the pads that wore the least were the yellow 90A Shore hardness pads. The other pads all wore down severely. This wear and the loose material acting like a lubricant is likely why the green pads rapidly lost friction, and the blue pads lost friction primarily at higher HCP, where wear is worse. The yellow pads did not wear much. Therefore, little material could act as lubrication between the pads and pipe. This might explain why the friction of these was the best out of the four different hardness pads, especially when the data points at the highest clamp forces are excluded. The hardest brown pads wore the most, but they did so in every experiment before, so their behaviour is unchanged.

4.8.1. Conclusions 12” bare steel pipe testing

For the 12” bare steel testing, the COF went down for all pads with increasing normal force. Its effect is smaller than seen in the graph, though, since the slip test machine could not provide enough hydraulic slip pressure at the last sets of tests. For this reason, the coefficient of friction is roughly independent of the normal force.

The 12” bare steel tests clearly show the influence of pad hardness. The softest material provides the most grip, whereas the hardest provides the least. The outlier is the pad that did not wear significantly. It seems important that in the case of a rough pipe, a more wear-resistant pad is more important than a soft pad, especially at the higher HCP.

The tests on the 12” bare steel pipes yielded some of the largest coefficients seen before. The rough surface could have caused the large numbers, but so could the relative humidity. With 61-66%, this was the most humid testing day. Considering the previous days where humidity improved friction, this must have had some influence.

5

New test pad design

Both literature and FEA were used as a basis for the design of new pads, which will serve as a basis for future work into friction research at Allseas. From the literature, maximising surface area in contact with the pipe and reducing stress in the polyurethane seemed a good choice. Maximising the surface area became key in the design of the new pad. With FEA, it was verified that maximising surface area leads to lower stress in the polyurethane.

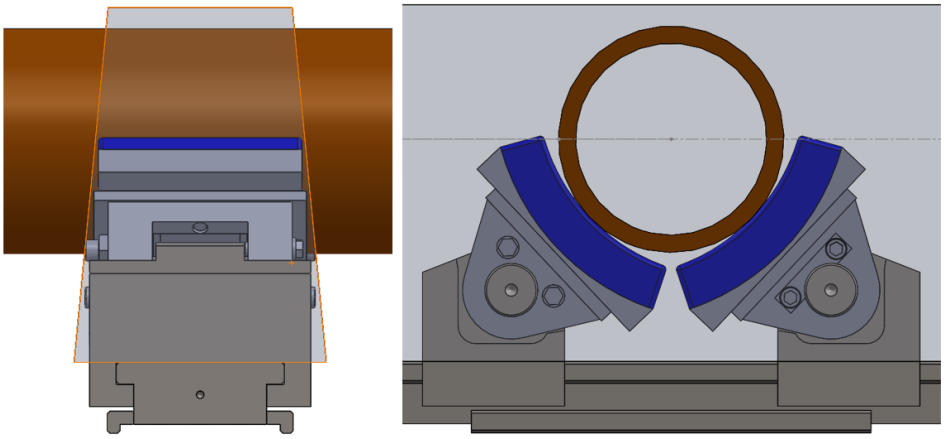

Figure 5.1: On the left is the transparent box from the side, showing the maximum possible dimensions the pad can have. On the right, the height and width restriction of a 10” pipe.

One way to maximise contact surface area is to make the pads as long and wide as possible. There were some design choices made at this point. The length and width of the pads are limited by the positive angles the crossties can make. These positive angles were first seen in figure 2.13 and make sure that the tensioners can still support a pipe if the diameter changes, for instance. A transparent box was inserted in CAD to ensure that the new pads would not stick out of the box to remove the chance of the pads colliding when the crossties reach their maximum positive angle. What can be seen from figure 5.1 is that the wider the pad becomes, the pad length should be decreased to still fit the box. Also, the wider the pads are, the smaller the pipe size that can be supported because of height restrictions. This is shown in figure 5.1 on the right, where a center line is drawn through the pipe. It is shown that, in this case, the unloaded polyurethane would touch the opposite pads. However, since the polyurethane pad can deform, and it is just a small deformation, it is still considered within limits. The pipe in the figure also has no coating, so its size is conservative.

5.1. Curvature

The most influential way to increase the surface area of the pads is to make the pads follow the curvature of the pipe. This immediately poses a problem since there is not one single pipe size that the vessels should be able to lay, but rather a range. For the vessel in focus, the range of pipes that can be laid is 6-68”. If one made a curved pad that can be used for all the pipes, one would have to choose a curve of 68”. This curvature will still result in a larger surface area than a flat pad for even the smallest 6” pipe, but improvements are marginal. Therefore, It was decided to split the pipe sizes into different groups, each with its own set of pads.

The groups were originally decided to be 6-16”, 16-32” and 32-48”. That means there is still a range of 48-68” missing, but this range was neglected for multiple reasons. First of all, the biggest pipes laid by Allseas are around 48”, nowhere near what the vessel is supposed to be capable of. As mentioned in the introduction, these large pipes tend to float since their wall thickness is small compared to their diameter. A concrete weight coating is used to keep the pipes fixed on the seabed. This concrete coating is very rough and offers plenty of grip on the current pads, omitting the need for new pads. The same reasoning could likely be used on the group of 32-48”, but this was not the group of main interest and pads were not designed for it.

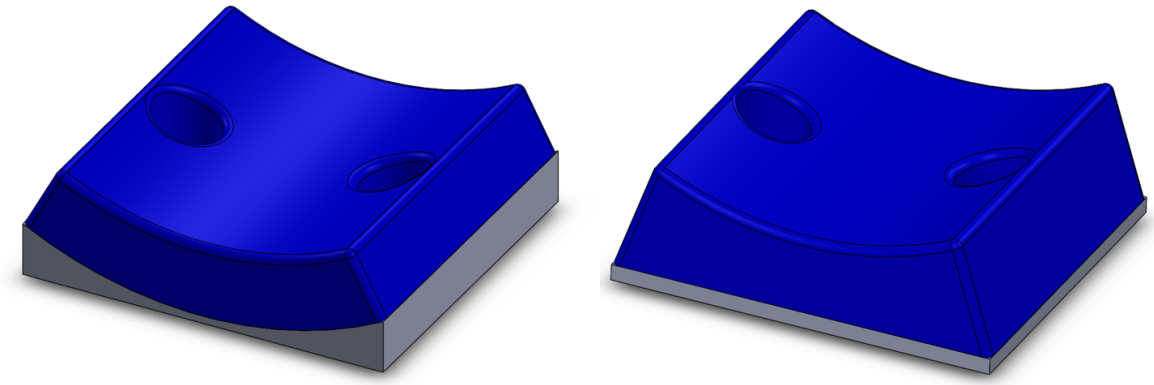

Figure 5.2: Two resulting designs for 10-16” pipe. On the left, the even polyurethane pad and on the right, the uneven polyurethane pad.

The groups of interest were mainly those of 6-16” and 16-32”. Out of the two the smaller one was worked out further since it was easier to produce and test. There was a problem when designing a pad for the 6-16”. To make the pads fit the 6” pipe, the width could not be larger than the original pads because the pads would touch. Therefore, the target size was decreased to 10-16” to widen the pads and increase the contact area. As shown in figure 5.2, there were two resulting designs from CAD. The difference is that the first one has a curved backplate, resulting in a 50-millimeter, even polyurethane layer. In contrast, the second pad has a flat backplate and an uneven layer of polyurethane with a thickness of 50 mm in the middle that forms the curved surface. Theoretically, the first pad would better distribute the pressure from the pipe, but the curved steel backplate would be much more expensive.

5.2. FEA new curved pad designs

To try to make a comparison between the two curved pad designs, they were tested in MSC Marc Mentat. There is one different variable in the results of the two sets. Due to an unidentified cause, there was an error in the 10mm mesh of the curved pad with an uneven polyurethane layer. This meant that the mesh size had to be reduced to a maximum of 9.5 mm instead of the maximum 10-mm mesh size used for the pad with an even polyurethane layer. As seen from chapter 3, this can influence the results slightly since simulation results were not converged. For extra clarity, the original PS pad with the same hardness and mesh size is also shown, all with the same scale for the Von Mises stresses in the material. For all FEA simulations in this chapter polyurethane of 75A Shore hardness was used.

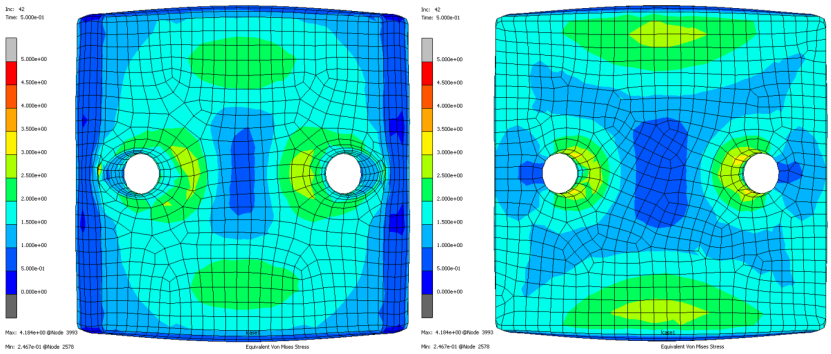

Figure 5.3: Curved pad design with curved backplate versus 16” pipe. On the left, the front and on the right, the back of the pad.

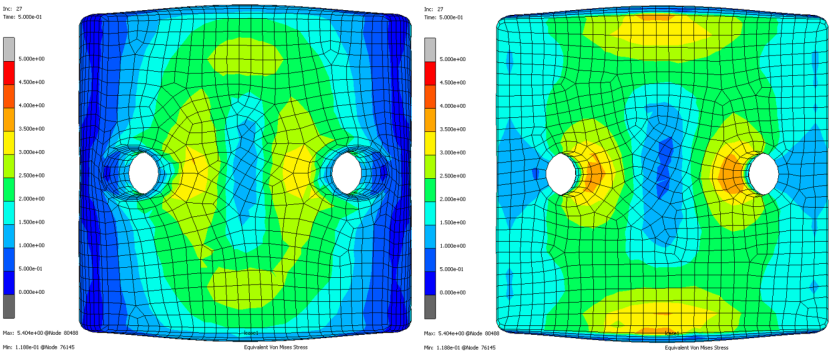

Figure 5.4: Curved pad design with flat backplate versus 16” pipe. On the left, the front and on the right, the back of the pad.

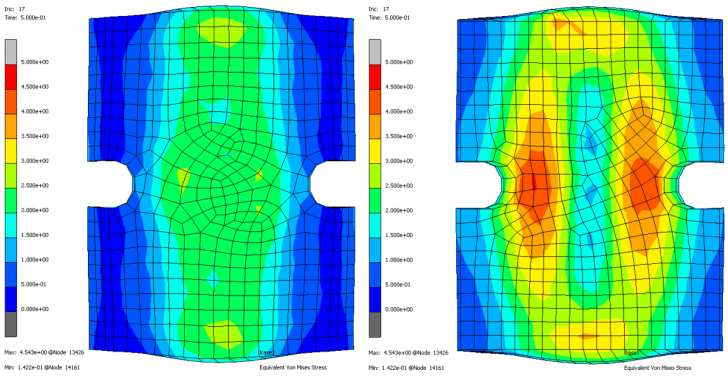

Figure 5.5: Original pad design of PS versus 16” pipe. On the left, the front and on the right, the back of the pad.

In figure 5.3, 5.4, and 5.5, the results from the FEA simulations are shown. The same load and material properties as before are used, with a mesh of maximum size 10 mm (9.5 mm for uneven polyurethane pad). For ease of comparison, the same scale is used for the different figures. The colour scales of the figures are, therefore, directly comparable.

Looking at the results of the FEA, it is immediately noticeable that the curved pad with the even layer of polyurethane seems to come out best in the comparison of the three pads. Stresses are the lowest in both the front and back of the pad; therefore, friction is likely the highest. It is not as clear to see what pad is performing second best. There are spots at the front of the pad where stresses are higher on the curved pad with a flat backplate than the original pad, suggesting lower friction. In turn, though, the overall contact surface is much larger, which would suggest higher friction.

Another result from the FEA is that the stresses at the backplate are greatly reduced in the curved designs. This is not necessarily because of the curved design but rather because of a thicker polyurethane layer, making it easier for the stresses to distribute through the material. It can also be seen that stresses are primarily concentrated around the bolt holes for the curved pads. This is not surprising since gaps in the material are usually where stresses build up. The new pads have a smaller hole for the bolts. In the figures shown in this section, the bolt holes were conical, which was believed to be needed for manufacturing. After talks with a polyurethane producer, this feature was removed, but because of time restrictions, not all simulations were run again.

One could argue that it is not a fair comparison to test a 16” pipe on curved pads that have almost the same curvature of 17”. Therefore another set of simulations was run for a smaller pipe size. The size of this new pipe was chosen as 12”. This pipe size was chosen because it was the same size as the pipes tested in Heijningen. From past FEA simulations performed at Allseas, it follows that the curvature of the pads would still benefit the smaller pipe sizes.

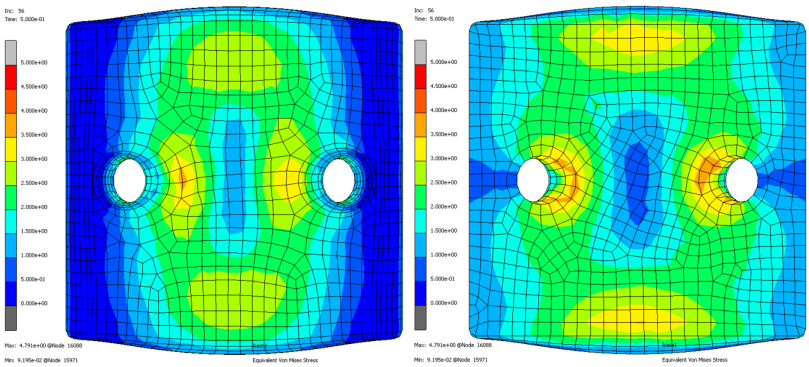

Figure 5.6: Curved pad design with curved backplate versus 12” pipe. On the left the front and on the right the back of the pad.

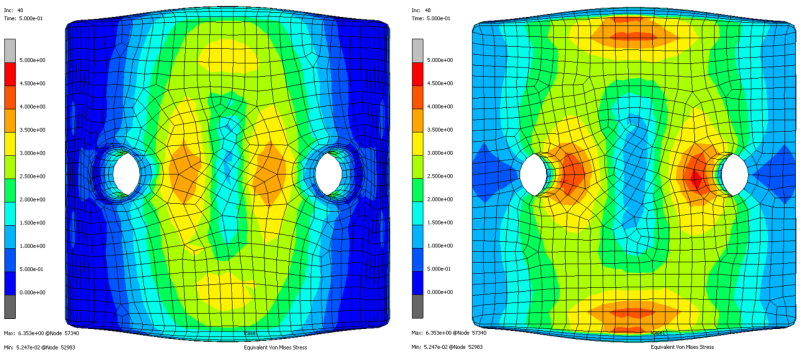

Figure 5.7: Curved pad design with flat backplate versus 12” pipe. On the left the front and on the right the back of the pad.

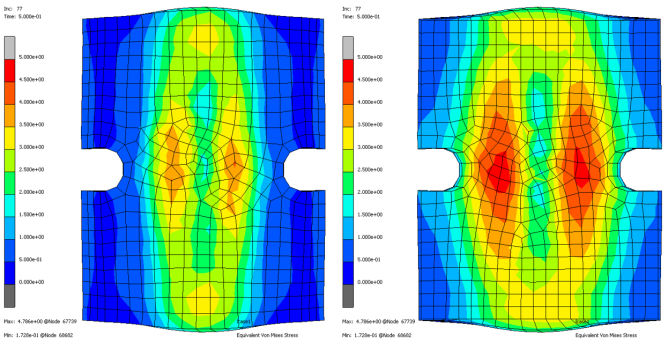

Figure 5.8: Original pad design of PS versus 12” pipe. On the left the front and on the right the back of the pad.

Since the scale is kept constant, figures 5.6, 5.7, and 5.8 can be directly compared to each other and versus the results of the 16” pipe. What can be seen is that the pad with the curved backplate is again the obvious winner in terms of the lowest stress concentration. It is again likely to yield the highest friction of the three pads. The second best pad based on contact patch would be the curved pad with a flat base. The back of the curved pads shows some stress concentrations along the front and rear sides and near the bolt holes again. Stress concentration at the front and rear of the pad should be minimised since this is where the material bonding with the backplate is most likely to fail.

Ultimately, the choice was made to produce the curved pad with a flat backplate. This was mainly because of the ease of manufacturing. Producing a few pads with curved backplates would be expensive, so it is unrealistic to expect multiple tensioners to be filled with pads with such curved backplates. With realism in mind, the choice was made to have some of the curved pads produced. Besides complexity in manufacturing, another advantage of this curved pad is that it is not necessarily bound to the maximum pipe size corresponding to its radius of curvature. The stress distribution might even improve when loading the pads with, for instance, a 20” pipe. This is because the material on the side is thicker than that in the middle, allowing it to deform more and, therefore, distributing stress more evenly.

The newly produced pads will be 78A Shore hardness, close to the 75A Shore hardness materials used in the FEA simulations. The literature showed that polyurethane can age, and material properties can change over time. The exact age of the polyurethane pads that were tested is not clear. Therefore, it is not known whether a fair comparison can be made between the old and the new polyurethane. Next to that, the different pads were made by different polyurethane producers. To make a fair comparison of geometry only, some PS pads were ordered next to the curved pads consisting of the same polyurethane.

5.3. Internal heating wire

From experiments at different temperatures, it was found there was an influence of temperature on friction. To better control the pads’ temperature, they must be heatable instead of putting them in an oven and then performing tests. It was found from previous heated testing that it was not easy to determine the temperature of the pads. In section 2.5, it was found that polyurethane is an excellent insulator. Since the polyurethane of the new pads would be thicker than the old pads, it was decided not to heat the baseplates but rather to heat the polyurethane from within.

With the cooling curves obtained in testing, the known masses, the ratio of polyurethane to steel, and the surface area of the old pads, a rough calculation was made to estimate the power requirements of the new pads. It was calculated that the new pads would need around 1.5W/K above ambient temperature. The calculations were not accurate, so a conservative estimation of 100W of heating per pad was made. The heating power was estimated conservatively since the pads would be tested against cold pipes. Therefore the pads will lose temperature more quickly than in the obtained cooling curves from the current pads.

It is easy to insert something in polyurethane pads when they are produced. Polyurethane enters the mould as a viscous liquid. After pouring the polyurethane, it hardens when it cools down and is cured. There were some challenges with internal heating, though. First, everything that one casts into the polyurethane influences its mechanical properties. With this in mind, it is not advisable to use commercially available heating mats since they are prone to get damaged as soon as one loads the pads in shear. The focus was shifted to a heating wire, which provided the next challenge. The heating wire that one wants to cast into the polyurethane must retain its shape when the polyurethane is cast around it. Also, the dimensions of the heating wire cannot be too large because of the risk of influencing the pads’ load-bearing properties. On the other hand, the heating wire should not be too small since local stress around the wire becomes large and can cause the polyurethane to tear internally.

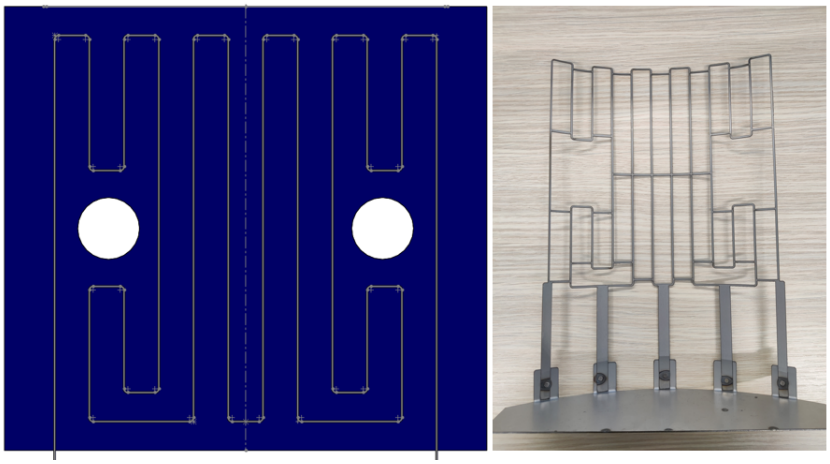

Figure 5.9: On the left, the pad where in grey the contour is shown that the heating wire would follow. On the right, a curved test frame that supports the heating wire is shown.

Since no commercially available solution was found, the choice was made to use nichrome resistance heating wire and to form it into a shape capable of heating the entire pad surface. To reach the 100W potential, roughly 2.5m length of wire in the pad was necessary. The pattern on the left in figure 5.9 was followed to reach this length. Since the pads were curved and to ensure that the pad's surface would be heated evenly, the wire needed to follow the curve of the pad's surface.

The nichrome wire is bendable in the right shape but is quite stiff and, therefore, hard to shape accurately. The choice was made to make a frame where the wire could be wrapped around to shape it. In this way, it was also easier to make the wire follow the curve of the surface. Since it is important not to influence the polyurethane pad too much, the frame was laser-cut from steel. This material was strong enough to mount the stiff nichrome wire on at a curve and could be made small enough not to influence the polyurethane too much. A prototype frame made to support the wire is shown in figure 5.9 on the right. The drawback of using a steel frame is that it conducts electricity better than the nichrome wire, so if it made contact with the wire, it would short out. This meant that the frame would have to be isolated from the wire.

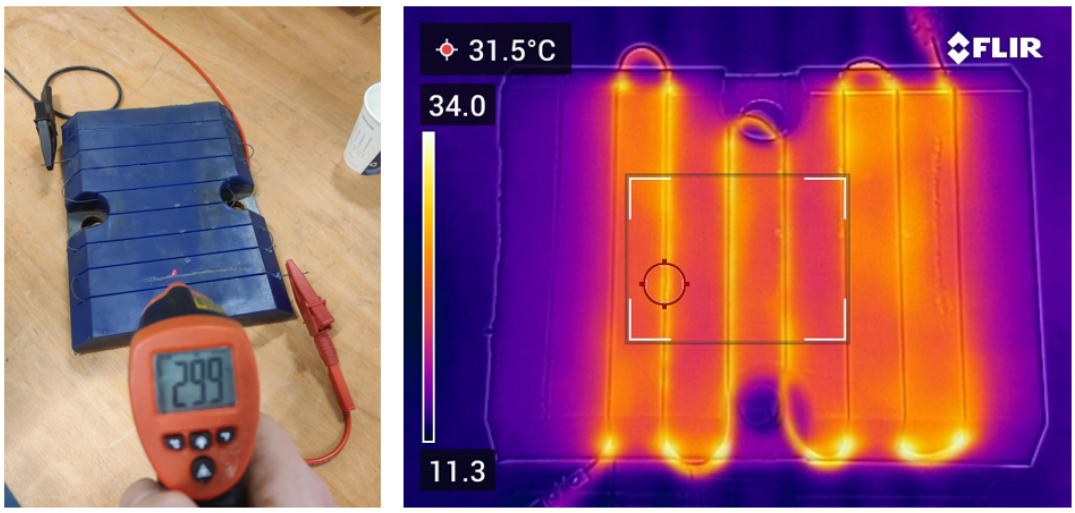

Figure 5.10: Test pad with heating wire fitted. On the left, it is shown with an infrared thermometer; on the right, the thermal image of the complete pad is shown.

At the same time as the production of the frame, an attempt was made to prove that the concept worked. An old pad was cut so that the nichrome wire could be fitted in it. This was tested because the wire diameter was quite small, and there was a chance that if the surface area of the wire was small,

and the polyurethane is an excellent insulator, the wire could not transfer its heat. This would mean the wire heats up to hundreds of degrees, melting the polyurethane around it. The results of this test pad are shown in figure 5.10. What can be seen in the figure on the right is how good of an insulator polyurethane is. In this case, the heating wire was spread further apart than in the new curved pads, but looking at the left side of the pad in the right figure, the heat does not travel far through the material. Now it was proven that the heating worked and that the power draw was only moderate before the wire melted the polyurethane, and production of the backplates was started.

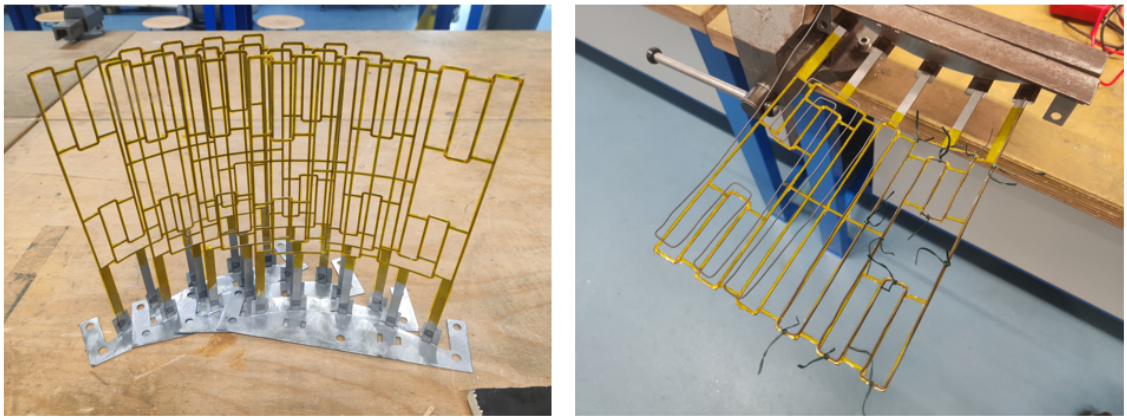

Figure 5.11: On the left, four frames are wrapped with Kapton tape to provide isolation. On the right, the process of mounting the nichrome wire on the frames before glueing it in place.

Frames were laser-cut and wrapped in Kapton tape, a special tape often used to isolate electronic components capable of withstanding a few hundred degrees of temperature. The result of this is seen in figure 5.11 on the left. After this, the pre-shaped wire was fixed to the frames, as seen in the same figure on the right. After the wire was fixed temporarily, it was glued to the frame permanently.

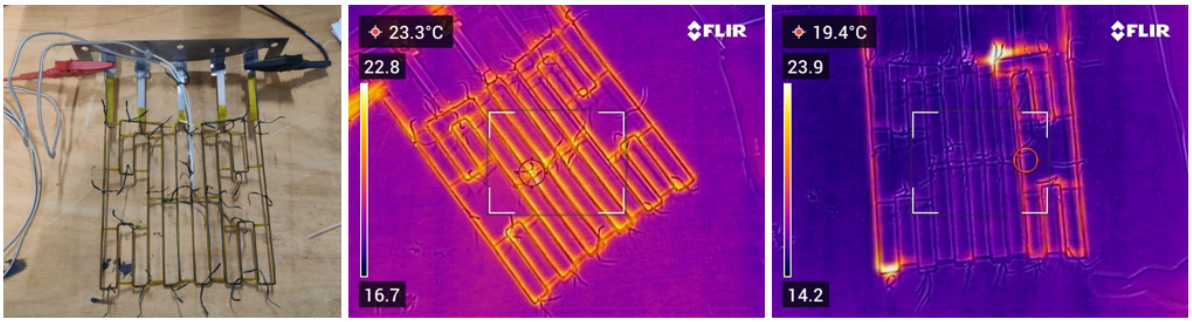

Figure 5.12: Last test of heating wireframes. On the left is the test setup, the intended result in the middle, and a short circuit on the right.

After the frames were fully assembled, they were tested again for shorts. When cast in the polyurethane, a short would not be fixable anymore. Therefore, it was absolutely vital that these frames were not shorting out, as shown in figure 5.12. Barely visible in the figure is that next to the heating wire, also two thermocouples were fixed to the steel frames. One of the thermocouples is placed directly on the wire to ensure it does not reach temperatures over roughly 130 °C, which would melt the polyurethane. The other thermocouple is placed between the heated frame and the surface, roughly 5mm below the pad's surface.

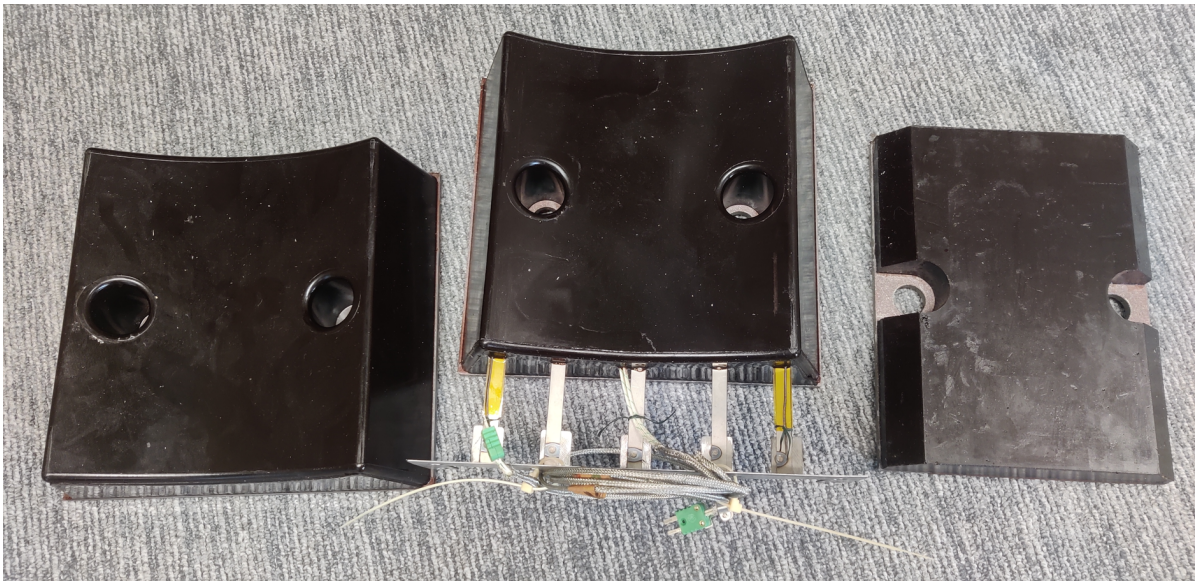

Figure 5.13: New pads delivered with on the left the curved pad, in the middle the heatable curved pad, and on the right the current PS pads to be able to compare geometry in testing.

Next to the pads that had the heating frames cast in them, another set of the same curved pads was ordered, so the influence of the metal frame and heating wire could be compared to a full polyurethane pad. Next to the two sets of curved pads, another set of current PS pads was also ordered. This was done so the variable of material was taken out of the equation, and solely the difference between two pad geometries could be tested. Figure 5.13 shows all three different pads. Due to time constraints and the wait for a new test setup, test results from the new pads are not part of this thesis, but instead, as mentioned before, the new pads will serve as a basis for future friction research at Allseas. The combination of being able to heat the pads and using a curved surface will provide more insight into friction behaviour between tensioner pads and pipes.

6

Discussion, conclusion and recommendations

6.1. Discussion

The aim was to find data for the static friction of polyurethane tensioner pads. The subject was first studied through literature and then full-scale tested. From the literature, it was learned that reducing the number of variables is important when testing the friction of polyurethane. Accurate numbers for static friction were not found due to the manner of sliding testing. It is impossible to accurately find a static coefficient of friction by only monitoring the hydraulic pressures of the test setup. Moreover, inaccuracies in the test setup led to an increased amount of variables. What was found was behavioural trends of polyurethane tensioner pads loaded against steel pipes. These behavioural trends might be indicative of tensioner pad behaviour in practice.

The friction of polyurethane can differ significantly. The variables that were tested all had a significant influence on the friction performance of the pads. Increasing normal force on the pads was also found to increase the COF, albeit this was most likely due to an increase in contact surface area. Softer grades of polyurethane generally provided better friction too. The geometry of pads was studied from FEA, and the results were not validated. Still, by changing the contact configuration, it is possible to decrease stresses in the polyurethane and, therefore, to increase friction. The last variable of the polyurethane that was tested was the temperature. The temperature was found to have an influence, but the results are unreliable. It was also found that relative humidity was an influential factor in the friction of polyurethane.

The test results indicate that increased normal force led to an increased coefficient of friction, which contradicts the literature, where most research shows a decay in friction. This contradiction in friction can be explained by an increase in contact surface area and the relation between apparent contact area A_a and real contact area A_r. The coefficient of friction was found to decline when A_a is near A_r. Since the pads were compressed more, A_a is continually increasing. Likely, A_r is also increasing, but not necessarily at the same rate. An attempt was done to measure the apparent contact area A_a, but the results were deemed inaccurate and were not published in this report. Since the contact area is unknown, it is impossible to link contact pressure to a friction coefficient decline, as found in the literature.

The geometry of the pads was only tested in MSC Marc. Testing with the new pads will more clearly define the influence of geometry. With the new pads, it is also possible to accurately tell the influence of temperature on the polyurethane since the pads can be tested repeatedly at the same temperatures. Because of the times in between tests due to the cooling of the pads, hysteresis might have played a big part in the results of heated pad testing. Next, the two thermocouples inside the pads will make it easier to determine the pad temperature than the three thermocouples placed in the current pads.

From the heated testing, the temperature window seems to change slightly with the applied normal

force, but not in a clear way. Changing the temperature of the pads might have changed the pad's hardness slightly. Stick-slip effects were less prominent when testing the yellow 90A Shore hardness pads at higher temperatures, indicating a possible softening of the polyurethane at higher temperatures.

Relative humidity and ambient temperature were first measured as a backup, so a difference in humidity or ambient temperature could explain small changes in friction. It, however, proved to increase the coefficient of friction. The ambient temperature was not changed much during the testing period, so its influence is still unknown.

Though not a main concern of this thesis, it was shown that wear is also important in the friction of polyurethane tensioner pads. On the rough 12" pipe, wear particles significantly reduced the pads' friction. In the tensioners, wear will be less present due to the smaller slip distance, but it should be monitored.

The results from this thesis showed that the current way of testing at Allseas is unreliable and many factors that were not cared for are of great importance. A new test setup is created because of the findings of this thesis. This will improve the coupling between tensioners in practice and testing onshore. Another implication is that ambient factors should be monitored on ships since they might play a crucial role in the friction of the tensioner pads. Hysteresis was also an effect that was never considered, but it significantly affected friction in the first few test runs.

Keeping variables to a minimum was not achieved. Variables that could and perhaps should have been constants were the pipe surfaces, test setup rigidity, and large relative humidity differences. Every experiment had multiple variables, making correlations between different experiments unreliable. The most reliable results were achieved on the 16" bare steel pipe since pad damage on this pipe was minimal, therefore not introducing loose particles acting as lubrication. The results found at larger normal forces could still be conservative because of the deformations of the test setup.

The relative humidity should have been recorded better. Its influence on friction was underestimated if it was solely the humidity and not other ambient factors. Relative humidity was measured once daily, or once for every set of tests, instead of for every experiment. Measuring the humidity for every experiment might have influenced the differences between the friction of different hardness pads.

Instead of normal force, contact pressure may have been a more clear variable in determining an influence on friction. The pads should have been tested on a flat piece of steel to measure the influence of contact pressure. In this way, it might have been possible to find at what contact pressure the apparent surface area is similar to the real surface area. Calculating the contact pressure from the Hertz contact formula is also possible, but then the pads' indentation must be measured accurately.

6.2. Conclusion

The research question that was answered in this thesis was:
What is the influence of normal force on the pads, pad hardness, pad geometry, and pad temperature on the friction performance of polyurethane tensioner pads?

The literature suggested that increased normal force leading to increased contact pressure could negatively affect the coefficient of friction of polyurethane. In the experiments performed, the coefficient of friction is more consistent and rises slightly rather than falling.

Pad hardness does seem to influence the coefficient of friction. The literature indicated that softer polyurethanes generally have a higher coefficient of friction than the harder varieties. In testing, it was also observed that the softer polyurethanes provided more friction than the harder polyurethanes.

The influence of geometry can only be answered by the literature and FEA simulations since testing with the new pads is reserved for future research. The geometry is important since it determines the contact configuration between the pad and the pipe. It was found from FEA simulations that increased surface area for the same normal force lowered the contact pressure. Another important factor in geometry is the pad thickness. When pads are thicker, the stresses in the material are better distributed through the pads, and friction is increased.

The influence of temperature seems to be the least straightforward. There is definitely an influence

of temperature on friction. Testing showed that two different polyurethanes seemed to have narrow windows of increased friction, depending on the material. A more definitive answer to this question can be given after testing with the new pads since they are continuously heated from within.

From testing, it seems that relative humidity was one of the most influential, if not the most influential, factors in the friction of polyurethane. In literature about polyurethane specifically, humidity was not mentioned as a factor of influence. It could be that there was another environmental factor at play that was not recorded. Still, it does not seem a coincidence that friction increased every time the humidity was significantly higher.

6.3. Recommendations

The first recommendation is to build a new test machine for tensioner pad testing. The process of designing a new test setup has already been started at Allseas, taking many findings from this thesis and applying it to the new concept. Many improvements can be made to the current test rig. The most important one is machine rigidity. A new hydraulic system controlled automatically instead of manually would also be an improvement. If one wants to find static friction, it should also have a slip cylinder controlled by hydraulic pressure instead of flow volume unless the volume is precisely controllable and the system has no leaks, so a certain pressure can be applied and kept constant. It is also highly advisable to upgrade the measuring tools on the test bench. Sensors should measure the distance slipped, the pads' shear angle, and the pads' indentation. Also, load cells should measure the force on the pads instead of hydraulic pressure.

The next recommendation is to test the new pads produced for this project. Testing the new pads should clarify the influence of geometry and temperature further. It is not recommended to test the new pads on the current test setup because there is a chance of damaging them while not extracting the data necessary to make clear claims regarding friction.

Another recommendation would be to place the test setup in a room where the climate can be controlled. The day-to-day differences in the hall where the current machine was positioned were massive, probably largely due to the differences in humidity. When these environmental variables can be controlled, testing is hopefully more repeatable. The conditions on the pipe-laying ships should also be measured to better correlate results between testing and practice.

The original test plan also had wet tests planned, meaning the pads would be intentionally wetted to simulate what would happen if a pipe is pulled back from the sea, for instance. It is advisable not to test with tap water but with seawater since it can have all kinds of living organisms that could influence friction beyond what one would see from tap water. The wet testing could then be done against coated pipes to add to the realism instead of using a bare steel one, which would oxidise anyways.

It is also advisable to use smooth steel pipes that are new. At the start of this project, the possibilities of using pieces of pipe were unknown. The pipes tested were not comparable in roughness, so their test results were not comparable. It is still interesting to see what happens when testing against a rough pipe and a slightly less rough piece of pipe, but when the point is to test the geometry, the results become irrelevant.

As mentioned in the discussion, it might be useful to test the effect of contact pressure on the coefficient of friction using a flat piece of steel instead of a round pipe. Combined With the measured indentation of the pads on a new test setup and the Hertz contact formula, the friction of round pipes on flat pads could be explained better.

There are plenty of potential influences not measured. Another possible factor of great influence is vibration. On board the pipe-laying ships, there are vibrations from ship engines, vortices around the pipe, and other equipment. It might be interesting to measure these vibrations and replicate them in the test setup to measure their influence.

With a test setup that can increase the slip force slowly, it is possible to test coating materials. Tests were performed on a pipe with fusion-bonded epoxy coating, and more were planned for tests on three-layer polypropylene. It was found that the quick wear of the coating affected friction behaviour significantly. The coated pipe testing results were not used, and further planned tests were cancelled.

Bibliography

[1] M. Alberto et al. “High-grip and hard-wearing graphene reinforced polyurethane coatings”. In: *Composites Part B: Engineering* (2021).

[2] M. Ashby, H. Shercliff, and D. Cebon. *Materials: Engineering, Science, Processing and Design 4th Edition*. Elsevier Ltd., 2014.

[3] H. Ashrafizadeh, P. Mertiny, and A. McDonald. “Evaluation of the effect of temperature on mechanical properties and wear resistance of polyurethane elastomers”. In: *Wear* (2016).

[4] O. Ben-David and J. Fineberg. “Static friction coefficient is not a material constant”. In: *Physical Review Letters* (2011).

[5] B. Bhushan. *Principles and Applications of Tribology, Second Edition*. John Wiley and Sons, Ltd., 2013.

[6] P. J. Blau. *Friction Science and Technology from concepts to applications*. CRC Press, 2009.

[7] D. Capanidis. “The influence of hardness of polyurethane on its abrasive wear resistance”. In: *Tribologia* (2016).

[8] D. Capanidis and J. Sokolska. “The effect of pressure and time of stationary contact under load on the static friction coefficient of polyurethane elastomers (EPUR) during friction on steel in various lubricating conditions”. In: *Tribologia* (2020).

[9] I. R. Clemitson. *Castable polyurethane elastomers*. CRC Press, 2008.

[10] B. Feeny et al. “A historical review on dry friction and stick-slip phenomena”. In: *Applied Mechanics Reviews* (1998).

[11] C. Hepburn. *Polyurethane elastomers*. Springer Netherlands, 1982.

[12] D. J. T. Hill et al. “Laboratory wear testing of polyurethane elastomers”. In: *Wear* (1997).

[13] H. Jiang et al. “Influence of surface roughness and contact load on friction coefficient and scratch behavior of thermoplastic olefins”. In: *Applied Surface Science* (2008).

[14] S. Maegawa, F. Itoigawa, and T. Nakamura. “Effect of normal load on friction coefficient for sliding contact between rough rubber surface and rigid smooth plane”. In: *Tribology International* (2015).

[15] R. Morgans, S. Lackovic, and P. Cobbold. “Understanding the IRHD and Shore Methods used in Rubber Hardness Testing”. In: *Rubber Division, American Chemical Society* (1999).

[16] C. Prisacariu. *Polyurethane Elastomers : From Morphology to Mechanical Aspects*. SpringerWienNewYork, 2011.

[17] V. Quaglini and P. Dubini. “Friction of polymers sliding on smooth surfaces”. In: *Advances in Tribology* (2011).

[18] R. Sahli et al. “Evolution of real contact area under shear and the value of static friction of soft materials”. In: *Proceedings of the National Academy of Sciences of the United States of America* (2018).

[19] E. Sharmin and F. Zafar. *Polyurethane: An Introduction*. IntechOpen, 2012.

[20] A.L. Smit. *Upscaling of pipe tensioners*. 2008.

[21] D. Tsukinovsky, E. Zaretsky, and I. Rutkevich. *Material Behavior in Plane Polyurethane-Polyurethane Impact with Velocities from 10 to 400 m/sec.* 1997.

[22] P. Wright and A. P. C. Cumming. *Solid polyurethane elastomers*. Maclaren, 1969.

[23] W. Xie et al. “Process parameter optimization for thin-walled tube push-bending using response surface methodology”. In: *International Journal of Advanced Manufacturing Technology* (2022).

[24] T. T. Yang et al. “Effect of cyclic straining with various rates on stress softening/hysteresis and structural evolution of filled rubber: A time-resolved SANS study”. In: *Composites Part B: Engineering* (2022).